

MASTER

Cooperative adaptive cruise control in a heterogeneous vehicle platoon a novel acceleration-based approach

Lambert, P.

Award date:
2019

[Link to publication](#)

Disclaimer

This document contains a student thesis (bachelor's or master's), as authored by a student at Eindhoven University of Technology. Student theses are made available in the TU/e repository upon obtaining the required degree. The grade received is not published on the document as presented in the repository. The required complexity or quality of research of student theses may vary by program, and the required minimum study period may vary in duration.

General rights

Copyright and moral rights for the publications made accessible in the public portal are retained by the authors and/or other copyright owners and it is a condition of accessing publications that users recognise and abide by the legal requirements associated with these rights.

- Users may download and print one copy of any publication from the public portal for the purpose of private study or research.
- You may not further distribute the material or use it for any profit-making activity or commercial gain

Cooperative Adaptive Cruise Control in a Heterogeneous Vehicle Platoon

A Novel Acceleration-Based Approach

Master's thesis

University: Eindhoven University of Technology
Department: Mechanical Engineering
Research group: Dynamics & Control

Author: P. Lambert
s1116821

Supervisors: Dr. ir. J. Ploeg
Dr. ir. A.A.J. Lefeber
Prof. dr. H. Nijmeijer

Document: DC 2019.072

Eindhoven, August 7, 2019

Summary

Cooperative Adaptive Cruise Control in a Heterogeneous Vehicle Platoon

What could solve the world's traffic congestion problem and reduce emission of greenhouse gasses at the same time? Cooperative Adaptive Cruise Control (CACC). Cruise Control (CC) and its successor Adaptive Cruise Control (ACC) are two well-known types of automated driving. Both systems aim to increase driver comfort and, therefore, operate at large inter-vehicle distances. In addition to the measurements used in ACC, CACC employs wireless communication between vehicles to realize significantly smaller inter-vehicle distances. This increases road throughput and, due to aerodynamics effects, decreases fuel consumption and emission of greenhouse gasses. Moreover, if string stability is guaranteed, disturbances are attenuated in upstream direction, preventing ghost traffic jams.

As a consequence of its high potential, CACC is well studied. The desired acceleration is commonly communicated between vehicles. To obtain the response of a preceding vehicle to this desired acceleration, a model describing its dynamic behaviour is required. The necessary knowledge to acquire an accurate model may not be available for various, e.g., reluctance of vehicle manufacturers to share information. To overcome this problem, homogeneity of vehicles is often assumed. However, this assumption is not accurate if vehicles have, for instance, different driveline dynamics, acceleration limits, or masses. Therefore, this thesis proposes a novel alternative CACC approach, where instead of the desired acceleration, the realized acceleration is communicated between platoon vehicles. As a result, this approach achieves string stability at close inter-vehicle distances in a heterogeneous platoon, without requiring knowledge of the dynamic behaviour or the limitations of a predecessor. Additionally, to allow for platooning in a scenario where vehicles have different and possibly unknown masses, both approaches are extended with an adaptive mass estimation.

Throughout this thesis, the two CACC approaches are compared using three scenarios: The first scenario shows that the alternative approach can guarantee string stability at slightly smaller inter-vehicle distances in a scenario of regular platooning, which means that the platoon is homogeneous and all vehicle parameters are *a priori* known. The second scenario illustrates the main advantage of the alternative approach in a platoon where vehicles have different drivelines or acceleration limitations. Due to this heterogeneity, the platoon becomes string unstable if the common approach is utilized, which may result in unsafe behaviour. However, if the alternative approach is adopted, the platoon remains string stable and safety is guaranteed. The third scenario compares the two approaches with the assumption of unknown vehicle masses, to illustrate the effectiveness of the mass estimation laws.

Finally, to validate the theoretical results and test the merit of the conclusions in a realistic environment, both approaches are implemented experimentally on a platoon of mobile robots.

Acknowledgements

With this opportunity I would like to express my gratitude to all who helped me during my graduation project. I would like to thank Jeroen Ploeg. Jeroen, I appreciate the willingness you have always had to read the endless number of pages I send your way. Throughout the project, your feedback helped me a lot and the occasional motivational speech was appreciated too. But most of all, the enthusiasm you brought to the project made it very much a pleasure to work with you. Also, I would like to express my gratitude to Erjen Lefeber and Henk Nijmeijer for the never ending stream of ideas, which always kept the project interesting. Moreover, I appreciate the time you made to provide my work with rigorous feedback and the patience you had throughout all our meetings. A word of appreciation also goes out to Maarten Lambert. Maarten, thank you for taking the time to improve the readability of my work with the many helpful suggestions on my style of writing. Finally, I would like to thank everyone at 2getthere B.V. for giving me the opportunity to work on this project. It has been a very pleasant and fun working environment for the past months.

Contents

1	Introduction	1
1.1	Cooperative automated driving	1
1.1.1	The background of advanced driver assistance systems	1
1.1.2	History and development of cooperative adaptive cruise control	2
1.2	Challenges in cooperative adaptive cruise control	3
1.3	Research objectives and contributions	3
1.4	Outline	4
2	Literature review	5
2.1	Cooperative adaptive cruise control	5
2.1.1	Longitudinal vehicle model	5
2.1.2	Control objectives	6
2.2	String stability	7
2.2.1	A literature overview	8
2.2.2	Definition of string stability	8
2.3	Heterogeneity	9
2.3.1	Different types of heterogeneity	9
2.3.2	Heterogeneity caused by different driveline dynamics	10
2.3.3	Heterogeneity caused by different acceleration limits	12
2.3.4	Discussion	12
2.4	Mass estimation	12
2.5	Summary	13
3	Cooperative adaptive cruise control: a common approach	15
3.1	Controller design	15
3.1.1	Closed loop dynamics	15
3.1.2	Input-to-state stability	16
3.1.3	String stability	18
3.2	Mass estimation	20
3.2.1	Closed loop dynamics	20
3.2.2	Individual vehicle stability	21
3.3	Platoon simulations	22
3.3.1	Regular platooning	23
3.3.2	Heterogeneity	23
3.3.3	Mass estimation	25
3.4	Summary	27
4	Cooperative adaptive cruise control: an alternative approach	29
4.1	Controller design	29
4.1.1	Closed-loop dynamics	29
4.1.2	Input-to-state stability	30
4.1.3	String stability	31

4.2	Mass estimation	32
4.2.1	Closed-loop dynamics	32
4.2.2	Individual vehicle stability	33
4.3	Platoon simulations	34
4.3.1	Regular platooning	34
4.3.2	Heterogeneity	35
4.3.3	Mass estimation	37
4.4	Summary	39
5	Experimental validation	41
5.1	Experimental setup	41
5.1.1	Hardware components	42
5.1.2	Characteristics of the experimental setup	42
5.1.3	Reference trajectory	43
5.2	Control structure	44
5.2.1	Low-level system	44
5.2.2	High-level system	45
5.3	Control structure validation using platoon simulations	46
5.3.1	Regular platooning	47
5.3.2	Heterogeneity	47
5.3.3	Mass estimation	50
5.4	Experimental results	51
5.4.1	Regular platooning	52
5.4.2	Heterogeneity	54
5.4.3	Mass estimation	55
5.5	Summary	59
6	Conclusions and recommendations	61
6.1	Conclusions	61
6.2	Recommendations	62
	Bibliography	63
	Appendix A Preliminaries	69
	Appendix B Input-to-state stability	71
	Appendix C A string stability condition	73
	Appendix D Negative definite quadratic form	75
	Appendix E Sensitivity in the presence of mass estimation errors	76
	Appendix F Experimental setup limitations	78
	Appendix G Additional experimental results	79

Nomenclature

Acronyms and abbreviations

ADAS	Advanced Driver Assistance Systems
ASP	Adaptive Spacing Policy
(C)ACC	(Cooperative) Adaptive Cruise Control
CC	Cruise Control
GAS	Global Asymptotic Stability
MRAC	Model Reference Adaptive Control
PF	Predecessor Following
PLF	Predecessor Leader Following

Roman symbols

A	system matrix
a	acceleration
B	input matrix
C	output matrix
D	delay transfer function
d	distance; drag coefficient
e	error
F	force
G	vehicle transfer function
H	spacing policy transfer function
h	time gap
j	imaginary number
K	feedback controller transfer function; Air resistance coefficient
k	gain
L	length
ℓ	output dimension
m	platoon length; vehicle mass
n	number of states
q	position; number of inputs
R	radius
r	standstill distance
S	sensitivity transfer function
s	Laplace variable
t	time
u	vehicle input
V	Lyapunov candidate function
v	velocity
x	state vector; position coordinate
y	position coordinate

Greek symbols

α	class \mathcal{K} function; control constant
β	class \mathcal{K} function; real-valued function
Γ	string stability complementary sensitivity
γ	control constant
Δ	time interval
ε	system state; state vector
ζ	auxiliary state
η	feedback linearisation input
θ	communication delay; orientation; orientation error
κ	trajectory curvature
λ	system eigenvalue
ρ	class \mathcal{K}
ξ	auxiliary input
τ	engine time constant
ϕ	uniformly continuous function
ω	angular velocity; frequency

Subscripts

a	alternative
d	derivative action; drag
dd	double derivative action
e	error
eq	equilibrium
i	indices
m	mechanical
max	maximum
min	minimum
p	proportional action
r	reference; desired

Miscellaneous

\mathbb{C}	set of complex numbers
$f(\cdot)$	real-valued function
\mathbb{N}	set of positive integer numbers
$\mathbb{R}^{n \times m}$	set of real $n \times m$ matrices
S_m	set of all vehicles in a platoon of length m
lim	limit value
x^T	transpose of x
\dot{x}	time derivative of x
\tilde{x}	estimation error of x
\hat{x}	estimated value of x
\bar{x}	equilibrium value of x
$ \cdot $	absolute value
$\ \cdot\ $	vector norm
$\ \cdot\ _{\mathcal{H}_\infty}$	\mathcal{H}_∞ system norm
$\ \cdot\ _{\mathcal{L}_p}$	\mathcal{L}_p signal norm, $p \in \{1, 2, \infty\}$

Chapter 1

Introduction

Cooperative automated driving is a promising field of research, that strives to fulfil the social demand for clean, safe and efficient traffic systems, driven by technological innovation. Cooperative Adaptive Cruise Control (CACC) is a form of cooperative driving, which automates the longitudinal control of vehicles strings. Wireless inter-vehicle communication is utilized to realize small distances between the vehicles, while guaranteeing safe driving behaviour. This chapter first presents a background of cooperative automated driving and gives an overview of the development towards CACC in Section 1.1. Subsequently, Section 1.2 discusses the main challenges existing in this field of research. Thereafter, Section 1.3 addresses the research objectives and contributions, which are specified based on the presented challenges. Finally, Section 1.4 presents the outline of this thesis.

1.1 Cooperative automated driving

This section presents a background overview of Advanced Driver Assistance Systems (ADAS) and introduces the main forces driving the development of ADAS. Thereafter, starting from regular Cruise Control (CC), the development towards Cooperative Adaptive Cruise Control (CACC) is explained, following several literature landmarks in the field of cooperative automated driving.

1.1.1 The background of advanced driver assistance systems

The urge to fulfil the social demand for clean, safe and efficient transportation, has created a surge of interest in the concept of automated driving in recent years. The demand for clean traffic systems has The Paris Agreement (UN, 2015) as one of the driving forces. Based on this agreement, the European Union has acceded to achieve a significant reduction of greenhouse emission gasses by 2030 (Rijksoverheid, 2017). Road vehicles are an important factor contributing to the emission of greenhouse emission gasses. It is well known that CACC, which is a type of advanced driver assistance systems, has the potential to significantly reduce fuel consumption (especially for heavy duty vehicles) through aerodynamic effects and, therewith, reduce the emission of greenhouse emission gasses. This was, for instance, shown by Ramakers et al. (2009). Moreover, both Browand et al. (2004) and Lammert et al. (2014) have experimentally shown a decrease in fuel consumption for both the leading and the following truck in a platoon of up to 10%. Bonnet and Fritz (2000) achieved a fuel consumption reduction of 20% in their experiments.

The desire for safe driving behaviour is obvious. It is known that many car accidents occur due to human errors when they are performing certain driving tasks. ADAS can relieve drivers from some of these tasks, giving ADAS the great potential of reducing car accidents and, thereupon, increasing road safety (Vahidi and Eskandarian, 2003).

Finally, in the European Union, road transport continues to have the largest share of inland freight transport, which has shown an increasing trend over recent years. Moreover, passenger cars

accounted for 83.4% of inland passenger transport in 2014 (Publications Office of the European Union, 2017). Because of this significance, road capacity has to be increased to an adequate level to create efficient traffic systems. Currently, the limited capacity of the road network results in congestion, which leads to severe traffic jams. If this problem is not dealt with, the large economic and environmental costs that are caused by traffic jams will drastically increase (Centre for Economics and Business Research, 2014). Schakel et al. (2010) and Netten et al. (2010) have demonstrated by means of simulations and experiments, respectively, that ADAS improve shockwave suppression and throughput. Arem et al. (2006) used simulations to investigate ADAS for a multiple-lane case with lane closure. With these simulations, an improved shock wave suppression was shown, thereby improving the traffic throughput.

In summary, ADAS show great potential to attain the social demand to have clean, safe and efficient traffic systems and to improve these systems to an adequate capacity level. There are many aspects to ADAS, e.g., environmental perception, human-machine interfacing, and functional safety. The focus of this study, however, is on control. Starting from regular cruise control (CC), the development towards cooperative adaptive cruise control (CACC) is explained in the following section.

1.1.2 History and development of cooperative adaptive cruise control

Cruise Control (CC) is a well-known vehicle speed-control mechanism that has been implemented in commercially available vehicles since 1948 (Teetor, 1948). Also, its successor, the Adaptive Cruise Control (ACC) functionality, is widespread and available in numerous commercially available vehicles. ACC automatically regulates the inter-vehicle distance to a desired value if there is a preceding vehicle. To this end, ACC employs data about the preceding vehicle, which is obtained by radar, lidar, or camera. However, ACC is primarily intended as a comfort system and, consequently, adopts relatively large inter-vehicle distances (Vahidi and Eskandarian, 2003).

Cooperative Adaptive Cruise Control (CACC) is an automatic vehicle-following system, which employs inter-vehicle wireless communication in addition to the data obtained by radar, lidar, or camera and was originally introduced by the California PATH program (Shladover, 1978). CACC is known to allow time gaps significantly smaller than 0.8 second, as is the standardized minimum value for current available ACC systems (International Organization for Standardization, 2010). Therefore, CACC exploits the benefits discussed in the previous section to a greater extent. Besides, Naus et al. (2010) have shown that ACC amplifies disturbances in upstream direction at small time gaps, similar to the disturbance amplification seen in the case of human drivers. These disturbances may, for instance, be induced by velocity variations of the first vehicle in a string of vehicles. As a result, fuel consumption and emissions increase. Moreover, so-called ghost traffic jams may occur, negatively influencing throughput, whereas safety might be compromised as well (Ploeg, 2014). As a consequence, string stability, roughly described as disturbance attenuation in upstream direction, is of the utmost importance and well studied. Swaroop and Hedrick (1996), for instance, have presented a comprehensively formalized definition of string stability based on Lyapunov stability with the focus on initial condition perturbations. Ploeg et al. (2014b) have presented an overview of the wide spectrum of different definitions of string stability and propose a novel definition for nonlinear cascaded systems. Then, they applied this definition to a case study considering homogeneous vehicle platoons, in which string stability is guaranteed.

Throughout the development process of ADAS towards CACC, heterogeneity within a vehicle platoon has always been one of the main challenges. This was for example illustrated by Sheikholeslam and Desoer (1992), who consider a heterogeneous vehicle platoon. They achieved string stability, with respect to a disturbance imposed by the platoon leader, in spite of variations in: vehicles masses; communication delays; and measurement noise. Another landmark study that considers a heterogeneous vehicle platoon was presented by Shaw and Hedrick (2007). Here, results from heterogeneous string stability analyses were presented and used to construct a controller design procedure that gives string stability and robustness to external disturbances. A more extensive literature overview of string stability and heterogeneity is presented in Chapter 2.

1.2 Challenges in cooperative adaptive cruise control

In the previous section, longitudinal vehicle automation, such as CACC, was introduced as a high potential solution to some of today's precessing issues in road transportation. As explained, CACC can contribute to reducing fuel consumption and emissions, safer and more comfortable driving behaviour and increasing road throughput. However, string stability of the vehicle platoon is a prerequisite for safety and driver comfort, as was shown by Ploeg (2014). String stability also increases the road throughput compared to human drivers or ACC and prevents ghost traffic jams (Arem et al., 2006). Moreover, reducing traffic congestion also decreases fuel consumption and greenhouse emissions (Barth and Boriboonsomsin, 2008). One of the main challenges in achieving string stable vehicle platoons originates in the nature of wireless communication. Complications in wireless communication occur due to impairments such as, (varying) latency and packet loss (Ploeg, 2014). Research in the field of networked control systems, focusing on the effects of varying latency, e.g. Öncü (2014), contributes to rigorous knowledge regarding the maximum allowable latency resulting in a string stable vehicle platoon.

Due to importance of the notion, string stability is well studied, see, e.g., Swaroop and Hedrick (1996); Desjardins and Chaib-draa (2011); Bayezit et al. (2012); Kianfar et al. (2012); Ploeg (2014); Ploeg et al. (2014a, 2015). All these studies use the desired acceleration of the preceding vehicle as input to the cooperative adaptive cruise controller. As a direct consequence of using the desired acceleration, knowledge about the dynamics and limitations of the preceding vehicle is required to understand how it reacts. To obtain this knowledge, the aforementioned studies assume a homogeneous vehicle platoon, i.e, there are no differences between the vehicles in the platoon. However, the practical relevance of studies considering homogeneous is limited to platoons with identical vehicles and loads, or to vehicles that have a low-level acceleration controller so that the dynamics of the acceleration-controlled vehicles are (nearly) identical (Arem et al., 2006).

In a realistic scenario of *ad hoc* platooning¹, the platoon consists of different vehicle types. This results in heterogeneity of the platoon with respect to the individual vehicle dynamics. Another cause of heterogeneity within a platoon can be different vehicle masses. This can, for instance, occur if platoon vehicles have varying loads, which account for a significant percentage of the total vehicle mass, e.g., trucks or buses. Due to the heterogeneity in these two examples, differences between the realizable accelerations of platoon vehicles may occur. Consequently, a platoon vehicle may not realize its desired acceleration. Moreover, the knowledge about a preceding vehicle required to anticipate these differences, might not be available due to, e.g., reluctance of vehicle manufacturers to share information. Hence, heterogeneity poses a serious challenge in the field of cooperative automated driving. Different vehicle types or loads are only two of the many possible causes of heterogeneity in a platoon. Many other differences between platoon vehicles, like differences in communication topology, spacing policies, controllers and definitions of the error signal can be thought of (Wang and Nijmeijer, 2015). In the development towards effective CACC approaches, heterogeneity has already been recognized as one of the main challenges by Shladover (1978). However, due to its many aspects, heterogeneity yet remains a challenge. Two landmark studies that consider a heterogeneous vehicle platoon were already mentioned in the previous section (Sheikholeslam and Desoer, 1992; Shaw and Hedrick, 2007). A more extensive literature overview of heterogeneity in vehicle platoons is presented in Chapter 2.

1.3 Research objectives and contributions

In line with the previously discussed challenges, the objective of this thesis is to develop a CACC approach that effectively achieves close vehicle following in a heterogeneous vehicle platoon, without requiring knowledge of the dynamics and limitations of the preceding vehicles. In order to maximize the benefits discussed in Section 1.1, string stability of the CACC approach is required. In addition, validation of the developed CACC approach is desired. Consequently, the

¹ *Ad hoc* platooning is vehicle following, which is characterized by a cluster of cooperative vehicle followers that are not necessarily aware of all members and do not rely on a leader (Ploeg, 2014).

following contributions are defined:

1. A commonly used CACC approach, which uses the desired acceleration of its predecessor as input, is extended with a dynamically updated mass estimation. This extension enables platooning in a scenario where vehicles carry (possibly varying) unknown loads that account for a significant percentage of the vehicle mass and is particularly relevant if vehicles have changing masses at every stop, such as buses or trucks.
2. To allow for platooning in heterogeneous vehicle platoons, without requiring knowledge of the dynamic behaviour and limitations of a predecessor, a novel alternative CACC approach is proposed. This alternative CACC approach uses the realized acceleration instead of the desired acceleration of its predecessor as input. Therefore, no knowledge of the dynamics of its predecessor is required to guarantee string stability. Moreover, differences between the desired and realized accelerations of a predecessor due to, e.g., power limitations of the driveline do not compromise safe driving behaviour.
3. The effectiveness of both CACC approaches is illustrated and their performance is compared by means of simulations. Additionally, both approaches are implemented experimentally on unicycle mobile robots, to validate the controller design and simulations in the presence of model uncertainties, delays, and sensor noise.

1.4 Outline

The organisation of this thesis is as follows: Chapter 2 presents a literature overview of the main subjects treated in this thesis, which are: the vehicle model and control objective utilized for the CACC design; string stability; heterogeneity; and parameter uncertainty. Chapter 3 presents a CACC approach that is commonly used in literature to achieve the control objectives and extends this approach with a dynamically updated mass estimation. The effectiveness of this common CACC approach, including mass estimation, is illustrated by means of simulations. Chapter 4 proposes a novel alternative to the common CACC approach, which does not require knowledge of the dynamics and limitations of its predecessor and, therefore, can achieve the control objectives in a heterogeneous platoon. The effectiveness of the proposed approach, including mass estimation, is again illustrated by means of simulations. Chapter 5 discusses the implementation of both approaches on mobile robots, to validate the controller design and simulations in the presence of model uncertainties, delays, and sensor noise. Finally, Chapter 6 summarizes the main conclusions and presents recommendations for future research.

Chapter 2

Literature review

As introduced in the previous chapter, a cooperative adaptive cruise controller is an advanced driver assistance system, which controls the longitudinal inter-vehicle distance of vehicles in a platoon. In this thesis, the merit of two CACC approaches is illustrated using three scenarios. The first scenario considers “regular platooning” with a focus on string stability. Regular platooning means that the vehicle platoon is assumed to be homogeneous and all vehicle parameters are assumed to be known. The second scenario considers a heterogeneous vehicle platoon, where the heterogeneity is either caused by different vehicle dynamics or different acceleration limits between the vehicles, and the third scenario assumes that the vehicle masses are unknown.

This chapter presents a literature overview of the topics treated in the three aforementioned scenarios and is organized as follows: Section 2.1 presents a longitudinal vehicle model and the control objectives, which are commonly used in literature. Section 2.2 discusses various string stability definitions available in literature and elaborates on the definition which is adopted in this work. Section 2.3 provides an overview of various types of heterogeneity and explains the focus of this thesis based on the provided overview. Section 2.4 briefly discusses adaptive and robust control, which are two well-known solutions to overcome the problem of unknown system parameters. Finally, the main conclusions are summarized in Section 2.5.

2.1 Cooperative adaptive cruise control

This section presents two necessities underlying the development of a CACC approach. Section 2.1.1 introduces the longitudinal vehicle model, which is adopted from Stankovic et al. (2000). Thereafter, Section 2.1.2 defines the control objectives that must be achieved by the designed controller, based on Ploeg (2014).

2.1.1 Longitudinal vehicle model

It is assumed that the road surface is horizontal, there is no wind gust, and the vehicles travel in the same direction at all times. Consequently, the nonlinear dynamics of the i^{th} platoon vehicle are described by:

$$m_i a_i = F_i - K_d v_i^2 - d_m \quad (2.1a)$$

$$\dot{F}_i = -\frac{F_i}{\tau_i} + \frac{\eta_i}{\tau_i}, \quad i \in S_m. \quad (2.1b)$$

Here, $S_m = \{i \in \mathbb{N} \mid 1 \leq i \leq m\}$ is the set of all vehicles in a platoon of length $m \in \mathbb{N}$. Equation (2.1a) represents Newton’s second law for the i^{th} vehicle, where a_i and v_i denote the acceleration and velocity of the vehicle, respectively, and $m_i > 0$ denotes the mass of the vehicle. The driving force produced by the engine is denoted by F_i , the constant d_m denotes the mechanical drag, and the force due to the air resistance is specified by $K_d v_i^2$, where K_d is a constant

coefficient. Equation (2.1b) models the i^{th} vehicle's engine dynamics, where $\tau_i > 0$ denotes the engine time constant, which is assumed to be constant, and η_i denotes the throttle input to the i^{th} vehicle's engine. Note that conventional or hybrid vehicles have complex nonlinear braking system dynamics, which are not captured by the engine dynamics (2.1b). These systems are for example studied in Kalberlah (1991); Gillespie (1992); Powell et al. (1998). However, in case of electric engines, which are for instance studied by Hori (2004); Khatun et al. (2003); Zheng et al. (2006) and in this thesis, the engine dynamics (2.1b) also represent the braking dynamics.

The model (2.1) can be expressed in kinematic variables. Substitute to this end the expression for F_i from (2.1a) into (2.1b), which gives

$$\dot{F}_i = -\frac{1}{\tau_i} \left[m_i a_i + K_d v_i^2 + d_m \right] + \frac{\eta_i}{\tau_i}, \quad i \in S_m. \quad (2.2)$$

Then, differentiating (2.1a) with respect to time and substituting (2.2) results in

$$\dot{a}_i = -\frac{2K_d}{m_i} v_i a_i - \frac{1}{\tau_i} \left[a_i + \frac{K_d}{m_i} v_i^2 + \frac{d_m}{m_i} \right] + \frac{\eta_i}{m_i \tau_i}, \quad i \in S_m. \quad (2.3)$$

The complete model of the i^{th} vehicle is then given by

$$\begin{aligned} \dot{q}_i &= v_i \\ \dot{v}_i &= a_i \\ \dot{a}_i &= -\frac{2K_d}{m_i} v_i a_i - \frac{1}{\tau_i} \left[a_i + \frac{K_d}{m_i} v_i^2 + \frac{d_m}{m_i} \right] + \frac{\eta_i}{m_i \tau_i}, \quad i \in S_m, \end{aligned} \quad (2.4)$$

where q_i is the rear bumper position of vehicle i . Note that the time argument is often omitted throughout this thesis to increase readability.

The system (2.4) is feedback linearisable and in the correct form for feedback linearisation, see Appendix A.1, i.e., there is no coordinate transformation required for input-state linearisation. Assume that all system parameters are *a priori* known and consider the following input transformation:

$$\eta_i = m_i u_i + K_d v_i^2 + d_m + 2K_d \tau_i v_i a_i, \quad i \in S_m, \quad (2.5)$$

where u_i is the new input signal. The input transformation is globally well defined since it was previously assumed that $m_i > 0$. After adopting this input transformation the longitudinal vehicle model is given by

$$\begin{aligned} \dot{q}_i &= v_i \\ \dot{v}_i &= a_i \\ \dot{a}_i &= -\frac{1}{\tau_i} a_i + \frac{1}{\tau_i} u_i, \quad i \in S_m. \end{aligned} \quad (2.6)$$

This linear vehicle model is adopted by many authors, see, e.g., Shladover (1978); Shaw and Hedrick (2007); Ploeg (2014). Another option, which is for instance used by Sheikholeslam and Desoer (1990); Ioannou and Chien (1993); Godbole and Lygeros (1994), is to use a triple integrator model, which is obtained if the following feedback linearisation is used instead of (2.5):

$$\eta_i = m_i \tau_i u_i + m_i a_i + K_d v_i^2 + d_m + 2K_d \tau_i v_i a_i, \quad i \in S_m. \quad (2.7)$$

2.1.2 Control objectives

In order to enable vehicle following in a CACC setting, individual vehicle stability is a prerequisite. This control objective is formalized hereafter. Thereto, consider a platoon of m vehicles, schematically depicted in Figure 2.1, where d_i is the distance between vehicle i and its preceding vehicle $i - 1$.

In the scope of CACC, platoon vehicles communicate information to achieve their control objectives. The communicated information can, for instance, be the desired acceleration u_{i-1} (Swaroop and Hedrick, 1996; Kianfar et al., 2012; Ploeg et al., 2014b) or the realized acceleration a_{i-1} (Naus

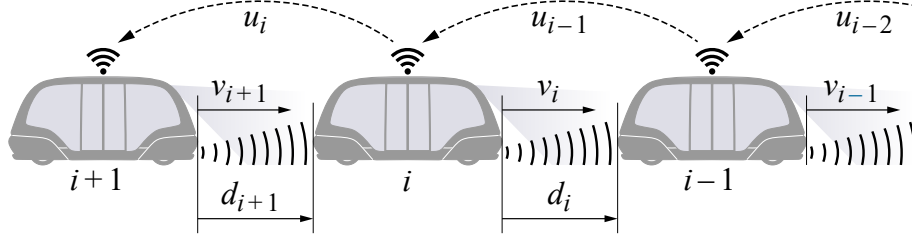


Figure 2.1: CACC-equipped vehicles in a platoon.

et al., 2010; Wang and Nijmeijer, 2015) of the preceding vehicle. To this end, a wireless communication topology must be adopted. Zheng et al. (2016) discussed six types of communication topologies: predecessor following, predecessor-leader following, bidirectional, bidirectional leader, two-predecessor following and two-predecessor-leader following. Complications in wireless communication such as (varying) latency and packet loss increase with an increasing communication distance (Öncü, 2014). Moreover, Ploeg et al. (2014a) have shown that multiple look-ahead topologies only improve the performance with respect to string stability at large communication delays. Therefore, an often adopted communication topology is predecessor following (PF), see, for instance, Sheikholeslam and Desoer (1990); Ioannou and Chien (1993); Ploeg et al. (2014b).

The first control objective of each vehicle is to follow its predecessor at a desired distance $d_{r,i}$, where the platoon leader (with index $i = 1$) follows a so-called virtual reference vehicle (with index $i = 0$). The desired distance $d_{r,i}$ is defined according to a constant time gap spacing policy, formulated as

$$d_{r,i}(t) = r_i + hv_i(t), \quad i \in S_m, \quad (2.8)$$

where h is the time gap and r_i is the standstill distance. Then, the spacing error $e_i(t)$ is defined as

$$\begin{aligned} e_i(t) &= d_i(t) - d_{i,r}(t) \\ &= (q_{i-1}(t) - q_i(t) - L_i) - (r_i + hv_i(t)), \quad i \in S_m, \end{aligned} \quad (2.9)$$

where L_i is the vehicle length. The vehicle following control objective is now formulated as ensuring that $\lim_{t \rightarrow \infty} e_i(t) = 0$, $\forall i \in S_m$. In other words, the control strategy should make sure that no steady state error exists. Additionally, the tracking errors should illustrate well-damped behaviour, which is not quantified here because of its application specific nature. Platoon simulations are presented throughout this thesis to analyze the behaviour of the tracking errors.

The constant time gap spacing policy (2.8) is known to improve string stability characteristics (Swaroop et al., 1994; Seiler et al., 2004) and also contributes to safety (Ioannou and Chien, 1993). Another frequently used spacing policy is the constant distance spacing policy, see, e.g., Shaw and Hedrick (2007). However, as a direct consequence of the latter spacing policy, string stability of the vehicle platoon can only be obtained by adopting communication topologies which are more complex than predecessor following, e.g., predecessor-leader following (Seiler et al., 2004). Achieving string stability is the second control objective, which is discussed in detail in the following section.

2.2 String stability

As explained in Chapter 1, it is of paramount importance that the control strategy of a CACC controlled vehicle platoon can guarantee string stability. Because of this importance, many authors have studied the notion of string stability, resulting in ambiguity concerning its definition. This section first discusses various definitions of string stability proposed in literature and, thereafter, presents the definition of string stability that is adopted in this thesis.

2.2.1 A literature overview

An extensive overview of string stability definitions was presented by Studli et al. (2017). They discuss various definitions starting from a general definition of $\mathcal{L}_{p,q}$ string stability. This rigorous general definition is the most versatile version of input-output stability, since it requires that, for any possible combination of inputs, the outputs of all platoon vehicles must be bounded. Consequently, this definition is highly relevant but also brings a lot of complexity to the analysis. On the other end of the spectrum, they present the definition “single with input α final $\mathcal{L}_{p,q}$ string stability”, which only considers the input of one selected vehicle and its influence on the output of the last vehicle. Various options in between these two extremities are discussed.

One of these variations is the definition presented by Ploeg et al. (2014b). This definition considers the external disturbance imposed by the platoon leader as input and looks at its influence on the outputs of all platoon vehicles. This definition also captures the definition of Swaroop and Hedrick (1996), which is one of the more formal approaches based on Lyapunov stability, because of the inclusion of initial condition perturbations. Both aforementioned definitions apply to both linear and nonlinear systems and include homogeneous as well as heterogeneous vehicle strings. The applicability to heterogeneous systems was, for example, illustrated by Naus et al. (2010); Wang and Nijmeijer (2015); Al-Jhayyish and Schmidt (2018). A more elaborate discussion of heterogeneity is presented in Section 2.3.

This work adopts the definition proposed by Ploeg et al. (2014b), which is formalized in the next section. Additional requirements on the (internal) system behaviour are explained in the following chapters. The particular definition is adopted for the following reasons: Firstly, the external input to the first platoon vehicle is the most relevant because, in case of vehicle platooning, the main disturbance is imposed by speed variations of the platoon leader. Secondly, only considering the influence of this input on a single vehicle, e.g., the last platoon vehicle, is considered a too weak condition since this would allow for undesired behaviour, such as collision of platoon vehicles. Hence, the influence of input variations imposed by the lead vehicle on the outputs of all platoon vehicles is considered.

2.2.2 Definition of string stability

In order to derive a general definition of string stability, consider the possibly nonlinear, heterogeneous interconnected system

$$\begin{aligned} \dot{x}_0 &= f_r(x_0, u_r) \\ \dot{x}_i &= f_i(x_i, x_{i-1}) \\ y_i &= h(x_i), \quad i \in S_m, \end{aligned} \tag{2.10}$$

where u_r is the external input, x_i is the state vector, and y_i is the output. Moreover, $f_r : \mathbb{R}^n \times \mathbb{R}^q \mapsto \mathbb{R}^n$, $f_i : \mathbb{R}^n \times \mathbb{R}^n \mapsto \mathbb{R}^n$, $i \in S_m$, and $h : \mathbb{R}^n \mapsto \mathbb{R}^\ell$. Then, using this system, the following definition of string stability is proposed.

Definition 2.1 (\mathcal{L}_p string stability). *Consider the interconnected system (2.10). Let $x^T = (x_0^T \dots x_m^T)$ be the lumped state vector and $\exists \bar{x}$ such that $f_i(\bar{x}_i, \bar{x}_{i-1}) = 0$, $\forall i \in S_m$, and $f_r(\bar{x}_0, 0) = 0$. The system (2.10) is \mathcal{L}_p string stable if there exist class \mathcal{K} functions¹ α and β , such that, for any initial state $x(0)$ and any u_r ,*

$$\|y_i(t) - h(\bar{x}_0)\|_{\mathcal{L}_p} \leq \alpha(\|u_r(t)\|_{\mathcal{L}_p}) + \beta(\|x(0) - \bar{x}\|), \quad \forall i \in S_m, \text{ and } \forall m \in \mathbb{N}.$$

If, in addition, with $x(0) = \bar{x}$ it holds that

$$\|y_i(t) - h(\bar{x}_0)\|_{\mathcal{L}_p} \leq \|y_{i-1}(t) - h(\bar{x}_0)\|_{\mathcal{L}_p}, \quad \forall i \in S_m \setminus \{1\}, \text{ and } \forall m \in \mathbb{N} \setminus \{1\},$$

¹A continuous function $\alpha : \mathbb{R}_{\geq 0} \mapsto \mathbb{R}_{\geq 0}$ is said to belong to class \mathcal{K} if it is strictly increasing and $\alpha(0) = 0$.

the system (2.10) is strictly \mathcal{L}_p string stable with respect to its input $u_r(t)$.

Here, $\|\cdot\|$ denotes any vector norm, $\|\cdot\|_{\mathcal{L}_p}$ denotes the signal p -norm, and \mathcal{L}_p^q is the q -dimensional space of vector signals that are bounded in the \mathcal{L}_p sense.

In addition, within the scope of the platooning problem, the linear heterogeneous system is considered as special case of (2.10), which, in lumped form, can be denoted by

$$\dot{x} = Ax + Bu_r, \quad (2.11)$$

with $x = (x_0^T \dots x_m^T)^T$. Moreover, consider linear output functions according to

$$y_i = C_i x, \quad i \in S_m \quad (2.12)$$

with output matrices C_i . The model (2.11), (2.12) can then be formulated in the Laplace domain as

$$\bar{y}_i(s) = P_i(s)\bar{u}_r(s) + O_i(s)x(0), \quad i \in S_m \quad (2.13)$$

with outputs $y_i(t)$ and exogenous input $u_r(t)$, whose Laplace transforms are denoted by $\bar{y}_i(s)$ and $\bar{u}_r(s)$ ². The initial condition is denoted by $x(0)$, whereas $P_i(s) = C_i(sI - A)^{-1}B$ and $O_i(s) = C_i(sI - A)^{-1}$. Then, Ploeg et al. (2014b) present the following (strict) string stability conditions for this linear system.

Theorem 2.1 *Assume that the pair (C_i, A) is such that unstable and marginally stable modes are unobservable and that $P_i(s)$ is square and nonsingular, for all $i \in \mathbb{N}$. Then, this system is \mathcal{L}_2 string stable if:*

$$\|P_1(s)\|_{\mathcal{H}_\infty} < \infty \quad \text{and} \quad (2.14a)$$

$$\|\Gamma_i(s)\|_{\mathcal{H}_\infty} \leq 1, \quad \forall i \in \mathbb{N} \setminus \{1\}, \quad (2.14b)$$

with $\Gamma_i(s) = P_i(s)P_{i-1}^{-1}(s)$. Moreover, the system is strictly \mathcal{L}_2 string stable if and only if conditions 1 and 2 hold.

2.3 Heterogeneity

This section presents an overview of literature that considers heterogeneous vehicle platoons. Firstly, Section 2.3.1 discusses various types of heterogeneity that can exist within a platoon. Then, the subsequent sections present a literature overview of two important types of heterogeneity.

2.3.1 Different types of heterogeneity

“Heterogeneous” is defined as: diverse, diversified, varied, varying or miscellaneous (Aarts et al., 2014). Various causes of heterogeneity are mentioned in literature, some of which are differences between platoon vehicles in communication topologies, spacing policies, controllers, definitions of the error signal, communication or actuator delays, vehicle dynamics and velocity or acceleration constraints (Wang and Nijmeijer, 2015). These causes of heterogeneity can be divided into three categories: vehicle characteristics, control objective and control strategy. Causes of heterogeneity in the first category, vehicle characteristics, are unavoidable, whereas the causes of heterogeneity in the other two categories are not. For the second and third categories, heterogeneity can be prevented by making agreements on common policies. With this reasoning, the first category is most important for vehicle manufacturers. Different types of heterogeneity are categorized in Table 2.1.

From the types of heterogeneity in the first category, (velocity) constraints are studied by, e.g., Zegers et al. (2017). They propose a distributed consensus control approach for longitudinal

²Note that throughout this thesis $\bar{\cdot}(s)$ denotes the Laplace transform of corresponding time domain variable $\cdot(t)$

Table 2.1: Causes of heterogeneity by category

Vehicle characteristics	Control objective	Control strategy
Dynamics	Spacing policies	Controllers
velocity/acceleration constraints	Definitions of the error signal	Communication topologies
Communication delays		
Actuator delays		

vehicular platoon control. This control law shows that members of a platoon can adjust their velocity based on the velocity constraints of other vehicles, to maintain the platoon cohesion.

An equally important notion is that of heterogeneity caused by vehicles with different delays. In a scenario of *ad hoc* platooning, vehicle-varying delay is an inevitable cause of platoon heterogeneity. In literature that considers heterogeneity caused by vehicle-varying delays, it is often assumed that delays are known and string stability is realized *a posteriori* by control parameter tuning, see, for instance, Naus et al. (2010); Wang and Nijmeijer (2015). Besides vehicle-varying delays, delays can also be time-varying. A distributed controller which achieves the close vehicle following control objective in the presence of time-varying and vehicle-varying communication delays is presented by di Bernardo et al. (2015). They guarantee string stability by assuming a constant upper bound for the considered delay.

The communication topology, which can be a cause of heterogeneity, has been studied by, e.g., Zheng et al. (2016). They discuss six types of communication topologies: predecessor following, predecessor leader following, bidirectional, bidirectional leader, two-predecessor following and two-predecessor-leader following. However, in their work it is assumed that all vehicles in a platoon use the same communication topology, so that the communication topology is not a type of heterogeneity. The communication topology is a type of heterogeneity in Zheng et al. (2017). They propose a distributed MPC algorithm for vehicle platoons with different (unidirectional) communication topologies within the platoon and derive a sufficient condition to guarantee asymptotic stability. Here, the heterogeneity is viewed as a type of uncertainty, whereas in later work (Zheng et al., 2019) heterogeneity is taken into account in the problem formulation. The latter allows for a deeper understanding of the influence of heterogeneity on the collective behaviour of a platoon of connected vehicles.

Rodonyi (2018) addressed the problem of heterogeneous spacing policies in multi-brand *ad hoc* platoons and demonstrates that this can result in collision of vehicles. To resolve this problem, they propose a leader-predecessor-follower (LPF) communication topology and use an adaptive spacing policy (ASP) with respect to the leader. Additionally, they derive conditions for string stability of platoons consisting of LPF-ASP vehicles and show that string stability with respect to acceleration and control effort can be guaranteed by appropriately choosing the LPF-ASP control parameters.

In summary, heterogeneity of vehicle platoons occurs if vehicles have different physical characteristics, control objectives, or control strategies. One of the contributions of this thesis, as specified in Chapter 1, is a novel alternative CACC approach that allows for *ad hoc* platooning within platoons which are heterogeneous with respect to vehicle dynamics and acceleration constraints. The following sections present an overview of literature which also focusses on these causes of heterogeneity.

2.3.2 Heterogeneity caused by different driveline dynamics

Shaw and Hedrick (2007) have presented an iconic study that considers heterogeneity due to different driveline dynamics. In their work they propose a definition for string stability of a heterogeneous vehicle platoon. Using this definition, they achieve string stability in a vehicle platoon that consists of vehicles with three different types of dynamics (fast, medium and slow). This is achieved with decentralized control laws, adopting a constant spacing policy and leader-predecessor following. As a direct consequence of the adopted spacing policy, string stability can

only be achieved by including leader communication (Seiler et al., 2004). Reliability of communication is one of the main issues in achieving string stability and becomes less when the distance between the communicating vehicles increases (Öncü, 2014). Reliability of communication was not addressed by Shaw and Hedrick (2007), but is a limitation of leader-predecessor following. Moreover, heterogeneity in the platoon is limited to three different vehicle types.

Various studies consider a feedforward strategy to achieve string stability in a vehicle platoon, which is heterogeneous with respect to the driveline dynamics, e.g., Naus et al. (2010); Wang and Nijmeijer (2015); Al-Jhayyish and Schmidt (2018). The study presented by Al-Jhayyish and Schmidt (2018) classifies these feedforward strategies into two categories. In the first category the desired acceleration is communicated, while in the second category the actual acceleration is communicated. Thereafter, they present a controller design for both categories, which achieves string stability, by *a posteriori* tuning of the controller. Consequently, knowledge of the differences between vehicles is required and no guarantees on string stability can be made in case of *ad hoc* platooning.

In the work presented by Wang and Nijmeijer (2015) the desired acceleration is communicated. Hence, this feedforward strategy fits in the first category described by Al-Jhayyish and Schmidt (2018). Due to the particular choice of feedforward controller, string stability is not influenced by differences in the dynamics of platoon vehicles. To achieve this, their feedforward controller uses τ_{i-1} , i.e., for the implementation of this controller knowledge of the preceding vehicle is required, which might not be available in case of *ad hoc* platooning.

The feedforward strategy presented by Naus et al. (2010) uses the actual acceleration as input signal. Hence, this feedforward strategy fits in the second category described by Al-Jhayyish and Schmidt (2018). As a direct consequence, string stability can be guaranteed without knowledge of the dynamics of the preceding vehicle, i.e., string stability can be guaranteed in a heterogeneous scenario of *ad hoc* platooning. The feedforward strategy presented by Naus et al. (2010), uses a lead-filter feedforward controller. Since the acceleration input signal is generally noisy, a serious drawback of this lead filter implementation is amplification of this noise. Moreover, their feedforward controller contains the inverted vehicle model. This vehicle model contains an actuator delay, which cannot be inverted. Hence, this feedforward controller cannot be implemented.

An interesting solution is presented by Harfouch et al. (2018), who assume that the driveline dynamics of the platoon leader τ_0 are known and the driveline dynamics of all other vehicles are assumed to consist of τ_0 plus an uncertainty $\Delta\tau$. Note that a more realistic assumption would be to assume that vehicle i knows its own driveline dynamics τ_i and that the driveline dynamics of the leading vehicle τ_0 are unknown. However, using the latter assumption is also possible with the proposed method. Using a Model Reference Adaptive Control (MRAC) augmentation method, Harfouch et al. (2018) analytically prove convergence of the heterogeneous platoon model to a string stable reference model and illustrate string stability by means of simulations. A known limitation, inherent to the proposed MRAC method, is that the adaptive gains lose their independence once steady state is reached. This raises the requirement of “persistent excitation” of the platoon reference acceleration to achieve convergence of the heterogeneous platoon model to the string stable reference model. As long as convergence is not achieved, string stability cannot be guaranteed. The tracking errors obtained by Harfouch et al. (2018) clearly show that the platoon is string unstable during convergence. Persistent excitation of the platoon reference acceleration is adopted by Harfouch et al. (2018) such that the platoon model converges to the reference model, after which the platoon is string stable. However, the adopted reference acceleration limits the adopted approach to vehicles that can achieve a velocity of 40 m/s and results in (undesired) velocity variations. Additionally, MRAC requires that the entire state vector of the heterogeneous platoon model follows the behaviour of the string stable reference platoon. This is only possible if both models are of the same order. While this is the case in the study presented by Harfouch et al. (2018), real world systems are usually of higher order compared to the system model. If these differences are too large, this might result in instability, i.e., model uncertainties have to be sufficiently small. The latter limitation is not discussed, since no real-world implementation of the MRAC approach is presented. Both of the aforementioned limitations appear if one only intends to guarantee stability of the system, before even mentioning performance (Barkana, 2007).

2.3.3 Heterogeneity caused by different acceleration limits

Different acceleration limits between platoon vehicles can occur for various reasons. Different acceleration limits can, for example, be caused by different driveline dynamics. This cause of differences in acceleration limits between vehicles is considered as a separate type of heterogeneity, of which a literature overview was presented in the previous section. Another cause of different acceleration limits can, for instance, be different (passenger) loads, if these loads have a significant influence on the achievable acceleration.

As mentioned, acceleration constraints are particularly relevant for truck-platooning. However, literature regarding these constraints is limited. Authors that focus on acceleration limits within truck platooning are, e.g., Chen et al. (2018); Zhai et al. (2019). Chen et al. (2018) present a scenario of truck-platooning with acceleration constraints that are caused by road slopes and illustrate that these constraints can compromise string stability. Zhai et al. (2019) have presented a switched control strategy to achieve various control objectives with platoon vehicles that have acceleration limits. However, the acceleration constraints are only imposed in a safety analysis, within the scope of collision avoidance, and not during the analysis of string stability. Moreover, both aforementioned studies focus on homogeneous constraints and are, therefore, not relevant for *ad hoc* platooning, where vehicles have different acceleration limits.

2.3.4 Discussion

The presented overview of the state-of-the-art shows that the proposed solutions to heterogeneous platooning, with respect to different driveline dynamics, have the following two limitations: the solutions either require knowledge of preceding vehicles, which means that *ad hoc* platooning is not possible (Naus et al., 2010; Wang and Nijmeijer, 2015; Al-Jhayyish and Schmidt, 2018); or have limitations regarding practical implementation, e.g., the reliability of long distance communication (Shaw and Hedrick, 2007), or the necessity of persistent excitation of the reference acceleration and sufficiently small model uncertainties (Harfouch et al., 2018). Hence, despite the large amount of research, no practically feasible solution is available for *ad hoc* platooning in a vehicle platoon which is heterogeneous with respect to different driveline dynamics, without requiring knowledge of these differences.

The second scenario, followed throughout this thesis, illustrates that heterogeneity with respect to acceleration limits is highly relevant in a case of *ad hoc* platooning and that these differences in achievable accelerations can result in unsafe driving behaviour, e.g., collisions between platoon vehicles. Despite its relevance, literature addressing heterogeneity with respect to acceleration limits is insufficient. To fill this gap, one of the contributions of this thesis is the proposal of a novel alternative CACC approach. As discussed in Chapter 1, this alternative approach does not require knowledge of the different acceleration limits between platoon vehicles to guarantee safe driving behaviour. Hence, the proposed alternative approach also achieves both control objectives in a platoon which is heterogeneous with respect to acceleration limits and, therewith, achieves effective platooning despite the occurrence of two of the most important types of heterogeneity.

2.4 Mass estimation

This work considers a scenario where platoon vehicles have different loads, which can change during stops. Moreover, the platoon vehicles are unaware of these (varying) differences and the loads take up a significant percentage of the total vehicle mass. Since the vehicle mass is part of the control input, this scenario requires a solution that allows for effective control without knowledge of the vehicle mass. Various solutions to parameter uncertainty are available in literature. Two well-known concepts that deal with this problem are robust control and adaptive control. Adaptive control is a method which requires no or little prior knowledge to estimate varying or unknown parameters and is studied by, e.g., Marino (1997); Pourboghraat and Karlsson (2002); Huang and Tsai (2008). Robust control, on the other hand, requires *a priori* knowledge of the bounds of the parameter variations and ensures robustness to these variations. Robust control is, for instance,

studied by Zhang et al. (1998); Jong-Min and Jong-Hwan (1999); Dixon et al. (2000). In general, the performance of an adaptive controller improves over time, while robust controllers aim to have acceptable performance right from the start (Tzafestas, 2014).

In case of vehicle platooning, the mass variations occur only during stops of the vehicles, i.e., only stepwise changes are expected, which is the main reason why adaptive control is adopted to estimate the vehicle mass in this work. An example of adaptive control was already discussed in the previous section. Here, MRAC was utilized as a solution to uncertainty in the dynamics of platoon vehicles. This discussion mentioned the requirement of persistent excitation, which is in general a limitation of adaptive control (Narendra and Annaswamy, 1987).

2.5 Summary

This chapter started with the introduction of the longitudinal vehicle model and the control objectives, which are required as basis for the design of a cooperative adaptive cruise controller, in Section 2.1. Thereafter, a literature overview of the main subjects treated in this thesis was presented. Firstly, Section 2.2 discussed studies that propose various definitions of string stability and motivated the use of one of these definitions. Secondly, Section 2.3 provided an overview of various types of heterogeneity. Finally, Section 2.4 briefly discussed two solutions proposed, in literature to allow for effective control in a scenario which assumes an unknown and possibly time-varying vehicle mass, which, in addition, may be different for each vehicle in the platoon.

Chapter 3

Cooperative adaptive cruise control: a common approach

In the most commonly used CACC approach in literature, platoon vehicles use the desired acceleration of their predecessors as feedforward input. As a direct consequence of this, knowledge of the dynamics of a predecessor is required to guarantee string stability. In a realistic case of *ad hoc* platooning this information is usually not available. To solve this problem, homogeneity of the platoon is often assumed, see, e.g., Ioannou and Chien (1993); Swaroop and Hedrick (1996); Ploeg (2014). Following Ploeg (2014), this chapter presents a “common CACC approach” with the assumption that the vehicle platoon is homogeneous and all system parameters are *a priori* known. Additionally, this work is extended with the assumption that the vehicle mass is unknown. Since the vehicle mass is part of the controller, see (2.5), an estimation of the vehicle mass is necessary to enable platooning with vehicles that have an unknown mass. With this extension, the presented common CACC approach is able to effectively platoon at close inter-vehicle distances, in case that platoon vehicles carry (possibly varying) unknown loads, which account for a significant percentage of the vehicle mass.

The organisation of this chapter is as follows: Section 3.1 presents the design of the common cooperative adaptive cruise controller and analyzes both the individual vehicle stability and string stability. Section 3.2 extends this approach with the assumption that the vehicle mass is unknown and presents the corresponding controller design and stability analyses. Section 3.3 illustrates the effectiveness of the common CACC approach by means of platoon simulations. This section follows the three scenarios that were introduced in the previous chapter. Finally, Section 3.4 summarizes the main conclusions.

3.1 Controller design

This section first presents the design of the common CACC approach, in which platoon vehicles use the desired acceleration of their predecessor as input and the platoon is assumed homogeneous. Thereafter, this section presents the analyses of individual vehicle stability and string stability of the presented CACC approach.

3.1.1 Closed loop dynamics

To achieve the vehicle following control objective, which was presented in Section 2.1.2, Ploeg (2014) defines the following error variables, obtained by differentiation of distance error (2.9).

$$\begin{aligned}\varepsilon_{i,1} &:= q_{i-1} - q_i - d_{i,r} \\ \varepsilon_{i,2} &:= \dot{\varepsilon}_{i,1} = v_{i-1} - v_i - h a_i \\ \varepsilon_{i,3} &:= \dot{\varepsilon}_{i,2} = a_{i-1} - \left(1 - \frac{h}{\tau}\right) a_i - \frac{h}{\tau} u_i, \quad i \in S_m.\end{aligned}\tag{3.1}$$

Here it is assumed that $L_i = 0$, which does not lead to a loss of generality since L_i can always be compensated for by a coordinate transformation. Differentiating these error variables, while substituting the longitudinal vehicle dynamics (2.6), results in the following error dynamics.

$$\begin{aligned}\dot{\varepsilon}_{i,1} &= \varepsilon_{i,2} \\ \dot{\varepsilon}_{i,2} &= \varepsilon_{i,3} \\ \dot{\varepsilon}_{i,3} &= -\frac{1}{\tau}\varepsilon_{i,3} - \frac{1}{\tau}\xi_i + \frac{1}{\tau}u_{i-1}, \quad i \in S_m,\end{aligned}\tag{3.2}$$

with

$$\xi_i = h\dot{u}_i + u_i, \quad i \in S_m,\tag{3.3}$$

which can be regarded as the new input to vehicle i . From the error dynamics (3.2) it is clear that the input ξ_i should be used to stabilize the error dynamics while compensating for the input u_{i-1} of the preceding vehicle in order to satisfy the vehicle-following control objective. Hence, the control law for ξ_i is chosen as

$$\xi_i := K \begin{bmatrix} \varepsilon_{i,1} \\ \varepsilon_{i,2} \\ \varepsilon_{i,3} \end{bmatrix} + u_{i-1}, \quad i \in S_m,\tag{3.4}$$

with $K := (k_p \ k_d \ k_{dd})$. Note that the feedforward term u_{i-1} is obtained through wireless communication with the preceding vehicle, which is the reason for the employment of a wireless communication link in the scope of CACC. Due to the additional controller dynamics (3.3), the error dynamics must be extended, to which end the input definition (3.3) can be employed, while substituting the control law (3.4). Then, a dynamic feedback law arises, with dynamics

$$\dot{u}_i = -\frac{1}{h}u_i + \frac{1}{h}(k_p\varepsilon_{i,1} + k_d\varepsilon_{i,2} + k_{dd}\varepsilon_{i,3}) + \frac{1}{h}u_{i-1}, \quad i \in S_m.\tag{3.5}$$

This results in the following closed loop dynamics:

$$\begin{bmatrix} \dot{\varepsilon}_{i,1} \\ \dot{\varepsilon}_{i,2} \\ \dot{\varepsilon}_{i,3} \\ \dot{u}_i \end{bmatrix} = \begin{bmatrix} 0 & 1 & 0 & 0 \\ 0 & 0 & 1 & 0 \\ -\frac{k_p}{h} & -\frac{k_d}{h} & -\frac{k_{dd}+1}{h} & 0 \\ \frac{k_p}{h} & \frac{k_d}{h} & \frac{k_{dd}}{h} & -\frac{1}{h} \end{bmatrix} \begin{bmatrix} \varepsilon_{i,1} \\ \varepsilon_{i,2} \\ \varepsilon_{i,3} \\ u_i \end{bmatrix} + \begin{bmatrix} 0 \\ 0 \\ 0 \\ \frac{1}{h} \end{bmatrix} u_{i-1}, \quad i \in S_m,\tag{3.6}$$

or, in short,

$$\dot{x}_i = Ax_i + Bu_{i-1}, \quad i \in S_m,\tag{3.7}$$

with x_i , A , and B defined accordingly. Note that this system is Hurwitz for $k_p > 0$, $k_d > 0$, $k_{dd} + 1 > 0$, and $k_d(1 + k_{dd}) > k_p\tau$. The analysis of input-to-state stability of these closed-loop dynamics is presented in the next section.

3.1.2 Input-to-state stability¹

The previous section has shown that, with the right controller gains, individual vehicles are asymptotically stable. Additionally, for individual vehicles, bounded inputs must result in bounded system states. Together, these two requirements pose as the requirement of input-to-state-stability of the individual vehicles. If input-to-state-stability of the individual vehicles is achieved, the cascaded string of vehicles is also input-to-state-stable (Khalil, 2002). In this work, the latter is considered a prerequisite before analysing string stability, based on the definition presented in Section 2.2.2.

Even though the closed-loop system (3.7) is linear, this section analyzes input-to-state stability separately. The purpose of this is that useful insights are obtained for the stability analysis of the system including mass estimation, presented in Section 3.2. The following input-to-state stability

¹Unless otherwise specified, all norms used in this section are vector 2-norms.

definition is adopted from Khalil (2002).

Definition (Input-to-state stability) *The system*

$$\dot{x} = f(t, x, u), \quad (3.8)$$

where $f : [0, \infty) \times \mathbb{R}^n \times \mathbb{R}^m \mapsto \mathbb{R}^n$ is piecewise continuous in t and locally Lipschitz in x and u , is said to be input-to-state stable if there exists a class \mathcal{KL} function β and a class \mathcal{K} function γ such that for any initial state $x(t_0)$ and any bounded input $u(t)$, the solution $x(t)$ exists for all $t \geq t_0$ and satisfies

$$\|x(t)\| \leq \beta(\|x(t_0)\|, t - t_0) + \gamma\left(\sup_{t_0 \leq \tau \leq t} \|u(\tau)\|\right). \quad (3.9)$$

Moreover, Khalil (2002) presents the following Lyapunov-like theorem, which gives sufficient conditions for input-to-state stability.

Theorem (Input-to-state stability) *There exist a continuously differentiable function $V : [0, \infty) \times \mathbb{R}^n \rightarrow \mathbb{R}$ such that*

$$\alpha_1(\|x\|) \leq V(t, x) \leq \alpha_2(\|x\|) \quad (3.10)$$

$$\frac{\partial V}{\partial t} + \frac{\partial V}{\partial x} f(t, x, u) \leq -W_3(x), \quad \forall \|x\| \geq \rho(\|u\|) > 0 \quad (3.11)$$

$\forall (t, x, u) \in [0, \infty) \times \mathbb{R}^n \times \mathbb{R}^m$, where α_1, α_2 are class \mathcal{K}_∞ functions, ρ is a class \mathcal{K} function, and W_3 is a continuous positive definite function on \mathbb{R}^n . Then, the system (3.8) is input-to-state stable with $\gamma = \alpha_1^{-1} \circ \alpha_2 \circ \rho$.

Now, consider the Lyapunov function

$$V(x_i) = x_i^T P x_i, \quad (3.12)$$

where P is a 4×4 positive definite matrix. This Lyapunov function satisfies

$$\lambda_{min}^P \|x_i\|^2 \leq x_i^T P x_i \leq \lambda_{max}^P \|x_i\|^2, \quad (3.13)$$

where λ_{min}^P and λ_{max}^P are the minimum and maximum eigenvalues of the matrix P , respectively. Hence, Lyapunov function (3.12) satisfies condition (3.10), with $\alpha_1 = \lambda_{min} \|x_i\|^2$ and $\alpha_2 = \lambda_{max} \|x_i\|^2$. Next, consider the derivative of Lyapunov function (3.12) along the trajectories of (3.7), which is given by

$$\dot{V}(x_i, u_{i-1}) = x_i^T (PA + A^T P) x_i + 2x_i^T P B u_{i-1}. \quad (3.14)$$

Suppose that the controller gains k_p , k_d , and k_{dd} are chosen such that A is Hurwitz, yielding existence of a positive definite matrix P that satisfies the Lyapunov equation $PA + A^T P = -Q$, where Q is a 4×4 identity matrix². This results in

$$\dot{V}(x_i, u_{i-1}) = -x_i^T Q x_i + 2x_i^T P B u_{i-1}. \quad (3.15)$$

Then, substituting $x_i^T Q x_i = \|x_i\|^2$ shows that

$$\begin{aligned} \dot{V}(x_i, u_{i-1}) &\leq -\frac{1}{2} \|x_i\|^2 - \frac{1}{2} \|x_i\|^2 + 2 \|x_i\| \|PB\| \|u_{i-1}\| \\ &\leq -\frac{1}{2} \|x_i\|^2 \quad \forall \|x_i\| \geq 4 \|PB\| \|u_{i-1}\|. \end{aligned} \quad (3.16)$$

² Appendix B shows that input-to-state stability can also be achieved with any other positive definite matrix Q .

From (3.16) it follows that the Lyapunov function (3.12) also satisfies condition (3.11), with $\rho = 4 \|PB\| \|u_{i-1}\|$. Hence, the system (3.7) is input-to-state stable with $\gamma = \alpha_1^{-1} \circ \alpha_2 \circ \rho$. In other words, there exists a t^* such that $\forall t \geq t^*$ it holds that

$$\|x_i(t)\| \leq 2 \|PB\| \|u_{i-1}(t)\|. \quad (3.17)$$

Therefore, it is concluded that bounded u_{i-1} results in bounded x_i and if u_{i-1} converges to zero, so does x_i . Note that input-to-state stability implies that the origin of the unforced system, i.e., with $u_{i-1} = 0$, is globally asymptotically stable (GAS) (Khalil, 2002).

3.1.3 String stability

The definition of string stability, used to analyse the disturbance propagation in a platoon of vehicles with closed loop dynamics (3.7), was presented in Section 2.2. To support the analysis, the closed-loop model of a platoon vehicle is presented in the Laplace domain. The first component of this closed-loop model is the vehicle transfer function

$$G_i(s) = \frac{\bar{a}_i(s)}{\bar{u}_i(s)} = \frac{1}{\tau s + 1}, \quad (3.18)$$

which directly follows from the vehicle model $\dot{\bar{a}}_i(s) = \frac{1}{\tau} \bar{a}_i(s) + \frac{1}{\tau} \bar{u}_i(s)$, see (2.6). Second, the spacing policy transfer function is introduced as $H_i(s) = \bar{\xi}_i(s)/\bar{u}_i(s)$. From (3.3) it follows that this transfer function is given by

$$H_i(s) = \frac{\bar{\xi}_i(s)}{\bar{u}_i(s)} = hs + 1. \quad (3.19)$$

Third, the control law (3.4) consists of a feedback term, with input $\bar{\varepsilon}_{i,1}(s)$, given by

$$K_i(s) = k_p + k_d s + k_{dd} s^2, \quad (3.20)$$

and feedforward $\bar{u}_{i-1}(s)$. This feedforward term is communicated and therefore subject to communication delay θ , represented by the delay transfer function

$$D_i(s) = e^{-\theta s}. \quad (3.21)$$

Together, these transfer functions form the block scheme of a controlled platoon vehicle, as depicted in Figure 3.1. The occurrence of the spacing policy transfer function $H(s)$ in the feedback loop of the block scheme can be easily understood from the error definition (3.1) in the Laplace domain, while substituting (3.19):

$$\begin{aligned} \varepsilon_{i,1}(s) &= \bar{q}_{i-1}(s) - \bar{q}_i(s) - h \bar{v}_i(s) \\ &= \bar{q}_{i-1}(s) - H(s) \bar{q}_i(s). \end{aligned} \quad (3.22)$$

To allow for the analysis of string stability, an output signal must be chosen. In this work, the choice of output signal is $y_i(t) = a_i(t)$. It then directly follows that $\|P_1(s)\|_{\mathcal{H}_\infty} < \infty$, such that condition (2.14a) is satisfied, see Appendix C. Hence, for a homogeneous vehicle platoon model, i.e., $G_i(s) = G_{i-1}(s)$, the only remaining condition for strict \mathcal{L}_2 string stability is

$$\|\Gamma_i(j\omega)\|_{\mathcal{H}_\infty} \leq 1, \quad \forall i \in \mathbb{N} \setminus \{1\}. \quad (3.23)$$

where Γ_i is the complementary sensitivity function, which can be derived from the control structure in Figure 3.1, and is given by

$$\Gamma_i(s) = \frac{\bar{a}_i(s)}{\bar{a}_{i-1}(s)} = \frac{1}{H_i(s)} \frac{D_i(s)s^2 + G_i(s)K_i(s)}{s^2 + G_i(s)K_i(s)}, \quad i \in S_m. \quad (3.24)$$

From (3.24), it follows that the vehicle transfer function $G_i(s)$ and the feedback controller $K_i(s)$ have very limited influence on string stability if $D_i(s)$ is close to 1, i.e., the delay θ is small. Hence,

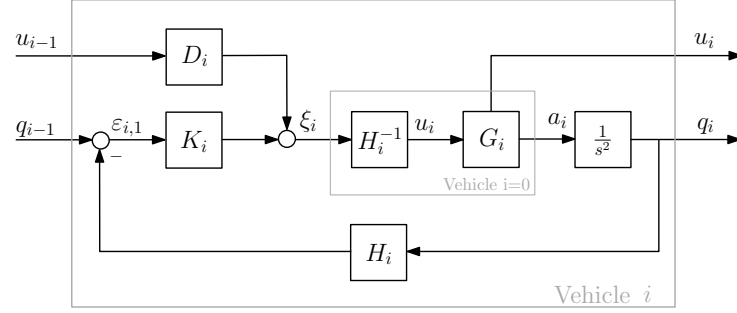
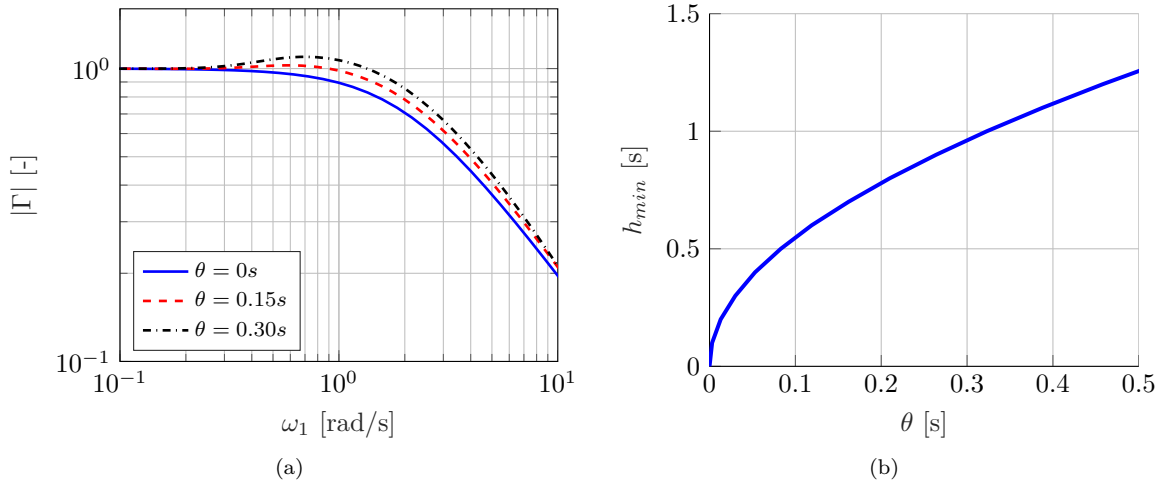


Figure 3.1: Control scheme of a controlled platoon vehicle.


 Figure 3.2: \mathcal{L}_2 string stability properties: (a) string stability complementary sensitivity magnitude $|\Gamma(j\omega)|$ for various communication delays and (b) the minimum time gap h_{min} that yields $\|\Gamma(s)\|_{\mathcal{H}_\infty} \leq 1$, as function of the communication delay θ .

the two main factors influencing string stability are the communication delay θ and the time gap h .

Wireless communication exhibits latency, which was discussed as one of the challenges in Chapter 1. This latency can compromise string stability, as indicated by (3.24). The influence of the communication delay on string stability is illustrated in Figure 3.2a. This figure shows the gain $|\Gamma(j\omega)|$ for several time delays. Here, the controller gains are $k_p = 0.2$, $k_d = 0.7$ and $k_{dd} = 0$, yielding asymptotic stability of the platoon and resulting in comfortable driving behaviour (Ploeg, 2014). Figure 3.2a shows that an increasing time delay yields an increased value of $\|\Gamma(j\omega)\|_{\mathcal{H}_\infty}$.

Additionally, (3.24) shows that increasing the time gap h decreases $\|\Gamma(s)\|_{\mathcal{H}_\infty}$. A more detailed explanation of the influence of the time gap on the string stability is presented in Ploeg (2014). The influence of the time gap h on string stability in the presence of a communication delay is illustrated in Figure 3.2b, showing the minimum time gap h_{min} that yields $\|\Gamma(s)\|_{\mathcal{H}_\infty} \leq 1$, as function of the communication delay θ . The curve shown here is calculated iteratively by taking a fixed value for θ and then searching for the smallest value of h for which $\|\Gamma(s)\|_{\mathcal{H}_\infty} = 1$. Since, the choice of output $y_i(t) = a_i(t)$ yields $\|P_1(s)\|_{\mathcal{H}_\infty} < \infty$, Theorem 2.1 of Ploeg (2014) shows that the given system is strictly \mathcal{L}_2 string stable if $\|\Gamma(s)\|_{\mathcal{H}_\infty} \leq 1$. Hence, Figure 3.2b shows the minimum time gap at a given communication delay, for which the system is \mathcal{L}_2 string stable.

3.2 Mass estimation

So far it was assumed that all vehicle parameters are known. As an extension, this section presents the common CACC approach with the assumption that the vehicle mass is an unknown parameter. As explained in Chapter 1, this is a more realistic assumption in a scenario where vehicles have varying loads, which take up a significant amount of the total mass, e.g., buses or trucks. First, the closed-loop dynamics are derived, followed by the analysis of individual vehicle stability.

3.2.1 Closed loop dynamics

To address the control problem where the mass m_i is unknown, this section presents a controller design based on the estimated mass \hat{m}_i , which is updated dynamically.

Let $\tilde{m}_i(t) = \hat{m}_i(t) - m_i$ denote the mass estimation error. Moreover, it is assumed that m_i only changes during full stops of the vehicle, such that $\dot{\tilde{m}}_i = \dot{\hat{m}}_i$ if the vehicle drives. Since, the input transformation (2.5) is part of the controller and the actual mass is assumed to be unknown, the input transformation now uses the estimated mass and is given by

$$\eta_i = \hat{m}_i u_i + K_d v_i^2 + d_m + 2K_d \tau v_i a_i, \quad i \in S_m. \quad (3.25)$$

This results in the vehicle model

$$\begin{aligned} \dot{q}_i &= v_i \\ \dot{v}_i &= a_i \\ \dot{a}_i &= -\frac{1}{\tau} a_i + \frac{1}{\tau} u_i + \frac{1}{\tau} \frac{\tilde{m}_i}{m_i} u_i, \quad i \in S_m. \end{aligned} \quad (3.26)$$

Then, defining the error variables as

$$\begin{aligned} \varepsilon_{i,1} &:= q_{i-1} - q_i - h v_i - r_i \\ \varepsilon_{i,2} &:= \dot{\varepsilon}_{i,1} = v_{i-1} - v_i - h a_i \\ \varepsilon_{i,3} &:= \dot{\varepsilon}_{i,2} + \frac{h}{\tau} \frac{\tilde{m}_i}{m_i} u_i = a_{i-1} - (1 - \frac{h}{\tau}) a_i - \frac{h}{\tau} u_i, \quad i \in S_m, \end{aligned} \quad (3.27)$$

results in the error dynamics

$$\begin{aligned} \dot{\varepsilon}_{i,1} &= \varepsilon_{i,2} \\ \dot{\varepsilon}_{i,2} &= \varepsilon_{i,3} - \frac{h}{\tau} \frac{\tilde{m}_i}{m_i} u_i \\ \dot{\varepsilon}_{i,3} &= -\frac{1}{\tau} \varepsilon_{i,3} - \frac{1}{\tau} (1 - \frac{h}{\tau}) \frac{\tilde{m}_i}{m_i} u_i - \frac{1}{\tau} \xi_i + \frac{1}{\tau} u_{i-1} + \frac{1}{\tau} \frac{\tilde{m}_{i-1}}{m_{i-1}} u_{i-1}, \quad i \in S_m, \end{aligned} \quad (3.28)$$

where ξ_i can be seen as the new input to vehicle i and is again given by $\xi_i = h \dot{u}_i + u_i$. Notice from (3.28) that \tilde{m}_{i-1} is required to analyze these error dynamics. As explained in the previous chapter, heterogeneity due to different controllers is not considered in the scope of this work. In other words, it is assumed that all vehicles $i \in S_m$ have equal mass estimation laws and \tilde{m}_{i-1} is an additional input. The same control law as in the previous section is used to stabilize these dynamics. This means that the control law for ξ_i is chosen as (3.4), yielding a dynamic controller, with dynamics

$$\dot{u}_i = -\frac{1}{h} u_i + \frac{1}{h} (k_p \varepsilon_{i,1} + k_d \varepsilon_{i,2} + k_{dd} \varepsilon_{i,3}) + \frac{1}{h} u_{i-1}, \quad i \in S_m. \quad (3.29)$$

Moreover, the update law for \hat{m}_i is defined as follows.

$$\dot{\hat{m}}_i = c_1 \varepsilon_{i,1} u_i + c_2 \varepsilon_{i,2} u_i + c_3 \varepsilon_{i,3} u_i, \quad i \in S_m, \quad (3.30)$$

where c_i , $i = 1, 2, 3$, are control constants. This particular choice of update law and the definition of the control constants is based on the stability analysis, as will become clear in the next section.

Then, the closed-loop system dynamics are given by

$$\begin{aligned}
 \dot{\varepsilon}_{i,1} &= \varepsilon_{i,2} \\
 \dot{\varepsilon}_{i,2} &= \varepsilon_{i,3} - \frac{h}{\tau} \frac{\tilde{m}_i}{m_i} u_i \\
 \dot{\varepsilon}_{i,3} &= -\frac{1}{\tau} (k_p \varepsilon_{i,1} + k_d \varepsilon_{i,2} + (k_{dd} + 1) \varepsilon_{i,3}) - (1 - \frac{h}{\tau}) \frac{\tilde{m}_i}{\tau m_i} u_i + \frac{\tilde{m}_{i-1}}{\tau m_{i-1}} u_{i-1} \\
 \dot{u}_i &= -\frac{1}{h} u_i + \frac{1}{h} (k_p \varepsilon_{i,1} + k_d \varepsilon_{i,2} + k_{dd} \varepsilon_{i,3}) + \frac{1}{h} u_{i-1} \\
 \dot{\tilde{m}}_i &= c_1 u_i \varepsilon_{i,1} + c_2 u_i \varepsilon_{i,2} + c_3 u_i \varepsilon_{i,3}, \quad i \in S_m.
 \end{aligned} \tag{3.31}$$

Adopting $k_{dd} = 0$, the steady-state solution of (3.31) is given by

$$\begin{aligned}
 \varepsilon_{i,1,eq} &= -\frac{c_3 h \tilde{m}_{i-1} u_{i-1}}{m_{i-1} (c_1 \tau - c_3 h k_p)} \\
 \varepsilon_{i,2,eq} &= 0 \\
 \varepsilon_{i,3,eq} &= \frac{c_1 h \tilde{m}_{i-1} u_{i-1}}{m_{i-1} (c_1 \tau - c_3 h k_p)} \\
 u_{i,eq} &= -u_{i-1} \frac{c_3 h k_p m_{i-1} - c_1 \tau m_{i-1} + c_3 h k_p \tilde{m}_{i-1}}{m_{i-1} (c_1 \tau - c_3 h k_p)} \\
 \tilde{m}_{i,eq} u_{i-1} &= -m_i u_{i-1} \frac{c_1 \tau \tilde{m}_{i-1}}{c_3 h k_p m_{i-1} - c_1 \tau m_{i-1} + c_3 h k_p \tilde{m}_{i-1}}, \quad i \in S_m.
 \end{aligned} \tag{3.32}$$

Note that these expressions give an infinite number of equilibrium values for $\tilde{m}_{i,eq}$ when $u_{i-1} = 0$.

3.2.2 Individual vehicle stability

For the individual vehicle stability analysis, consider the unforced system, i.e., $u_{i-1} = 0$, and $\tilde{m}_{i-1} = 0$:

$$\begin{aligned}
 \dot{\varepsilon}_{i,1} &= \varepsilon_{i,2} \\
 \dot{\varepsilon}_{i,2} &= \varepsilon_{i,3} - \frac{h}{\tau} \frac{\tilde{m}_i}{m_i} u_i \\
 \dot{\varepsilon}_{i,3} &= -\frac{1}{\tau} (k_p \varepsilon_{i,1} + k_d \varepsilon_{i,2} + (k_{dd} + 1) \varepsilon_{i,3}) - (1 - \frac{h}{\tau}) \frac{\tilde{m}_i}{\tau m_i} u_i \\
 \dot{u}_i &= \frac{1}{h} (k_p \varepsilon_{i,1} + k_d \varepsilon_{i,2} + k_{dd} \varepsilon_{i,3}) - \frac{1}{h} u_i \\
 \dot{\tilde{m}}_i &= c_1 u_i \varepsilon_{i,1} + c_2 u_i \varepsilon_{i,2} + c_3 u_i \varepsilon_{i,3}, \quad i \in S_m.
 \end{aligned} \tag{3.33}$$

Denote $x = [\varepsilon_{i,1}, \varepsilon_{i,2}, \varepsilon_{i,3}, u_i, \tilde{m}_i]^T$, $A = \begin{bmatrix} 0 & 1 & 0 \\ 0 & 0 & 1 \\ -\frac{k_p}{\tau} & -\frac{k_d}{\tau} & -\frac{k_{dd}+1}{\tau} \\ \frac{1}{h} & \frac{1}{h} & \frac{1}{h} \\ c_1 & c_2 & c_3 \end{bmatrix}$, suppose that the controller gains are chosen such that A is Hurwitz and let $\bar{P} = P^T > 0$ be such that $PA + A^T P = -Q$ with $Q = Q^T > 0$. Furthermore, let

$$[c_1 \quad c_2 \quad c_3] = -\tilde{\gamma}_i \left[0 \quad -\frac{h}{\tau} \quad -(1 - \frac{h}{\tau}) \frac{1}{\tau} \right] P, \tag{3.34}$$

where $\tilde{\gamma}_i = \frac{2}{\gamma_i \tilde{m}_i}$ and $\gamma_i > 0$ is a control constant. The particular choices for c_i , $i = 1, 2, 3$, and update law (3.30) are motivated by the following stability analysis, since these choices enable to come to a conclusion on the convergence of the system states, using the standard Lyapunov function

$$V(\varepsilon, u_i, \tilde{m}_i) = \varepsilon^T P \varepsilon + \frac{\alpha}{2} u_i^2 + \frac{\gamma_i}{2} \tilde{m}_i^2, \quad (3.35)$$

where $\varepsilon = [\varepsilon_{i,1}, \varepsilon_{i,2}, \varepsilon_{i,3}]^T$ and $\alpha > 0$ is a constant. Differentiating this Lyapunov function with respect to time, along the solutions of (3.33), while utilizing (3.30) and (3.34) results in

$$\begin{aligned} \dot{V}(\varepsilon, u_i, \tilde{m}_i) &= -\varepsilon^T Q \varepsilon + \frac{\alpha}{h} u_i [k_p \quad k_d \quad k_{dd}] \varepsilon - \frac{\alpha}{h} u_i^2 \\ &\leq -\lambda_{min}^Q \|\varepsilon\|^2 + \frac{\alpha}{h} \|k\| |u_i| \|\varepsilon\| - \frac{\alpha}{h} |u_i|^2, \end{aligned} \quad (3.36)$$

where $k = [k_p \quad k_d \quad k_{dd}]$. This time derivative is a negative definite quadratic form in $\|\varepsilon\|$ and $|u_i|$ for $0 < \alpha < \frac{4\lambda_{min}^Q h}{\|k\|^2}$, see Appendix D, yielding it negative semi-definite because \tilde{m}_i does not appear on the right-hand side. Since the Lyapunov function (3.35) is radially unbounded, the set $\Omega_c = \{x \in \mathbb{R}^5 \mid V(\varepsilon, u_i, \tilde{m}_i) \leq c\}$ is compact and positively invariant, for every $c > 0$. The set of points where $\dot{V}(\varepsilon, \tilde{m}_i) = 0$ is given by $E = \{x \in \Omega_c \mid \varepsilon = 0, u_i = 0\}$, which is invariant because the dynamics (3.33) show that in this set $\dot{\tilde{m}}_i = 0$. Then LaSalle's theorem (Khalil, 2002) shows that all solutions starting in Ω_c approach E as $t \rightarrow \infty$. Hence, the following can be concluded on the convergence of the system states:

$$\lim_{t \rightarrow \infty} \varepsilon(t) = 0, \quad \lim_{t \rightarrow \infty} u_i(t) = 0, \quad \lim_{t \rightarrow \infty} \tilde{m}_i(t) = \bar{m}_i, \quad (3.37)$$

where \bar{m}_i is some constant. Moreover, since the Lyapunov function (3.35) is radially unbounded, the conclusion hold for all initial conditions. This is true because for any $x(0)$, the constant c can be chosen large enough such that $x(0) \in \Omega_c$. Analysis of the forced system (3.31), i.e., with $u_{i-1} \neq 0$ and $\tilde{m}_i \neq 0$, is done by means of simulations, which are presented in the next section.

3.3 Platoon simulations

To illustrate the effectiveness and analyse the tracking behaviour of the common CACC approach, this section presents simulations of a vehicle platoon. As introduced in Chapter 2, three scenario's are followed. Firstly, Section 3.3.1 presents the results of simulations in a scenario of regular platooning, with a focus on string stability. These simulations are included to be able to compare them to the results of the simulations presented in the subsequent sections and to the alternative approach. Secondly, Section 3.3.2 analyzes the performance of the CACC approach in a heterogeneous vehicle platoon. Finally, Section 3.3.3 discusses the simulation results when it is assumed that the vehicle mass is unknown.

The platoon considered in this section consists of four vehicles with index $i = 1, 2, 3, 4$. These vehicles are described by the dynamics (2.4), input transformation (2.5) and dynamic controller (3.5). The first platoon vehicle follows virtual vehicle with index $i = 0$, which has the same vehicle dynamics but no feedback control, as indicated in Figure 3.1. The system parameters are adopted from the vehicles at 2getthere B.V. and given in Table 3.1. Unless otherwise indicated, the control parameters are as specified by Table 3.2. These controller gains are adopted from Ploeg (2014) and result in individual vehicle stability as well as comfortable driving behaviour. The time gap $h = 0.5$ s guarantees string stability at a communication delay of $\theta = 0.02$ s, see Section 3.1.3. Since the aim of the CACC approach is to drive at a close inter-vehicle distance, while achieving string stability, the simulations focus on the performance without initial position errors, i.e., $q_i(0) = -10 \cdot i$ m, $v_i(0) = 0$, $a_i(0) = 0$, $u_i(0) = 0$. For the following two sections, Section 3.3.1 and Section 3.3.2, the reference acceleration is specified by

$$u_0 = \begin{cases} 2, & 0 < t < 4, \\ -2, & 40 < t < 42, \\ 0, & 52 < t < 54, \\ 0, & \text{otherwise.} \end{cases} \quad (3.38)$$

Table 3.1: Vehicle system parameters

Parameter	Symbol	Value	Unit
Tare mass	m_i	4500	kg
Crush load	m_{crush}	2000	kg
Air resistance coefficient	K_d	1.40	-
Mechanical drag coefficient	d_m	0.01	-
communication delay	θ	0.02	s
Engine time constant	τ	0.10	s
Maximum velocity	$v_{i,max}$	11.11	m/s

Table 3.2: Control parameters

Parameter	Symbol	Value	Unit
Desired inter-vehicle distance	r_i	10	m
Spacing policy time gap	h	0.5	s
Proportional feedback gain	k_p	0.2	-
Derivative feedback gain	k_d	0.7	-
Double derivative feedback gain	k_{dd}	0.0	-

3.3.1 Regular platooning

The complementary sensitivity transfer function from Section 3.1.3, with initial condition $x(0) = 0$, is given by: $\Gamma(j\omega) = a_i(t)/a_{i-1}(t)$, which is stable and strictly proper for the adopted controller gains. Assume that the input $a_i(t) \in \mathcal{L}_2$ and output $a_{i-1}(t) \in \mathcal{L}_2$ are piecewise continuous. Then Doyle et al. (1990) (p18) show that the output is bounded according to

$$\|a_{i-1}(t)\|_{\mathcal{L}_2} \leq \|\Gamma(j\omega)\|_{\mathcal{H}_\infty} \|a_i(t)\|_{\mathcal{L}_2}, \quad (3.39)$$

and that there exists an input signal $a_i(t)$ for which (3.39) becomes an equality. Then, it follows that

$$\|\Gamma(j\omega)\|_{\mathcal{H}_\infty} = \max_{a_i(t) \neq 0} \frac{\|a_{i-1}(t)\|_{\mathcal{L}_2}}{\|a_i(t)\|_{\mathcal{L}_2}}, \quad (3.40)$$

which means that \mathcal{L}_2 (strict) string stability is guaranteed if

$$\max_{a_i(t) \neq 0} \frac{\|a_{i-1}(t)\|_{\mathcal{L}_2}}{\|a_i(t)\|_{\mathcal{L}_2}} \leq 1. \quad (3.41)$$

Notice that the output response to all possible inputs (except $a_i(t) = 0$) must be tested, to assess \mathcal{L}_2 (strict) string stability. This is not possible because there are an infinite number of possible inputs. Therefore, string stability cannot be guaranteed in general, as was done in Section 3.1.3, but only for the specific input that is used in the simulation. The accelerations a_i of the platoon simulation are presented in Figure 3.3a and the corresponding 2-norms are given in Table 3.3. These 2-norms are decreasing over the vehicle index, indicating that, conform expectation, the platoon is string stable for the chosen settings.

Since the reference acceleration converges to zero, the errors $\varepsilon(t)$ also converge to zero, as was shown in Section 3.1.2. Figure 3.3b presents the tracking errors $\varepsilon_{i,1}$ and confirms that these converge to zero. However, the vehicles do have a tracking error during acceleration and deceleration. These tracking errors are a direct consequence of the communication delay θ . If no communication delay is present the tracking errors are (approximately) zero throughout the simulation.

3.3.2 Heterogeneity

This section illustrates the performance of the common CACC approach in two different heterogeneous scenarios. First, an example is presented of a vehicle platoon which is heterogeneous with

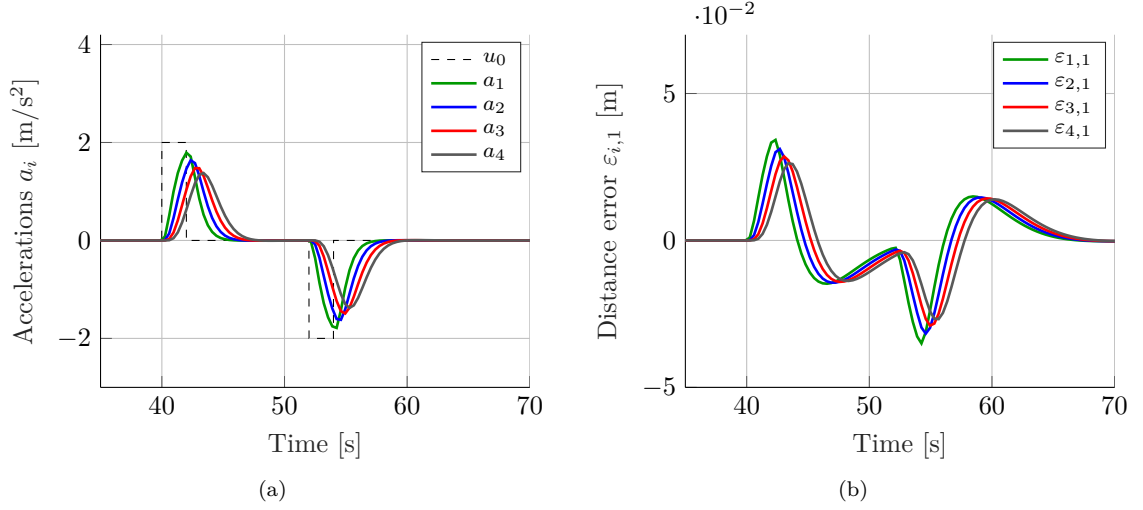

 Figure 3.3: Response of (a) the accelerations a_i and (b) the position errors $\varepsilon_{i,1}$.

 Table 3.3: Regular platooning: acceleration norms calculated over the simulation time $t = [0 \ 70]$.

vehicle index	Norm value
$\ a_1\ _2$	48.4011
$\ a_2\ _2$	46.5709
$\ a_3\ _2$	45.0998
$\ a_4\ _2$	43.8659

respect to the driveline dynamics. Thereafter, an example is presented of a vehicle platoon which is heterogeneous with respect to acceleration limits.

Different driveline dynamics

In the considered heterogeneous platoon, all vehicles are the same as previously discussed except the second vehicle which now has an engine time constant, representing the driveline dynamics, of $\tau_2 = 1.0$ s. Even though the differences between platoon vehicles are usually smaller in a realistic scenario, this example is used because it clearly illustrates the differences between the alternative and the common approach. Moreover, the initial conditions, system parameters, control parameters and reference acceleration remain the same as in the previous section. Because of the large difference between the driveline dynamics in this example it is expected that the common CACC approach is not able to maintain string stability and has tracking errors which are significantly larger than the errors obtained in the previous section.

Figures 3.4a and 3.4b present the response of the acceleration a_i and the position errors $\varepsilon_{i,1}$, respectively. Conform expectations, these figures show large tracking errors and clearly illustrate that the platoon is not string stable. In other words, in the presented example of a platoon which is heterogeneous with respect to the driveline dynamics, the common approach is not able to achieve the control objectives.

Different acceleration limits

So far, it was assumed that there are no limitations on the achievable accelerations of the platoon vehicles, such that the continuous model (2.6) accurately describes the vehicles. In reality, the vehicle engines can only produce forces up to a certain maximum, which directly limits the achievable acceleration, cf. (2.1a). This section investigates the behaviour of a platoon that is het-

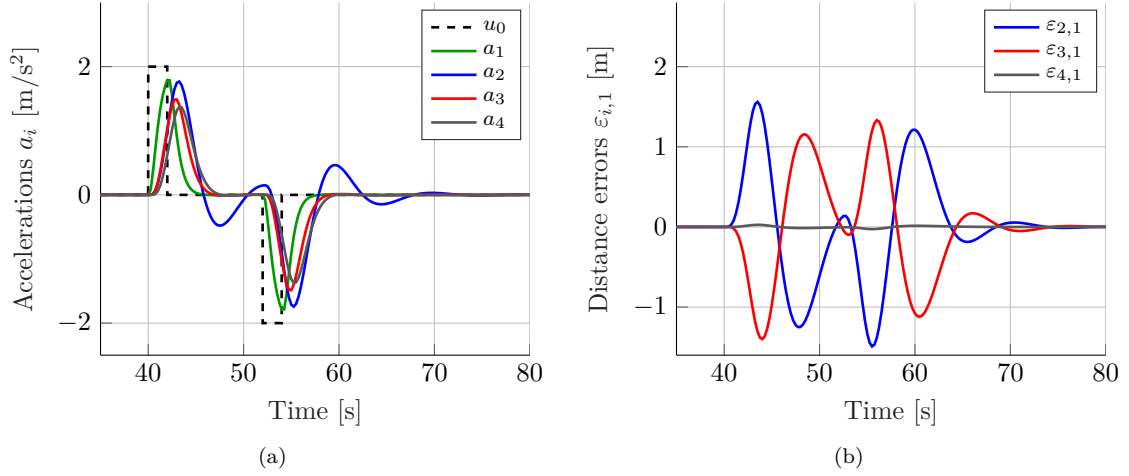


Figure 3.4: Simulation results of a platoon with different driveline dynamics, response of: (a) the accelerations a_i and (b) the tracking errors $\varepsilon_{i,1}$.

erogeneous with respect to these acceleration limits. This can, for instance, be caused by different loads in identical vehicles. To this end, vehicle $i = 2$ has a maximum acceleration of $a_{2,max} = 1.5 \text{ m/s}^2$, such that $a_2 = a_{2,max}$ if this maximum is reached. For $a_2(t) < a_{2,max}$ and vehicles $i \neq 2$, the dynamics are given by continuous model (2.6). The initial conditions, system parameters, control parameters and reference acceleration remain the same as in Section 3.3.1. The considered example results in differences between the desired acceleration u_2 and the actual acceleration a_2 of the second vehicle. Therefore, the expectation is that the vehicle platoon does not exhibit strictly string stable behaviour, resulting in large positions errors.

Figure 3.5a and Figure 3.5b present the response of the acceleration a_i and the position errors $\varepsilon_{i,1}$, respectively. As mentioned, the maximum acceleration limit of the second vehicle yields a_2 to be lower than would be expected from u_2 . Because u_{i-1} is used as feedforward, the acceleration of the third vehicle is larger than that of the second vehicle. This behaviour is clearly illustrated in Figure 3.5a, which indicates that the platoon is not strictly string stable.

Figure 3.5b shows that the second vehicle has a positive distance error. This is expected because its acceleration is limited. Moreover, because u_{i-1} is communicated instead of a_{i-1} , the third vehicle is unaware of the acceleration limitations in the second vehicle. This results in a significant tracking error for the third vehicle. Note that the tracking error of the third vehicle is negative, which means that the vehicle drives closer to its predecessor than desired. This illustrates that acceleration limitations can result in dangerous driving behaviour.

3.3.3 Mass estimation

Section 3.2.2 has shown that for $u_{i-1} = 0$ and $\tilde{m}_{i-1} = 0$, the states $\varepsilon(t)$ and $u_i(t)$ converge to zero, while $\hat{m}_i(t)$ converges to a constant value. The aim of this section is to investigate the system behaviour, for $u_{i-1} \neq 0$ and $\tilde{m}_{i-1} \neq 0$, via simulations. For these simulations the controller gains are re-tuned, which now also includes tuning for the mass estimation update gain $\tilde{\gamma}_i$. The gains are tuned with the aim of realizing a settling time of the mass estimates $t_s \leq 11 \text{ s}$, such that convergence is achieved before the maximum velocity is exceeded. Additionally, the gains k_p , k_d , and $\tilde{\gamma}_i$ are kept as small as possible, to realize comfortable driving behaviour. The resulting controller gains are: $k_p = 0.8$, $k_d = 2.8$, $k_{dd} = 0$, and $\tilde{\gamma}_i = 50$.

Since the vehicle mass is unknown and can vary between the tare mass of 4500 kg and the tare mass plus crush load of 2000 kg, the initial mass estimates are chosen as $\hat{m}_i(0) = 5500 \text{ kg}$, to minimize $\tilde{m}_i(0)$. All other system parameters, control parameters and initial conditions are the same as previously discussed. Hence, all vehicles have initial conditions $q_i(0) = -10 \cdot i \text{ m}$,

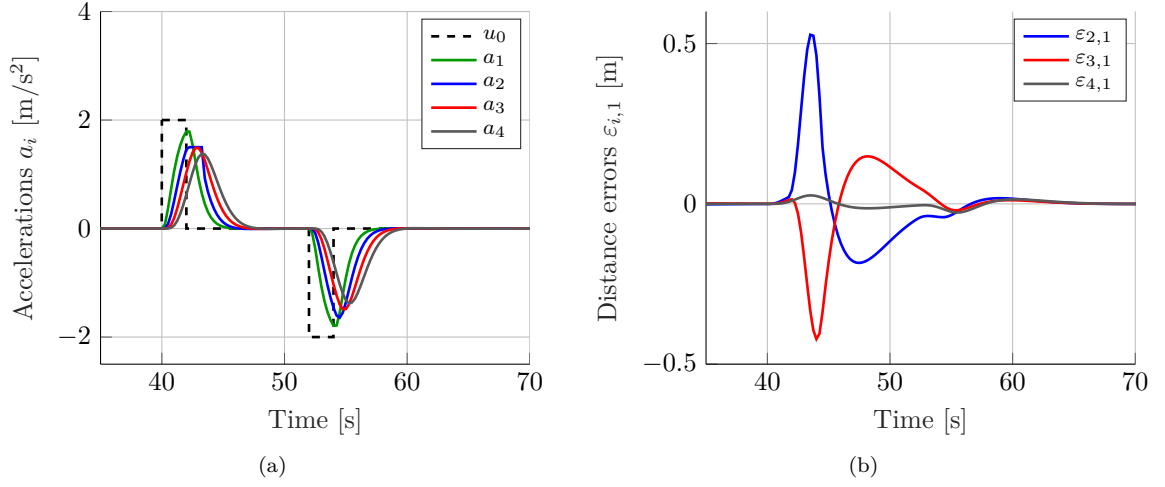


Figure 3.5: Simulation results with acceleration limitations on the second vehicle, response of: (a) the accelerations a_i and (b) the tracking errors $\varepsilon_{i,1}$.

$v_i(0) = 0$, $a_i(0) = 0$, $u_i(0) = 0$, and $\hat{m}_i(0) = 5500$ kg.

The virtual leader follows a reference acceleration of $u_0 = 1.0$ m/s^2 for $0 < t \leq 11$. After this period, the vehicles drive just below their maximum velocities, such that the model (3.31) accurately describes the dynamic behaviour of the vehicles. For the remainder of the simulation the reference acceleration is given by $u_0 = -2.0$ m/s^2 for $40 < t \leq 42$, $u_0 = 2.0$ m/s^2 for $52 < t \leq 54$ and $u_0 = 0$ for all other time intervals. The model of the virtual leader is given by (2.6), yielding $\tilde{m}_{i-1} = 0$ for vehicle $i = 1$. Then (3.32) shows that for a constant $u_0 \neq 0$, the equilibrium point is given by $\tilde{m}_{1,eq} = 0$. A similar reasoning holds for the vehicles $i = 2, 3, 4$. Figure 3.6a presents the mass estimates obtained in the platoon simulations. These simulations show that (near) convergence to $\tilde{m}_{i,eq}$ is achieved during the first constant acceleration period. Since $\tilde{m}_i \approx 0$ after this period, the mass estimates are fixed for $t > 11$ s.

The string stability analysis presented in Section 3.1.3 is not valid if $\tilde{m}_i \neq 0$. Therefore, string stability is analysed by means of simulations. Figure 3.7 shows that a_i is smooth and has a decreasing amplitude over the vehicle index. To investigate string stability, the 2-norms of the acceleration signals are given in Table 3.4a. These values show that $\|a_i\|_2$ is decreasing over the vehicle index, from which it is concluded that the platoon is string stable for this specific scenario. Since u_0 captures a wide range of frequencies, this simulation gives a strong indication that the platoon is string stable in general. However, using time domain simulations, string stability cannot be guaranteed.

Figure 3.6b shows the obtained tracking errors. The overall effect of assuming an unknown mass appears to have little influence on the tracking performance. This can be explained by the effectiveness of the mass estimation and by the robustness of the controller to external disturbances, as explained in Appendix E. Table 3.4b shows $\|\varepsilon_{i,1}\|_2$ for the presented simulation and compares these with the case without update law, which means that the estimates are $\hat{m}_i = 5500$ kg throughout the simulation. These error norms confirm that the mass estimation has very limited influence on the tracking performance.

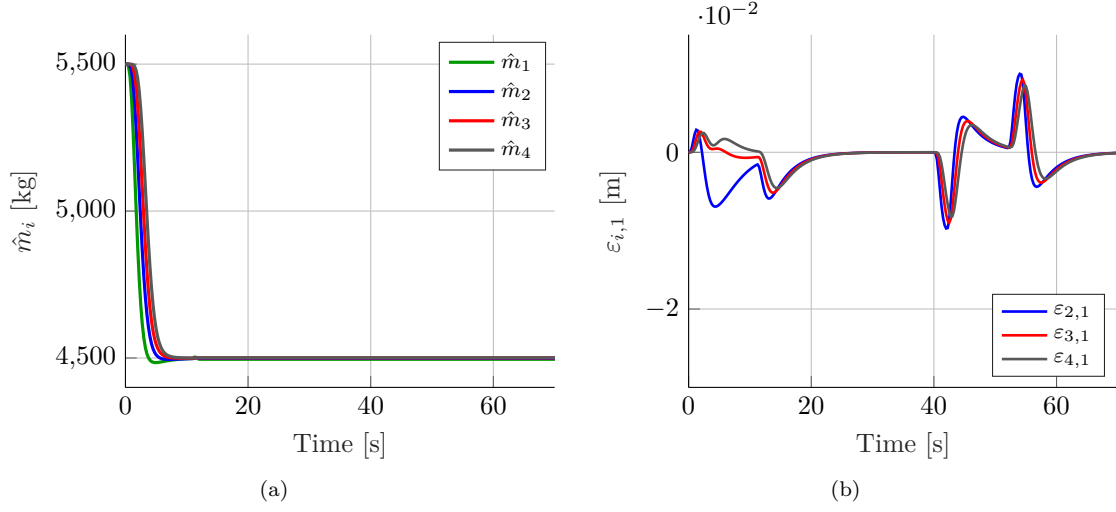
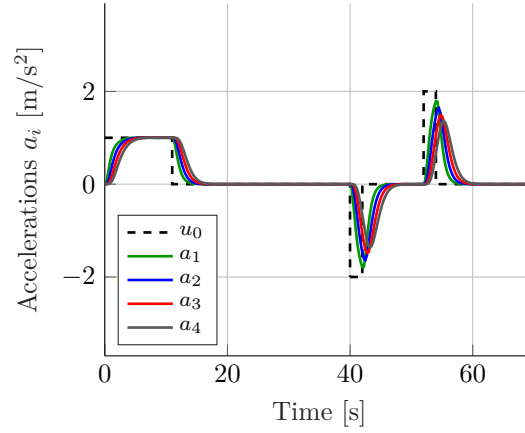

 Figure 3.6: Simulation results (a) mass estimates \hat{m}_i and (b) distance errors $\varepsilon_{i,1}$.

 Figure 3.7: Reference acceleration u_0 and the response of accelerations a_i .

 Table 3.4: Results of the simulations including mass estimation, calculated over the simulation time $t = [0 \ 80]$: (a) acceleration norms and (b) average of the distance error signal 2-norms $\|\varepsilon_{i,1}\|_2$, over all vehicles.

vehicle index	Norm value
$\ a_1\ _2$	45.2752
$\ a_2\ _2$	43.7745
$\ a_3\ _2$	42.5998
$\ a_4\ _2$	41.6434

(a)

Case	$\ \varepsilon_{i,1}\ _2$
1. With mass estimate \hat{m}_i	0.2254
3. No mass estimate \hat{m}_i	0.1796

(b)

3.4 Summary

This chapter started in Section 3.1 with the design and stability analyses of the common CACC approach. Thereafter, in Section 3.2, this approach was extended with the assumption that the vehicle mass is unknown. An adaptive mass estimation law was presented such that the CACC

approach achieves the vehicle-following objective, while indicating string stable behaviour without *a priori* knowledge of the vehicle mass. The effectiveness of the presented CACC approach was further illustrated by means of platoon simulations in Section 3.3. Using platoon simulations, this section analyzed the performance of the common CACC approach in a scenario of regular platooning, a scenario of heterogeneous platooning, and a scenario where vehicles have unknown masses.

Chapter 4

Cooperative adaptive cruise control: an alternative approach

In literature, CACC approaches often use the desired acceleration of preceding vehicles as control input. An example of such a common CACC approach was presented in the previous chapter. It was shown that, as a direct consequence of using this desired acceleration, knowledge of the dynamics of a predecessor vehicle is required in order to guarantee string stability. Because this knowledge is often not available, homogeneity of the platoon is commonly assumed, see, e.g., Ioannou and Chien (1993); Swaroop and Hedrick (1996); Ploeg (2014). However, in a scenario of *ad hoc* platooning, this is not always a realistic assumption.

To allow for *ad hoc* platooning within a heterogeneous vehicle platoon, without requiring exact knowledge of the dynamic behaviour and limitations of a predecessor, this chapter presents a novel alternative CACC approach. This alternative CACC approach uses the realized acceleration instead of the desired acceleration of its predecessor as input. As a consequence, no knowledge of the dynamics of its predecessor is required to guarantee string stability and differences between the desired and realized accelerations of a predecessor do not compromise safe driving behaviour.

The organisation of this chapter is as follows: Section 4.1 presents the design of the novel alternative cooperative adaptive cruise controller and analyzes both individual vehicle stability and string stability. Section 4.2 extends this CACC approach with the assumption that the vehicle mass is unknown and presents the corresponding controller design and stability analyses. Section 4.3 illustrates the effectiveness of the proposed CACC approach by means of platoon simulations. These simulations follow again the three scenarios: regular platooning, heterogeneous platooning, and platooning with unknown vehicle masses. Finally, Section 4.4 summarizes the main conclusions.

4.1 Controller design

This section first presents the design of the alternative CACC approach, in which platoon vehicles use the realized acceleration of their predecessor as input. Thereafter, the analyses of individual vehicle stability and string stability are presented.

4.1.1 Closed-loop dynamics

The difference between the proposed alternative CACC approach and the common CACC approach presented in the previous chapter originates in the definition of the error variables. These error

variables are now defined as follows.

$$\varepsilon_{i,1} := q_{i-1} - q_i - hv_i - r_i \quad (4.1a)$$

$$\varepsilon_{i,2} := \dot{\varepsilon}_{i,1} = v_{i-1} - v_i - ha_i \quad (4.1b)$$

$$\varepsilon_{i,3} := v_{i-1} - v_i, \quad i \in S_m. \quad (4.1c)$$

Here, the distance error (4.1a) and velocity error (4.1b) remain unchanged, but $\varepsilon_{i,3}$ is now given by (4.1c). The motivation behind this definition is that a stabilizing controller can be formulated based on these variables, which uses a_{i-1} instead of u_{i-1} as feedforward input, as becomes clear in the remainder of this section. Differentiating the error variables, while substituting the longitudinal vehicle dynamics (2.6), results in the following error dynamics.

$$\begin{aligned} \dot{\varepsilon}_{i,1} &= \varepsilon_{i,2} \\ \dot{\varepsilon}_{i,2} &= a_{i-1} - \left(1 - \frac{h}{\tau_i}\right)a_i - \frac{h}{\tau_i}u_i \\ \dot{\varepsilon}_{i,3} &= a_{i-1} - \frac{\varepsilon_{i,3} - \varepsilon_{i,2}}{h}, \quad i \in S_m. \end{aligned} \quad (4.2)$$

Next, choose the input u_i as

$$u_i := \frac{\tau_i}{h}\xi_i + \left(1 - \frac{\tau_i}{h}\right)a_i, \quad i \in S_m, \quad (4.3)$$

where ξ_i is an auxiliary input, which results in

$$\begin{aligned} \dot{\varepsilon}_{i,1} &= \varepsilon_{i,2} \\ \dot{\varepsilon}_{i,2} &= a_{i-1} - \xi_i \\ \dot{\varepsilon}_{i,3} &= a_{i-1} - \frac{\varepsilon_{i,3} - \varepsilon_{i,2}}{h}, \quad i \in S_m. \end{aligned} \quad (4.4)$$

These dynamics clearly show that the auxiliary input ξ_i should be used to stabilize the error dynamics while compensating for the input a_{i-1} of the preceding vehicle in order to satisfy the vehicle following control objective. Hence, the control law for ξ_i is chosen as follows.

$$\xi_i := K \begin{bmatrix} \varepsilon_{i,1} \\ \varepsilon_{i,2} \\ \varepsilon_{i,3} \end{bmatrix} + a_{i-1}, \quad i \in S_m, \quad (4.5)$$

with $K := (k_p \ k_d \ k_{dd})$. Note that, as opposed to the common approach, the control law now uses a_{i-1} instead of u_{i-1} as feedforward input. This input is obtained through wireless communication with the preceding vehicle and the reason for the employment of a wireless communication link in the scope of CACC. The resulting closed loop dynamics are given by

$$\begin{bmatrix} \dot{\varepsilon}_{i,1} \\ \dot{\varepsilon}_{i,2} \\ \dot{\varepsilon}_{i,3} \end{bmatrix} = \begin{bmatrix} 0 & 1 & 0 \\ -k_p & -k_d & -k_{dd} \\ 0 & \frac{1}{h} & -\frac{1}{h} \end{bmatrix} \begin{bmatrix} \varepsilon_{i,1} \\ \varepsilon_{i,2} \\ \varepsilon_{i,3} \end{bmatrix} + \begin{bmatrix} 0 \\ 0 \\ 1 \end{bmatrix} a_{i-1}, \quad i \in S_m, \quad (4.6)$$

or, in short,

$$\dot{x}_i = Ax_i + Ba_{i-1}, \quad i \in S_m, \quad (4.7)$$

with x_i , A , and B defined accordingly. From now on $k_{dd} = 0$, resulting in a Hurwitz system for $k_p > 0$ and $k_d > 0$. The analysis of input-to-state stability of these closed-loop dynamics is presented in the section below.

4.1.2 Input-to-state stability

To show that the closed-loop dynamics (4.7) are input-to-state stable, the exact analysis as presented in Section 3.1.2 can be followed. The only difference is that the matrix P is now a 3×3 positive definite matrix and Q is the 3×3 identity matrix because the system (4.7) is of third order. Here it is again assumed that the control gains are chosen such that A is Hurwitz. Hence, the system (4.7) is input-to-state stable, which also implies that the origin of the unforced system, i.e., with $a_{i-1} = 0$, is globally asymptotically stable (GAS) (Khalil, 2002). Therefore, it can be concluded that bounded a_{i-1} results in bounded x_i and if a_{i-1} converges to zero, so does x_i .

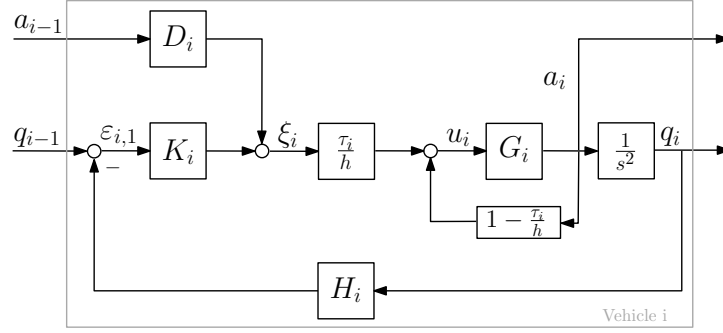


Figure 4.1: Control scheme of a controlled platoon vehicle in the alternative CACC approach.

4.1.3 String stability

The definition of string stability, used to analyse the disturbance propagation in a platoon of vehicles with closed loop dynamics (4.7), was presented in Section 2.2. To support the analysis, the closed-loop model of a platoon vehicle, utilizing the alternative approach, is presented in the Laplace domain. The vehicle transfer function $G_i(s)$, spacing policy transfer function $H_i(s)$, delay transfer function $D_i(s)$, and feedback controller transfer function $K_i(s)$ are defined equal to those presented in the previous chapter. The difference with the block diagram of the common approach comes from the definition of the control inputs u_i and ξ_i . From (4.3) it follows that u_i is, in Laplace domain, now given by

$$\bar{u}_i(s) = \frac{\tau_i}{h} \bar{\xi}_i(s) + (1 - \frac{\tau_i}{h}) \bar{a}_i(s), \quad i \in S_m, \quad (4.8)$$

and from (4.5) it follows that ξ_i , in Laplace domain, is now given by

$$\bar{\xi}_i(s) = k_p \bar{\varepsilon}_{i,1} + k_d \bar{\varepsilon}_{i,2} + k_{dd} \bar{\varepsilon}_{i,3} + \bar{a}_{i-1}, \quad i \in S_m. \quad (4.9)$$

The resulting block diagram for a controlled platoon vehicle in the alternative CACC approach is depicted in Figure 4.1.

The acceleration is again chosen as output signal, i.e., $y_i(t) = a_i(t)$. Consequently, $\|P_1(s)\|_{\mathcal{H}_\infty} < \infty$, such that condition (2.14a) is satisfied, see Appendix C. Hence, the only remaining condition for strict \mathcal{L}_2 string stability is

$$\|\Gamma_i(j\omega)\|_{\mathcal{H}_\infty} \leq 1, \quad \forall i \in \mathbb{N} \setminus \{1\}. \quad (4.10)$$

The complementary sensitivity function Γ_i can be derived from the block diagram, depicted in Figure 4.1, and is given by

$$\Gamma_i(s) = \frac{\bar{a}_i}{\bar{a}_{i-1}} = \frac{1}{H_i(s)} \frac{D_i(s)s^2 + K_i(s)}{s^2 + K_i(s)}, \quad i \in S_m. \quad (4.11)$$

The main difference with the complementary sensitivity function of the common approach, (3.24), is that (4.11) does not depend on the vehicle model transfer function $G_i(s)$, i.e., it is independent of the driveline dynamics. This is a direct consequence of using the feedforward input a_{i-1} instead of u_{i-1} . As a result, string stability of the vehicle platoon can be guaranteed without knowledge of a predecessors driveline dynamics, which is the motivation behind the definition of the error variables (4.1) and the main qualitative advantage of the alternative CACC approach over the common CACC approach.

To compare both approaches in a quantitative manner, the influence of the time gap h on string stability in the presence of a communication delay is illustrated in the same manner as in the previous chapter, see Figure 4.2. This figure shows that a tuning can be obtained ($k_p = 0.2$, $k_d = 0.7$) for which the minimum achievable time gap at a given communication delay is slightly

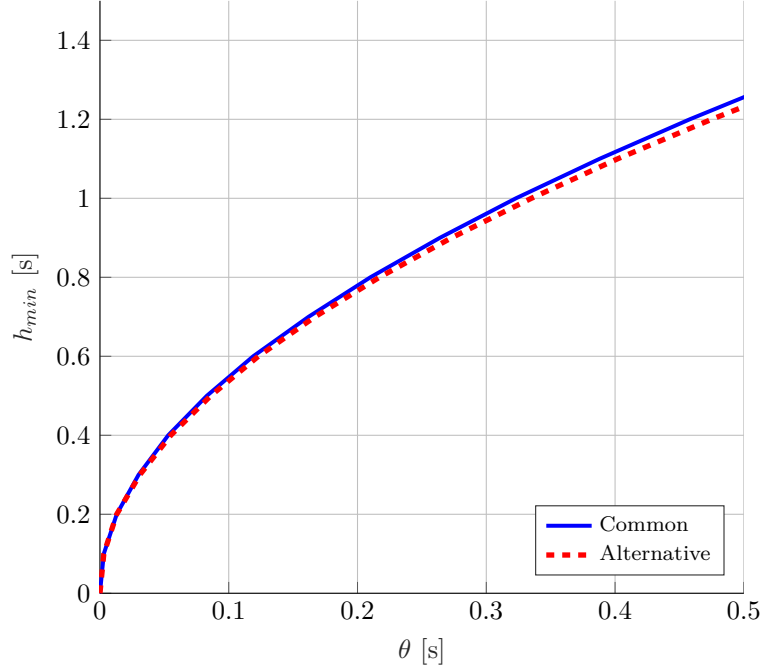


Figure 4.2: The minimum time gap h_{min} that yields $\|\Gamma(s)\|_{\mathcal{H}_\infty} \leq 1$, as function of the communication delay θ : comparison of the common and alternative CACC approaches.

smaller in the alternative approach. Hence, besides the aforementioned qualitative advantage, it is also possible to find control parameters that guarantee string stability at smaller distances than the common CACC approach, yielding a quantitative advantage of the alternative approach.

4.2 Mass estimation

So far, the alternative CACC approach proposed in this chapter assumed that all vehicle parameters are known. In line with the previous chapter, the alternative approach is extended with the assumption that the vehicle mass is an unknown parameter. First, the closed-loop dynamics are derived, followed by the analysis of individual vehicle stability.

4.2.1 Closed-loop dynamics

To address the control problem where the mass m_i is unknown, this section presents a controller design based on the estimated mass \hat{m}_i , which is updated dynamically.

As in the previous chapter, $\tilde{m}_i(t) = \hat{m}_i(t) - m_i$ denotes the mass estimation error. Moreover, it is assumed that m_i only changes during full stops of the vehicle, such that $\dot{\tilde{m}}_i = \dot{\hat{m}}_i$ if the vehicle drives. Since the input transformation (2.5) is part of the controller and the actual mass is assumed to be unknown, the input transformation now uses the estimated mass and is given by:

$$\eta_i = \hat{m}_i u_i + K_d v_i^2 + d_m + 2K_d \tau v_i a_i, \quad i \in S_m. \quad (4.12)$$

This results in the vehicle model

$$\begin{aligned} \dot{q}_i &= v_i \\ \dot{v}_i &= a_i \\ \dot{a}_i &= -\frac{1}{\tau} a_i + \frac{1}{\tau} u_i + \frac{1}{\tau} \frac{\tilde{m}_i}{m_i} u_i, \quad i \in S_m. \end{aligned} \quad (4.13)$$

Defining the error variables as (4.1) results in the error dynamics:

$$\begin{aligned}\dot{\varepsilon}_{i,1} &= \varepsilon_{i,2} \\ \dot{\varepsilon}_{i,2} &= a_{i-1} - \left(1 - \frac{h}{\tau}\right)a_i - \frac{h}{\tau}u_i - \frac{h\tilde{m}_i}{\tau m_i}u_i \\ \dot{\varepsilon}_{i,3} &= a_{i-1} - \frac{\varepsilon_{i,3} - \varepsilon_{i,2}}{h}, \quad i \in S_m.\end{aligned}\tag{4.14}$$

To stabilize these dynamics the input u_i is chosen as (4.3) and auxiliary input ξ_i is given by (4.5), with $k_{dd} = 0$. Additionally, the update law for \hat{m}_i is defined as follows.

$$\dot{\hat{m}}_i := \beta_1(x_i)\varepsilon_{i,1} + \beta_2(x_i)\varepsilon_{i,2}, \quad i \in S_m,\tag{4.15}$$

where $\beta_1(x_i)$ and $\beta_2(x_i)$ and the particular choice of update law (4.15) follow from the stability analysis in the next section. Then, the closed-loop system dynamics are given by

$$\begin{aligned}\dot{\varepsilon}_{i,1} &= \varepsilon_{i,2} \\ \dot{\varepsilon}_{i,2} &= -k_p\varepsilon_{i,1} - k_d\varepsilon_{i,2} - \left(k_p\varepsilon_{i,1} + \left(k_d + \frac{1}{h} - \frac{1}{\tau}\right)\varepsilon_{i,2} - \left(\frac{1}{h} - \frac{1}{\tau}\right)\varepsilon_{i,3}\right)\frac{\tilde{m}_i}{m_i} - \frac{\tilde{m}_i}{m_i}a_{i-1} \\ \dot{\varepsilon}_{i,3} &= \frac{1}{h}\varepsilon_{i,2} - \frac{1}{h}\varepsilon_{i,3} + a_{i-1} \\ \dot{\tilde{m}}_i &= \beta_1(x_i)\varepsilon_{i,1} + \beta_2(x_i)\varepsilon_{i,2},\end{aligned}\tag{4.16}$$

which has equilibrium point

$$\varepsilon_{i,1} = 0 \quad \varepsilon_{i,2} = 0 \quad \varepsilon_{i,3} = ha_{i-1} \quad \tilde{m}_i a_{i-1} = 0.\tag{4.17}$$

4.2.2 Individual vehicle stability

For the individual vehicle stability analysis, consider the unforced system, i.e., with $a_{i-1} = 0$:

$$\begin{aligned}\dot{\varepsilon}_{i,1} &= \varepsilon_{i,2} \\ \dot{\varepsilon}_{i,2} &= -k_p\varepsilon_{i,1} - k_d\varepsilon_{i,2} - \left(k_p\varepsilon_{i,1} + \left(k_d + \frac{1}{h} - \frac{1}{\tau}\right)\varepsilon_{i,2} - \left(\frac{1}{h} - \frac{1}{\tau}\right)\varepsilon_{i,3}\right)\frac{\tilde{m}_i}{m_i} \\ \dot{\varepsilon}_{i,3} &= \frac{1}{h}\varepsilon_{i,2} - \frac{1}{h}\varepsilon_{i,3} \\ \dot{\tilde{m}}_i &= \beta_1(x_i)\varepsilon_{i,1} + \beta_2(x_i)\varepsilon_{i,2}.\end{aligned}\tag{4.18}$$

Denote $x = [\varepsilon_{i,1}, \varepsilon_{i,2}, \varepsilon_{i,3}, \tilde{m}_i]^T$, $x_a = [\varepsilon_{i,1}, \varepsilon_{i,2}]^T$, $A = \begin{bmatrix} 0 & 1 \\ -k_p & -k_d \end{bmatrix}$, suppose that the control gains are chosen such that A is Hurwitz and let $P = P^T > 0$ be such that $PA + A^T P = -Q$ with $Q = Q^T > 0$. Furthermore, let

$$[\beta_1(x_i) \quad \beta_2(x_i)] = -\tilde{\gamma} \left[0 \quad k_p\varepsilon_{i,1} + \left(k_d + \frac{1}{h} - \frac{1}{\tau}\right)\varepsilon_{i,2} - \left(\frac{1}{h} - \frac{1}{\tau}\right)\varepsilon_{i,3} \right] P,\tag{4.19}$$

where $\tilde{\gamma} = \frac{2}{\gamma m_i}$ and $\gamma > 0$ is a control constant. The particular choices for $\beta_1(x_i)$, $\beta_2(x_i)$, and update law (4.15) are motivated by the following stability analysis because these choices enable to come to a conclusion on the convergence of the system states, using the standard Lyapunov function

$$V(\varepsilon, \tilde{m}_i) = x_a^T P x_a + \frac{\alpha}{2}\varepsilon_{i,3}^2 + \frac{\gamma}{2}\tilde{m}_i^2,\tag{4.20}$$

where $\alpha > 0$ is a control constant. Differentiating this Lyapunov function with respect to time, along the solutions of (4.18), while utilizing (4.15) and (4.19) results in

$$\begin{aligned}\dot{V}(\varepsilon, \tilde{m}_i) &= -x_a Q x_a + \frac{\alpha}{h}\varepsilon_{i,2}\varepsilon_{i,3} - \frac{\alpha}{h}\varepsilon_{i,3}^2 \\ &\leq -\lambda_{min}^Q \|x_a\|^2 + \frac{\alpha}{h} \|x_a\| |\varepsilon_{i,3}| - \frac{\alpha}{h} |\varepsilon_{i,3}|^2.\end{aligned}\tag{4.21}$$

Table 4.1: Controller gains.

Parameter	Symbol	Value	Unit
Desired inter-vehicle distance	r_i	10	m
Spacing policy time gap	h	0.5	s
Proportional feedback gain	k_p	0.2	-
Derivative feedback gain	k_d	0.7	-
Double derivative feedback gain	k_{dd}	0.0	-

This time derivative is a negative definite quadratic form in $\|x_a\|$ and $|\varepsilon_{i,3}|$ for $0 < \alpha < 4\lambda_{min}^Q h$, see Appendix D, yielding it negative semi-definite because \tilde{m}_i does not appear in (4.21). Since the Lyapunov function (4.20) is radially unbounded, the set $\Omega_c = \{x \in \mathbb{R}^4 \mid V(\varepsilon, \tilde{m}_i) \leq c\}$ is compact and positively invariant, for every $c > 0$. The set of points where $\dot{V}(\varepsilon, \tilde{m}_i) = 0$ is given by $E = \{x \in \Omega_c \mid \varepsilon = 0\}$, which is invariant because the dynamics (4.18) show that in this set $\dot{\tilde{m}}_i = 0$. Then LaSalle's theorem (Khalil, 2002) shows that all solutions starting in Ω_c approach E as $t \rightarrow \infty$. Hence, the following can be concluded on the convergence of the system states:

$$\lim_{t \rightarrow \infty} x_a(t) = 0, \quad \lim_{t \rightarrow \infty} \varepsilon_{i,3}(t) = 0, \quad \lim_{t \rightarrow \infty} \tilde{m}_i(t) = \bar{m}_i, \quad (4.22)$$

where \bar{m}_i is some constant. Moreover, since the Lyapunov function (3.35) is radially unbounded, the conclusion hold for all initial conditions. This is true because for any $x(0)$, the constant c can be chosen large enough such that $x(0) \in \Omega_c$. Analysis of the forced system, i.e., with $a_{i-1} \neq 0$, is done by means of platoon simulations in the next section.

4.3 Platoon simulations

To illustrate the effectiveness of the alternative CACC approach and compare its performance with the common CACC approach, this section presents platoon simulations. In line with the previous chapter, three scenarios are given. Section 4.3.1 presents the results of simulations in a scenario of regular platooning, with a focus on string stability. These simulations are compared to the results of the subsequent sections and to the simulations presented in Section 3.3.1. Thereafter, Section 4.3.2 analyzes the performance of the alternative CACC approach in a heterogeneous vehicle platoon, illustrating its main advantage over the common approach. Finally, Section 4.3.3 discusses the simulation results when it is assumed that the vehicle mass is unknown.

The same platoon vehicles are considered as in the previous chapter, which means that the system parameters are still specified by Table 3.1. Moreover, throughout this section the initial conditions are $q_i(0) = -10 \cdot i$ m, $v_i(0) = 0$, $a_i(0) = 0$.

4.3.1 Regular platooning

The controller gains are given in Table 4.1. These gains are tuned such that string stability is guaranteed at the same h_{min} compared to the common approach, as explained in Section 4.1.3. Once this is achieved the gains k_p and k_d are minimized with the aim of achieving comfortable driving behaviour. Consequently, the time gap $h = 0.5$ s again guarantees string stability at a communication delay of $\theta = 0.02$ s. The virtual leader follows a reference acceleration, specified by

$$u_0 = \begin{cases} 2, & 0 < t < 4, \\ -2, & 40 < t < 42, \\ 0, & 52 < t < 54, \\ 0, & \text{otherwise.} \end{cases}$$

Since this reference acceleration converges to zero, so will the states x_i , as was shown in Section 4.1.2.

Table 4.2: Regular platooning: acceleration norms calculated over the simulation time $t = [0 \ 70]$.

vehicle index	Norm value
$\ a_1\ _2$	51.1845
$\ a_2\ _2$	48.6588
$\ a_3\ _2$	46.7902
$\ a_4\ _2$	45.2909

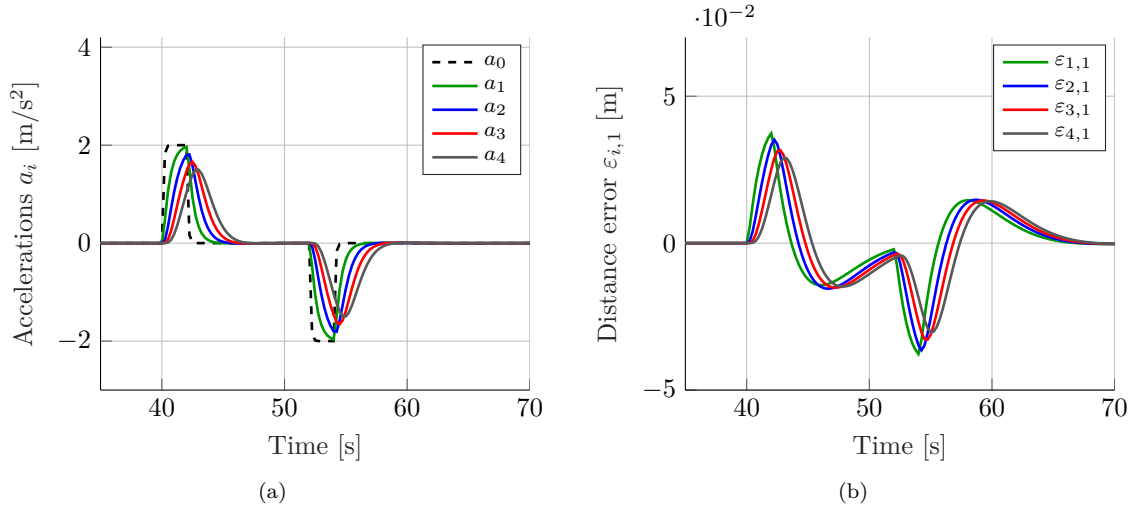


Figure 4.3: Regular platooning: response of (a) the accelerations a_i and (b) the tracking errors $\varepsilon_{i,1}$.

Figure 4.3a presents the accelerations a_i and shows that a_i is smooth and has a decreasing amplitude over the vehicle index. To investigate string stability, the 2-norms of the acceleration signals are given in Table 4.2. These values confirm that $\|a_i\|_2$ is decreasing over the vehicle index, which indicates that, conform expectation, the platoon is string stable for the chosen settings.

Figure 4.3b presents the tracking errors and shows that these have approximately the same amplitude compared to the common approach, as presented in Section 3.3.1. Section 4.1.2 has shown that the tracking errors $\varepsilon_{i,1}$ converge to zero when a_{i-1} goes to zero. Additionally, Figure 4.3b shows that the vehicles have a tracking error during acceleration and deceleration. These tracking errors are a direct consequence of the communication delay θ .

4.3.2 Heterogeneity

This section illustrates the performance of the alternative CACC approach in two different heterogeneous scenarios. Firstly, an example is presented of a vehicle platoon which is heterogeneous with respect to the driveline dynamics. Thereafter, an example is presented of a vehicle platoon which is heterogeneous with respect to acceleration limits.

Different driveline dynamics

In line with the previous chapter, all vehicles are the same as previously discussed except vehicle $i = 2$. This vehicle now has an engine time constant, which represents the driveline dynamics, of $\tau_2 = 1.0$ s. The initial conditions, system parameters, control parameters and reference acceleration remain the same as in the previous section.

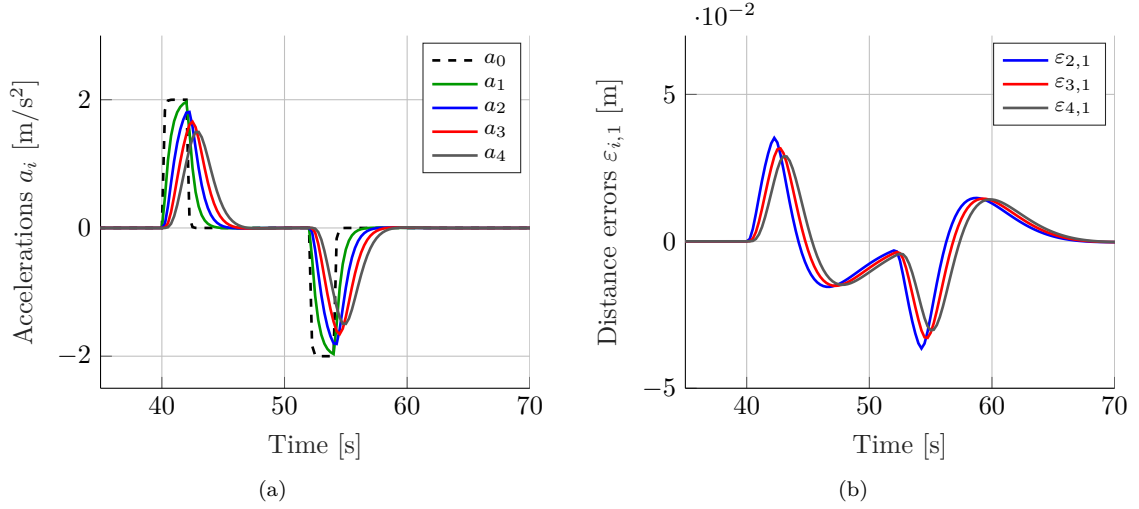


Figure 4.4: Simulation results of a platoon with different driveline dynamics, response of (a) the accelerations a_i and (b) the tracking errors $\varepsilon_{i,1}$.

It was shown in Section 4.1.3 that the alternative approach is able to guarantee string stability independent of the driveline dynamics. Hence, it is expected that, despite the large difference between the driveline dynamics, the platoon exhibits string stability and that the tracking errors do not increase. Figures 4.4a and 4.4b present the response of the acceleration a_i and the tracking errors $\varepsilon_{i,1}$, respectively, and confirm these expectations. The presented example clearly illustrates that the alternative CACC approach is able to achieve the control objectives in a platoon which is heterogeneous with respect to the driveline dynamics. Since this was not the case for the common CACC approach, this example highlights the main advantage of the alternative approach over the common approach.

Different acceleration limits

In the second heterogeneous example, all vehicles are the same as in Section 4.3.1, except vehicle $i = 2$. This vehicle now has a maximum acceleration of $a_{2,max} = 1.5 \text{ m/s}^2$, such that $a_2 = a_{2,max}$ if this maximum is reached. For $a_2(t) < a_{2,max}$ and vehicles $i \neq 2$, the dynamics are given by continuous model (2.6). The initial conditions, system parameters, control parameters and reference acceleration remain the same as in Section 4.3.1. This example results in differences between the desired acceleration u_2 and the actual acceleration a_2 of the second vehicle. Because of the acceleration limit, it is expected that the second vehicle is not able to accurately track its predecessor. However, as opposed to the common approach, it is expected that the upstream platoon vehicles are able to accurately track their predecessors, resulting in string stable behaviour.

Figure 4.5a presents the acceleration responses a_i . Because u_{i-1} is used as feedforward in the common approach, the platoon is not strictly string stable, as was shown in Section 3.3.2. For the alternative approach on the other hand, Figure 4.5a shows that the third and fourth vehicle follow their predecessor, which shows that the platoon is string stable in the specific simulation. Figure 4.5b presents the tracking errors $\varepsilon_{i,1}$ and shows that, in line with the common approach, vehicle $i = 2$ has a positive tracking error. This is expected because vehicle $i = 2$ has the an acceleration limit. The main difference between the two approaches can be seen in the distance error of vehicle $i = 3$. As was discussed in Section 3.3.2, this vehicle is unaware of the acceleration limitations in the second vehicle in the common approach. As a result, vehicle $i = 3$ has a negative tracking error in the common approach. A negative tracking error means that the vehicle drives closer to its predecessor than desired, which illustrates that the common approach can result in dangerous situations, while these situations do not occur in the alternative approach.

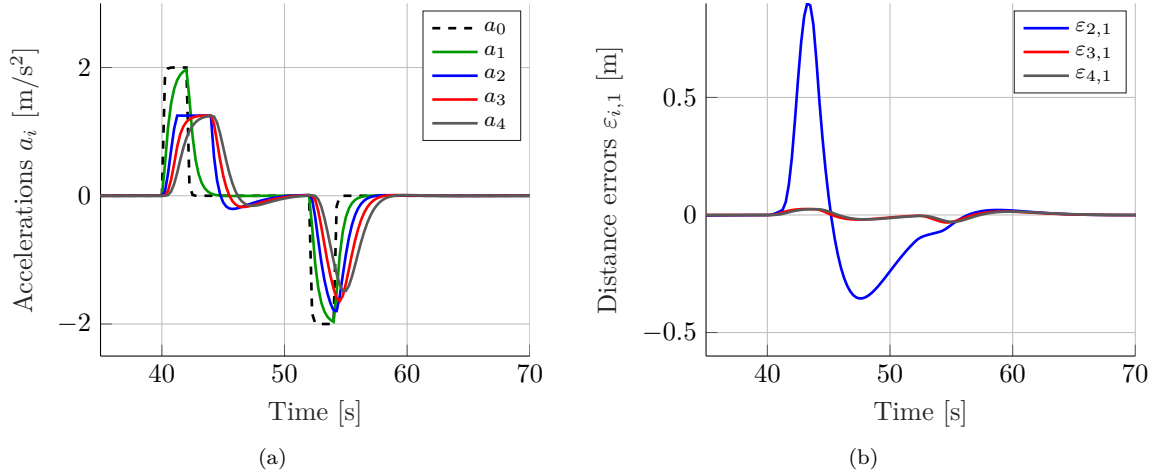


Figure 4.5: Simulation results with acceleration limitations on the second vehicle, response of (a) the accelerations a_i and (b) the tracking errors $\varepsilon_{i,1}$.

4.3.3 Mass estimation

Section 4.2.2 has shown that for $a_{i-1} = 0$ the states $\varepsilon(t)$ converge to zero, while $\hat{m}_i(t)$ converges to a constant value. The aim of this section is to investigate the system behaviour for $a_{i-1} \neq 0$, via simulations. The simulations are also used to tune the controller gains. Since a settling time for \hat{m}_i smaller than 11 seconds is not achieved, the tuning goal is now to minimize this settling time. Additionally, the gains k_p , k_d , and $\tilde{\gamma}_i$ are kept as small as possible, to realize comfortable driving behaviour. Convergence of \hat{m}_i to m_i is achieved after approximately 40 seconds with the following gains: $k_p = 1.5$, $k_d = 5.0$, $k_{dd} = 0$, and $\tilde{\gamma}_i = 250$. All other system parameters, control parameters and initial conditions are the same as previously discussed. Hence, all vehicles have initial conditions $q_i(0) = -10 \cdot i$ m, $v_i(0) = 0$, $a_i(0) = 0$, and $\hat{m}_i(0) = 5500$ kg.

For a constant a_{i-1} , the equilibrium point $\tilde{m}_{i,eq} = 0$, see (4.17). As mentioned, convergence to this equilibrium is achieved after approximately 40 seconds. Since the vehicles would exceed the maximum velocity when a constant $a_{i-1} = 1$ m/s^2 is used for 40 seconds, a continuous reference acceleration is designed for the first 40 seconds, such that $v_{i,\max}$ is not exceeded and the model (4.16) accurately describes the dynamic behaviour of the vehicles. For the remainder of the simulation the reference acceleration is given by $u_0 = -2.0$ m/s^2 for $55 < t \leq 57$, $u_0 = 2.0$ m/s^2 for $67 < t \leq 69$ and $u_0 = 0$ for all other time intervals, the corresponding profile is presented in Figure 4.7. In line with Chapter 3, the mass estimates are again fixed after the first acceleration period.

Figure 4.6a presents the mass estimates and shows that these converge to (approximately) the actual mass. However, during convergence $\tilde{m}_i \neq 0$ and the stability analysis presented in Section 4.1.3 is not valid. Therefore, string stability is analysed by means of simulations. Figure 4.7 shows that a_i is smooth and has a decreasing amplitude over the vehicle index. To investigate string stability, the 2-norms of the acceleration signals are given in Table 4.3a. These values show that $\|a_i\|_2$ is decreasing over the vehicle index, from which it is concluded that the platoon is string stable for this specific scenario. Since u_0 captures a wide range of frequencies, this simulation gives a strong indication that the platoon is string stable in general. However, using time domain simulations, string stability cannot be guaranteed.

Figure 4.6b presents the tracking errors. During convergence of the mass estimates these errors are much larger than in the common approach, which can be explained by the larger settling time and the higher sensitivity to disturbances, see Appendix E. These tracking errors depend on tuning and can be reduced by increasing the controller gains. However, as explained, the controller gains are minimized in both approaches to maximize driver comfort. The reduction of the errors

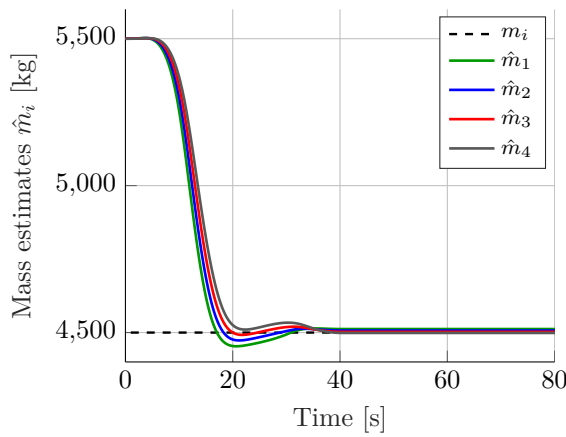
Table 4.3: Results of the simulations including mass estimation calculated over the simulation time $t = [0 \ 80]$: (a) acceleration norms and (b) average of the distance error signal 2-norms $\|\varepsilon_{i,1}\|_2$, over the all vehicles.

vehicle index	Norm value
$\ a_1\ _2$	50.1452
$\ a_2\ _2$	48.1548
$\ a_3\ _2$	46.6767
$\ a_4\ _2$	45.4992

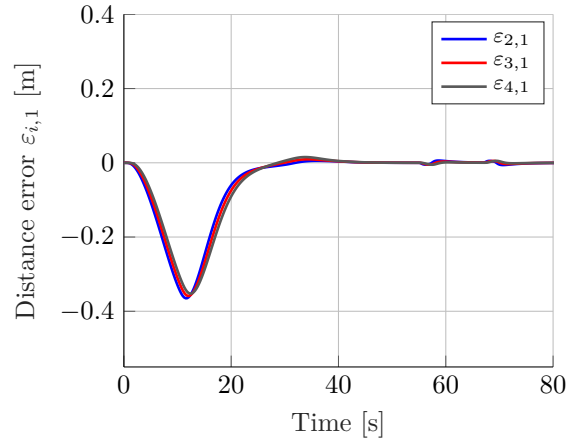
(a)

Case	$\ \varepsilon_{i,1}\ _2$
1. With mass estimate \hat{m}_i	9.7070
2. Without mass estimate \hat{m}_i	22.237

(b)



(a)



(b)

Figure 4.6: Simulation results (a) mass estimates \hat{m}_i and (b) tracking errors $\varepsilon_{i,1}$.

after convergence of the mass estimates, clearly illustrates the effectiveness of the update laws. Moreover, Table 4.3b presents the corresponding error norms and compares these to the scenario without mass estimation, i.e., $\hat{m}_i = 5500$ kg throughout the simulation. The presented values confirm the two aforementioned conclusions: assuming an unknown mass has more influence on the tracking error compared to the common approach and utilizing the mass estimation reduces the tracking errors significantly.

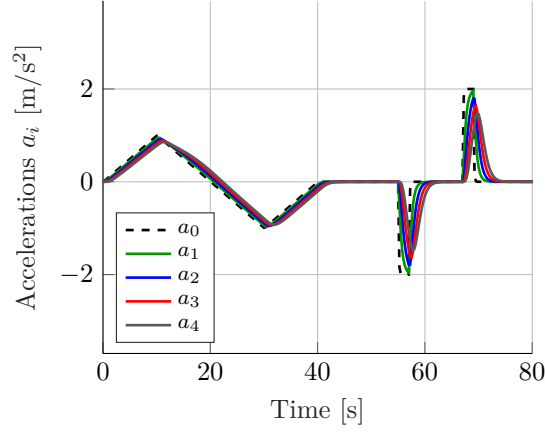


Figure 4.7: Reference acceleration a_0 and the response of accelerations a_i .

4.4 Summary

This chapter started in Section 4.1 with the design and stability analyses of a novel alternative CACC approach in a regular platooning situation. Section 4.2 extended this approach with the assumption that the vehicle mass is unknown. An adaptive mass estimation law was presented such that the CACC approach achieves the vehicle-following objective, while exhibiting string-stable behaviour without knowledge of the vehicle mass. The effectiveness of the proposed alternative CACC approach was further illustrated by means of platoon simulations in Section 4.3. The performance of the alternative approach was compared to the common approach, presented in Chapter 3. This section showed that the performance of both approaches is similar in a scenario of regular platooning. Thereafter, the main advantage of the alternative over the common approach was clearly illustrated in two scenarios of heterogeneous platooning. In both heterogeneous scenarios, the common approach resulted in string instability and safety was compromised, while this was not the case with the alternative approach presented in this chapter. Finally, it was shown that the control objectives are also achieved in a scenario where vehicles have unknown masses. However, due to the higher sensitivity to disturbances and the longer settling time of the alternative approach, the tracking errors are larger compared to the common approach.

Chapter 5

Experimental validation

To validate and compare the CACC approaches presented in Chapter 3 and Chapter 4, this chapter discusses the implementation and presents the results of experiments carried out on a platoon of so called “e-puck” mobile robots, depicted in Figure 5.1. Both CACC approaches control the longitudinal inter-vehicle distance between vehicles in a platoon, which is a one-dimensional control problem. However, because of the limited space in the experimental area, a lateral controller is also included in the control strategy. This makes it possible to test multiple straight sections in one experiment, which enables testing of the longitudinal performance of the CACC approaches without initial errors. The results of experiments with the e-pucks are used to validate assumptions made in the simulations and to provide insight into the performance of both control strategies when subject to sensor noise, delays and model uncertainties.

The outline of this chapter is as follows: Section 5.1 introduces the hardware components and characteristics of the experimental setup. Section 5.2 explains the control structure that is adopted for testing of the CACC approaches. The results of the simulations and experiments are presented in Sections 5.3 and 5.4, respectively. Finally, Section 5.5 summarizes the main conclusions.

5.1 Experimental setup

This section introduces the experimental setup. Firstly, all hardware components of the setup are described after which the characteristics of the setup and the reference trajectory are discussed.



Figure 5.1: Validation platform used for experimental validation: (left) a platoon of e-puck mobile robots, (right) a single e-puck.

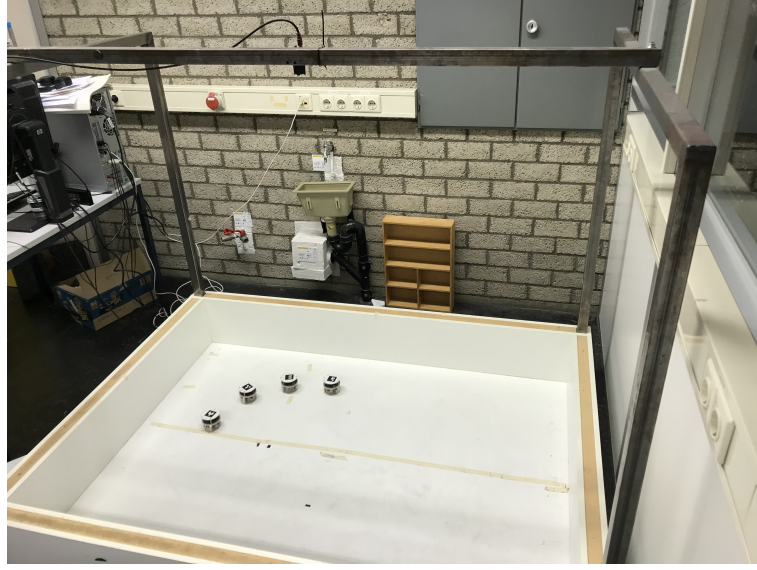


Figure 5.2: Experimental setup.

5.1.1 Hardware components

The e-puck mobile robot platform is chosen for the validation of the CACC approaches. This experimental platform, depicted in Figure 5.2, was originally designed to investigate coordination control of unicycle mobile robots using a virtual structure approach (van den Broek et al., 2009). The setup has proven to be useful for testing of various control strategies, e.g., Kostic et al. (2010); Bayuwindra et al. (2016); Beumer (2017). The four main components of the setup are: the e-puck mobile robot, the arena, the camera localization system and the main computer equipped with Bluetooth communication. These four components are briefly introduced in this section.

The e-puck mobile robot has been developed at the EPFL, Switzerland (Goncalves et al., 2009). The main specifications of an e-puck are given in Table 5.1. Since an e-puck is a differential-drive mobile robot, the left and right wheels are driven separately by stepper motors. The left and right wheel speeds are denoted as $v_{i,\text{left}}$ and $v_{i,\text{right}}$, respectively, and calculated based on the longitudinal velocity v_i and the angular velocity ω_i according to

$$v_{i,\text{left}} = v_i - \frac{L_a}{2}\omega_i, \quad v_{i,\text{right}} = v_i + \frac{L}{2}\omega_i,$$

where L_a is the wheelbase.

The experimental arena used in this thesis has a size of 1.75×2.20 meters. The overhead camera, which uses the unique markers fitted on top of the robots for localization, is placed in the middle of the arena. This camera (Firewire 1032×778 camera AVT Guppy F-080b b/w combined with reactIVision software) samples at approximately 30 Hz and is directly coupled to the PC. All control is done by the main PC, because the on-board processor of the e-puck does not have the computational power to do this locally, which also means that no measurements are done on-board of the e-puck. All available information is obtained by the overhead camera. The PC is also used to process the images obtained by the camera, to get the position data of the e-puck. Finally, the PC communicates the control signal to the e-pucks via a Bluetooth communication protocol.

5.1.2 Characteristics of the experimental setup

According to the technical manual (Allied Vision Technologies, 2008), the accuracy of the position measurements is approximately $0.25 \cdot 10^{-3}$ m in x- and y-direction and $0.9 \cdot 10^{-2}$ rad in θ direction.

Table 5.1: E-puck specifications.

Specification	Value	Unit
Robot weight	0.2	kg
Robot radius	0.0370	m
Wheel radius	0.0205	m
Axle length (L_a)	0.0520	m
Maximum velocity	0.13	m/s
Maximum angular velocity	5	rad/s

Due to this high accuracy, the quality of the measurements in x- and y-direction is not of major concern. To obtain more accurate orientation measurements, an observer could be included in the control strategy, see for example Beumer (2017). However, the lateral performance is not considered in the scope of this thesis. A more relevant camera characteristic is the frame rate, which is approximately 30 Hz and determines the sampling time of the experimental setup. Due to this slow update rate, it is expected that the control structure introduces additional tracking error. This is explained in more detail in the next sections.

The second characteristic of concern is the stability of the wireless protocol that is used to communicate the control signal from the PC to the e-pucks. During several experiments, the communication with one or more e-pucks was lost. If an e-puck does not receive a control signal due to a loss in communication, the e-puck stops. This results in peaks in the tracking error and velocity control signal. To ensure fair comparison between the two CACC approaches, the experiments with communication losses are not taken into account. These experiments are discussed separately in Appendix F. The results presented in Appendix F illustrate that the platoon is able to recover from a loss in communication, if the communication is restored in time.

Delays due to the Bluetooth communication, image processing and computation of the control signal, inevitably occur in the experimental setup. The delay due to communication is expected to be the most significant. Beumer (2017) reports that the average communication delay is around 0.133 seconds. The influence of the communication delay on string stability of the platoon was discussed in detail in Section 3.1.3 and Section 4.1.3. Following these string stability analyses a time gap of $h = 0.5$ seconds is chosen throughout the experiments, yielding string stability of the platoon.

The last two characteristics considered are the maximum velocity and battery life of the e-pucks. The stepper motors of the e-pucks are only able to generate reliable results at low speed. Therefore, the forward velocity of the e-pucks is limited to a maximum of 0.13 m/s. Moreover, battery life can be of significant influence to the performance of the e-pucks, which is taken into account to obtain reliable results. To ensure fair comparison between the two approaches, three runs of all the experiments are carried out in alternate order.

5.1.3 Reference trajectory

Because of the emphasis on the longitudinal performance of the CACC approaches, a reference trajectory is specified which maximizes the straight sections within the limits of the experimental area. This reference trajectory, with starting point $(x, y) = (0.5, 0.1)$, is presented in Figure 5.3. From the starting point, the curvature of the trajectory is specified, as function of the curvilinear position $q_{i,r}$, as follows:

$$\kappa_i = f(q_{i,r}) = \begin{cases} 0 & \text{if } q_{i,r} \bmod (\pi R + L) \in [0, L), \\ 1/R & \text{otherwise,} \end{cases} \quad (5.1)$$

where $R = 0.4$ m is the radius of the curved part of the trajectory and $L = 0.4$ m is the length of the straight part of the trajectory. The mentioned reference e-puck is introduced in Section 5.2.

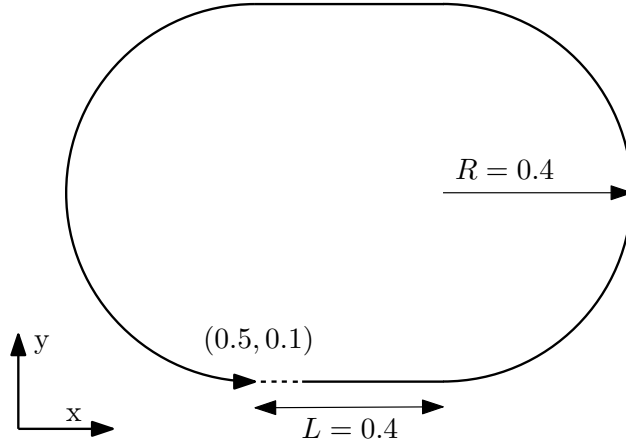


Figure 5.3: Reference trajectory.

5.2 Control structure

For the implementation of the two CACC approaches on the mobile robots, two control levels are distinguished. Firstly, the “low-level system” is presented in Section 5.2.1. This lower-level handles the actual control of every e-puck such that it drives according to a desired trajectory. Secondly, Section 5.2.2 presents the “high-level system”. The high-level system contains the longitudinal CACC controller, which controls the inter-vehicle distance between two adjacent vehicles. Moreover, the high-level system also transforms the desired acceleration control input, generated by the CACC controllers, into a reference velocity input, which is required for the e-pucks.

5.2.1 Low-level system

A kinematic model of a mobile robot is presented to facilitate simulations since this model appears to adequately describe the e-pucks behaviour (Beumer, 2017). Assuming no slip, the nonholonomic kinematic unicycle model is described by the following differential equations:

$$\begin{aligned} \dot{x}_i &= v_i \cos \theta_i \\ \dot{y}_i &= v_i \sin \theta_i \\ \dot{\theta}_i &= \omega_i, \quad i \in S_m, \end{aligned} \quad (5.2)$$

where the x_i and y_i coordinates describe the position of the center of the mobile robot with respect to the fixed earth frame O . The orientation angle θ_i is the angle between the heading of the vehicle and the x -axis, taken counter-clockwise. The forward velocity v_i and the angular velocity ω_i are the inputs.

The goal of the experiments is to test the CACC approaches, which control the longitudinal motion, while the e-pucks drive according to a desired trajectory. In order to make the e-pucks follow this desired trajectory, a lateral controller is required. Hence, the control objective in the lower-level is, for every e-puck, to follow a virtual reference e-puck which is projected onto reference trajectory (5.1). The dynamics of these reference vehicles are given by

$$\begin{aligned} \dot{x}_{i,r} &= v_{i,r} \cos \theta_{i,r} \\ \dot{y}_{i,r} &= v_{i,r} \sin \theta_{i,r} \\ \dot{\theta}_{i,r} &= v_{i,r} \kappa_{i,r}, \quad i \in S_m, \end{aligned} \quad (5.3)$$

where $x_{i,r}$ and $y_{i,r}$ describe the position and $\theta_{i,r}$ the orientation of the reference vehicle. The velocity $v_{i,r}$ and the curvature of the reference trajectory $\kappa_{i,r}$ are the inputs. Note that the

Table 5.2: Lead vehicle control parameters.

Parameter	Description	Value	Unit
c_1	Position gain	0.1	-
c_2	Position gain	600	-
c_3	Orientation gain	5	-
c_4	Velocity gain	1	-

angular velocity of the reference vehicle is given by $\omega_{i,r} = v_{i,r}\kappa_{i,r}$. The error between vehicle i and the corresponding reference vehicle is defined as the difference between the postures and expressed in the local frame of vehicle i . Applying a coordinate transformation from the global frame to the local frame of vehicle i results in the following error coordinates (Beumer, 2017):

$$\begin{bmatrix} x_{i,e} \\ y_{i,e} \\ \theta_{i,e} \end{bmatrix} = \begin{bmatrix} \cos \theta_i & \sin \theta_i & 0 \\ -\sin \theta_i & \cos \theta_i & 0 \\ 0 & 0 & 1 \end{bmatrix} \begin{bmatrix} x_{i,r} - x_i \\ y_{i,r} - y_i \\ \theta_{i,r} - \theta_i \end{bmatrix}, \quad i \in S_m. \quad (5.4)$$

A tracking controller needs to be adopted to make these errors converge to zero. To this end, the tracking controller proposed by Beumer (2017), which is based on the tracking controller proposed by Jiang and Nijmeijer (1997), is adopted in this work. This controller is defined as

$$\begin{aligned} \omega_i &= \omega_{i,r} - c_2 v_{i,r} y_{i,e} + c_3 \dot{\theta}_{i,e} \\ \dot{\zeta}_i &= c_1 x_{i,e} + c_4 v_{i,e} \\ v_i &= v_{i,r} + \zeta_i, \end{aligned} \quad (5.5)$$

where c_i , $i = 1, 2, 3, 4$, are controller gains, $v_{i,e} = v_{i,r} - v_i$, and ζ_i is an auxiliary state. For details on the derivation of this controller and proof of convergence of the error states to zero, the reader is referred to Beumer (2017) and Jiang and Nijmeijer (1997). The controller gains of the tracking controller are based on Beumer (2017) and given in Table 5.2. Here, the orientation gain is increased to $c_3 = 5$, to achieve faster convergence of θ_e to zero.

Now, the reference trajectory (5.1), the e-puck model (5.2), the virtual reference vehicle (5.3), and the tracking controller (5.5), which makes the errors (5.4) converge to zero, are classified as the “low-level” system. This system is depicted in Figure 5.4, where q_i is calculated based on the position of the e-puck using

$$q_i(t + \Delta t) = q_i(t) + \sqrt{(x_i(t + \Delta t) - x_i(t))^2 + (y_i(t + \Delta t) - y_i(t))^2}, \quad i \in S_m,$$

with sample time $\Delta t = 0.033$ s. If the tracking controller achieves perfect tracking, the low-level system can be seen as a single integrator model, which requires a desired longitudinal velocity as input and has the corresponding curvilinear position as output. However, as mentioned in the previous section, the controller has an update rate of 30 Hz. Therefore, it is expected that the low-level control structure introduces a tracking error and does not resemble a perfect integrator. This is further investigated by means of platoon simulations in Section 5.3. The desired longitudinal velocity is specified by the high-level system, which is explained in the section below.

5.2.2 High-level system

The high-level system assumes that the entire low-level system is a single integrator, which replaces the equation $\dot{q}_i = v_i$ of longitudinal vehicle model (2.6). Since the CACC controllers specify a desired acceleration $u_{i,r}$ and the low-level system requires a reference velocity $v_{i,r}$ as input signal, the following longitudinal vehicle model is used for conversion.

$$\begin{aligned} \dot{v}_{i,r} &= a_{i,r} \\ \dot{a}_{i,r} &= -\frac{1}{\tau} a_{i,r} + \frac{1}{\tau} u_{i,r}, \quad i \in S_m, \end{aligned} \quad (5.6)$$

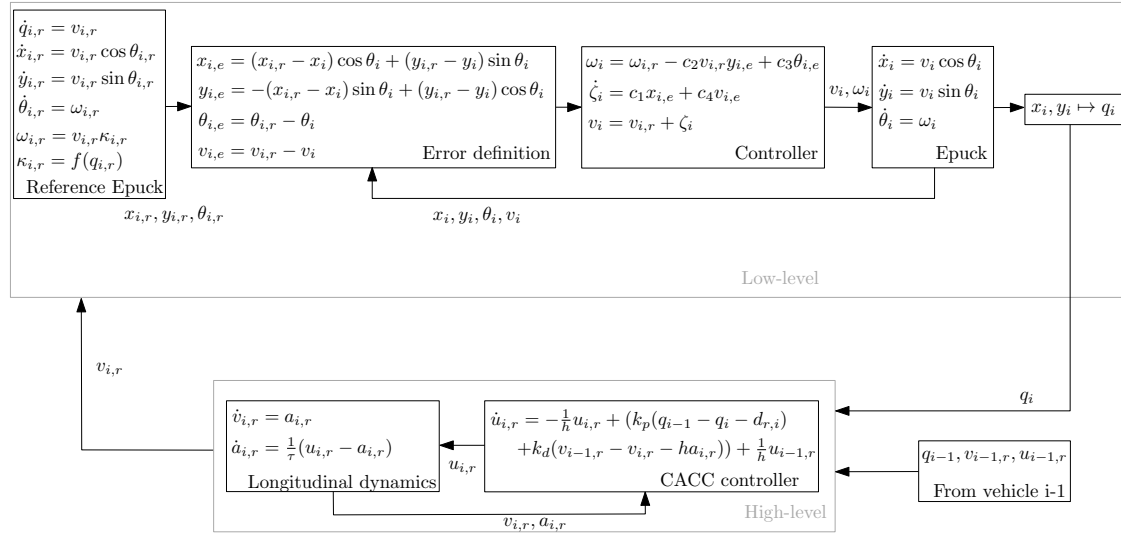


Figure 5.4: Overview of combined high- and low-level control schemes.

where $u_{i,r}$ is the input specified by a CACC controller. The kinematic variables are extended with a subscript r to indicate that the model is used to specify a reference velocity for the low-level system. Hence, $a_{i,r}$, $v_{i,r}$, and $q_{i,r}$ denote the reference acceleration, velocity, and curvilinear position, respectively. The second component of the high-level system is either of the CACC controllers (3.5) or (4.3), for the common and alternative approaches, respectively. The overview of the total control structure is given in Figure 5.4. In this figure, the CACC controller of the common approach is adopted. Before implementing the presented control structure in an experimental setting, the validity of the assumption that the low-level system represents a single integrator is tested by means of platoon simulations in the next section.

5.3 Control structure validation using platoon simulations

Before implementation on the experimental setup, this section aims to validate the control structure described in the previous section. To this end, platoon simulations with the presented control structure are compared to the simulation results obtained in Chapter 3 and Chapter 4. In line with these chapters, this section subsequently focuses on regular platooning, heterogeneity, and mass estimation. Assuming that the low-level system is an accurate approximation of a pure integrator, it is expected that the simulations throughout this section closely resemble the simulations presented in Chapter 3 and Chapter 4.

The simulation conditions are, where possible, equal to the simulation conditions in the previous chapters, to ensure fair comparisons. However, scaling is required because the vehicles in this chapter have different system parameters, see Table 5.1. For all scenarios, the starting positions of the four platoon vehicles are given in Table 5.3. These initial positions are chosen such that $\varepsilon_{i,1}(0) = 0$ with standstill distance $r_i = 0.1\text{m}$ and time gap $h = 0.5\text{s}$. Moreover, the initial curvilinear positions are chosen such that $q_i = 0$ at the starting point of the reference trajectory. Unless indicated otherwise, all other system states are initiated from zero. As explained in the previous chapters, the controller gains $k_p = 0.2$, $k_d = 0.7$ and $k_{dd} = 0$ are well validated for the common approach by previous authors. These gains are also adopted in this chapter for the scenario's where m_i is assumed to be known. Additionally, the controller gains for the alternative approach are tuned such that the amplitude of the tracking errors does not exceed that of the common approach. Once that performance is achieved, the gains are minimized to realize comfortable driving behaviour. For the alternative approach the resulting gains are: $k_p = 0.2$, $k_d = 0.7$ and $k_{dd} = 0$.

Table 5.3: Initial vehicle positions.

Vehicle	$x_i(0)$	$y_i(0)$	$\theta_i(0)$	$q_i(0)$
$i = 1$	0.4	0.1	0.0	-0.1
$i = 2$	0.3	0.1	0.0	-0.2
$i = 3$	0.2	0.1	0.0	-0.3
$i = 4$	0.1	0.1	0.0	-0.4

Table 5.4: Acceleration norms of the common and alternative approach calculated over the simulation time $t = [0 \ 70]$.

Acceleration norm	Common	Alternative
$\ a_1\ _2$	0.2853	0.2798
$\ a_2\ _2$	0.2669	0.2646
$\ a_3\ _2$	0.2531	0.2533
$\ a_4\ _2$	0.2421	0.2443

Finally, because the aim of this section is only to validate the low-level approximation, no delays are considered.

5.3.1 Regular platooning

Following sections 3.3.1 and 4.3.1, the simulations start from steady state and focus on the response of the follower vehicles during acceleration and deceleration of the lead vehicle. This lead vehicle follows a reference acceleration, which is specified by

$$u_{0,r} = \begin{cases} 0.02, & 0 < t < 4, \quad 40 < t < 42, \\ -0.02, & 52 < t < 54, \\ 0, & \text{otherwise.} \end{cases}$$

Figure 5.5 and Figure 5.6 present the accelerations $a_{i,r}$ and tracking errors $\varepsilon_{i,1}$ for the common and alternative approaches, respectively. These figures show that both $a_{i,r}$ and $\varepsilon_{i,1}$ have different amplitudes, compared to the results presented in sections 3.3.1 and 4.3.1. This is a direct consequence of the scaling in the reference acceleration $u_{0,r}$, which is required due to the use of different vehicles. As was the case in the previous chapters, these amplitudes are similar for both approaches.

Since no delays are considered in the presented simulations, it is expected that the platoon exhibits string stable behaviour. Figure 5.5a and Figure 5.6a show that, for both approaches, $a_{i,r}$ is smooth and has a decreasing amplitude over the vehicle index. To investigate the string stability, the 2-norms of the acceleration signals are given in Table 5.4. These values confirm that $\|a_{i,r}\|_2$ is decreasing over the vehicle index, which indicates that the platoon is string stable for the chosen settings.

The simulations in sections 3.3.1 and 4.3.1 illustrated that the tracking errors are caused by the communication delay, without communication delay the tracking errors are expected to be approximately zero. This indicates that the tracking errors shown in Figure 5.5b and Figure 5.6b occur because the low-level system is not an exact representation of a pure integrator.

5.3.2 Heterogeneity

In line with Section 3.3.2 and Section 4.3.2, this section presents two examples of heterogeneous platoons. Firstly, a platoon is considered which is heterogeneous with respect to the acceleration limits. Secondly, a platoon is considered which is heterogeneous with respect to the vehicle dynamics.

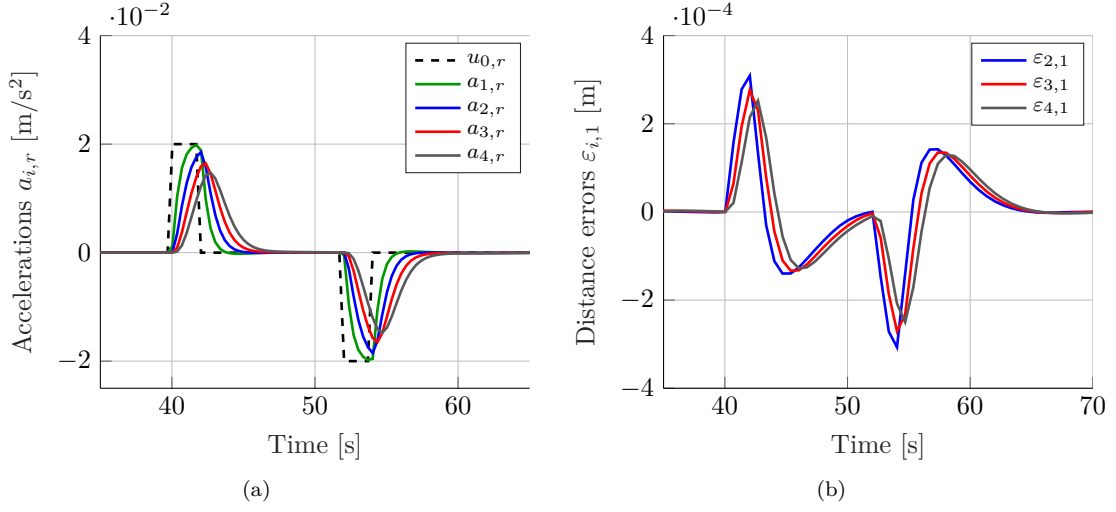


Figure 5.5: Simulation results of the common CACC approach in a regular platooning scenario: (a) accelerations $a_{i,r}$ and (b) tracking errors $\varepsilon_{i,1}$.

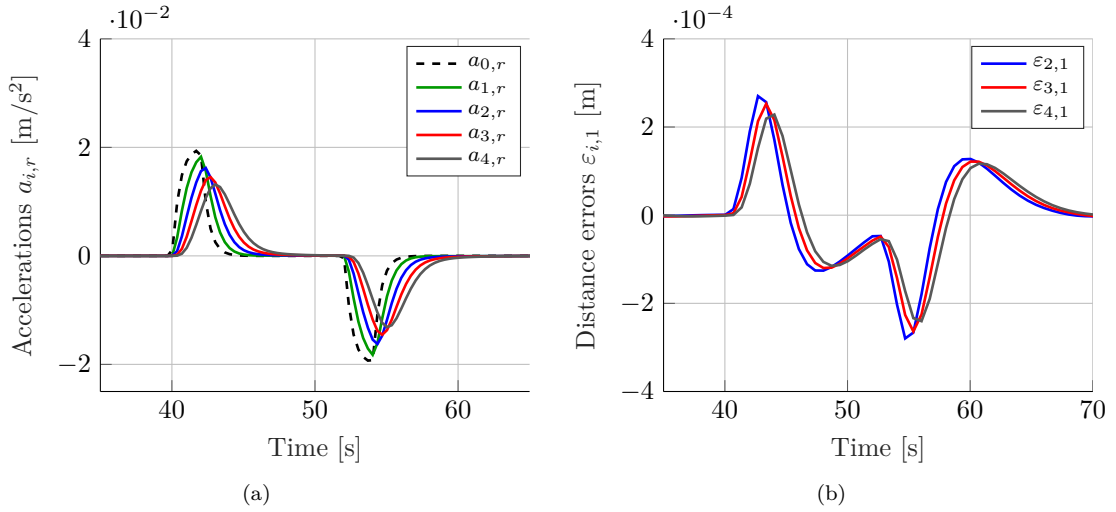


Figure 5.6: Simulation results of the alternative CACC approach in a regular platooning scenario: (a) accelerations $a_{i,r}$ and (b) tracking errors $\varepsilon_{i,1}$.

Different acceleration limits

In this first example vehicle $i = 2$ has a maximum acceleration of $a_{2,r,max} = 0.01 \text{ m/s}^2$, whereas all other simulation conditions remain the same as in Section 5.4.1.

It was illustrated that the low-level system introduces a tracking error. However, this tracking error occurs in both approaches and is significantly smaller than the tracking error introduced by the acceleration limits. Hence, it is expected that there is a similar difference between the alternative and common approach as in the previous chapters.

Figure 5.7 and Figure 5.8 present the accelerations $a_{i,r}$ and tracking errors $\varepsilon_{i,1}$ for the common and alternative approaches, respectively. Both figures show, apart from scaling, similar behaviour compared to the simulation results presented in Section 3.3.2 and Section 4.3.2, respectively. Hence, the presented simulations illustrate that the adopted control structure, with the low-level approximation, can be used to compare the performance of the CACC approaches.

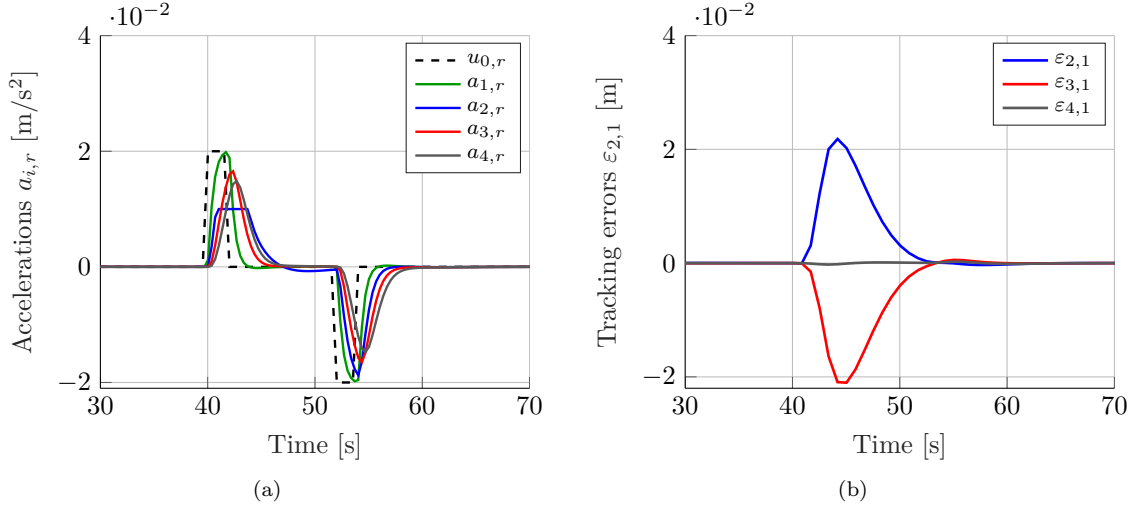


Figure 5.7: Simulation results of the common approach in a platoon with different acceleration limits: (a) accelerations $a_{i,r}$ and (b) tracking errors $\varepsilon_{i,1}$.

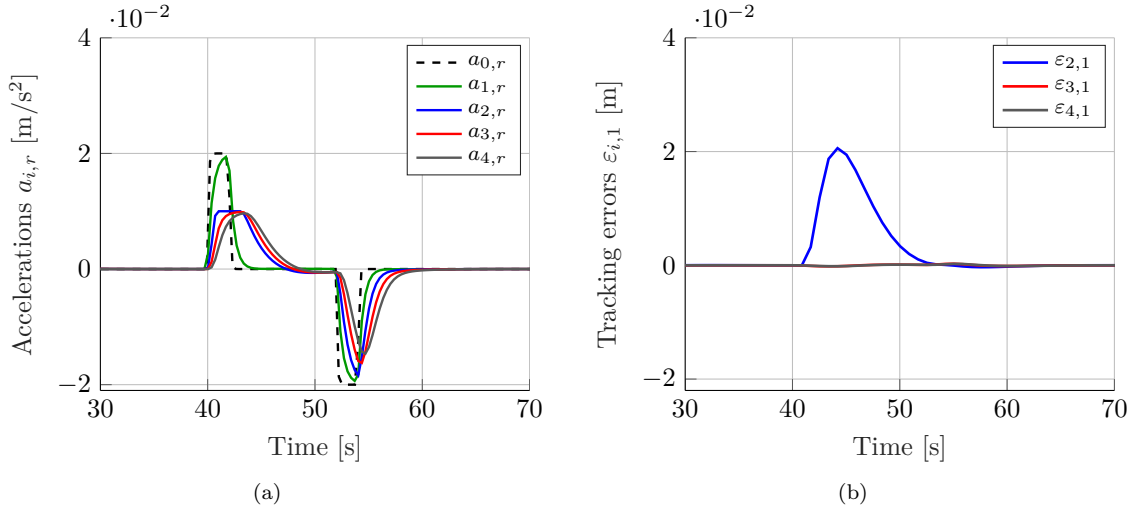


Figure 5.8: Simulation results of the alternative approach in a platoon with different acceleration limits: (a) accelerations $a_{i,r}$ and (b) tracking errors $\varepsilon_{i,1}$.

Different vehicle dynamics

In this second example vehicle $i = 2$ has an engine time constant of $\tau_2 = 1.0\text{s}$, whereas all other simulation conditions remain the same as in Section 5.4.1. Based on the previous sections, it is expected that the presented example shows similar differences between the common and alternative approach as in the corresponding heterogeneity example presented in Chapter 3 and Chapter 4.

Figure 5.9 and Figure 5.10 present the accelerations $a_{i,r}$ and tracking errors $\varepsilon_{i,1}$ for the common and alternative approaches, respectively. Both figures again show similar behaviour compared to the simulation results presented in Section 3.3.2 and Section 4.3.2. Hence, the conclusions for the presented example remain as discussed in the previous chapters.

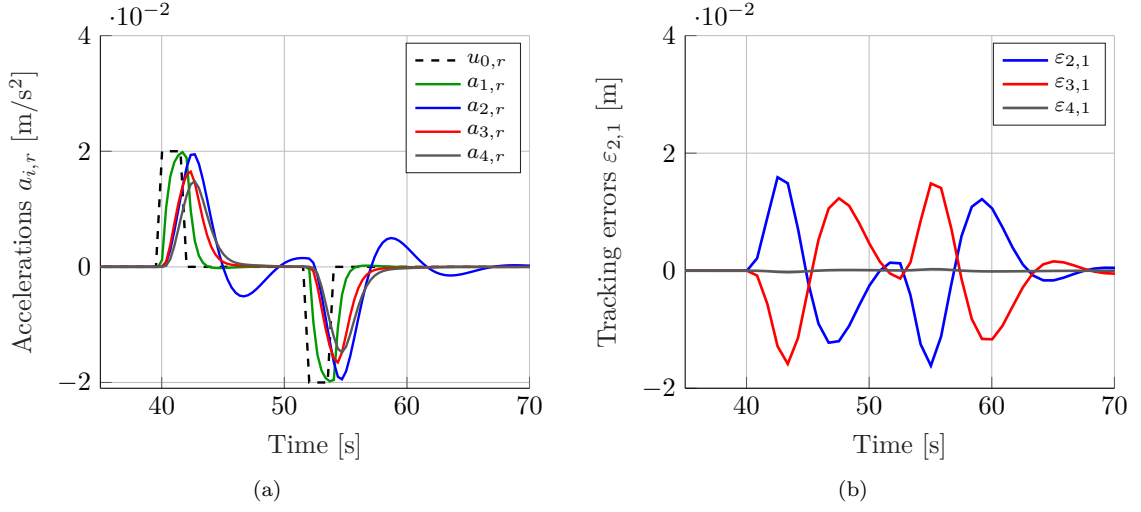


Figure 5.9: Simulation results of the common approach in a platoon with different vehicle dynamics: (a) accelerations $a_{i,r}$ and (b) tracking errors $\varepsilon_{i,1}$.

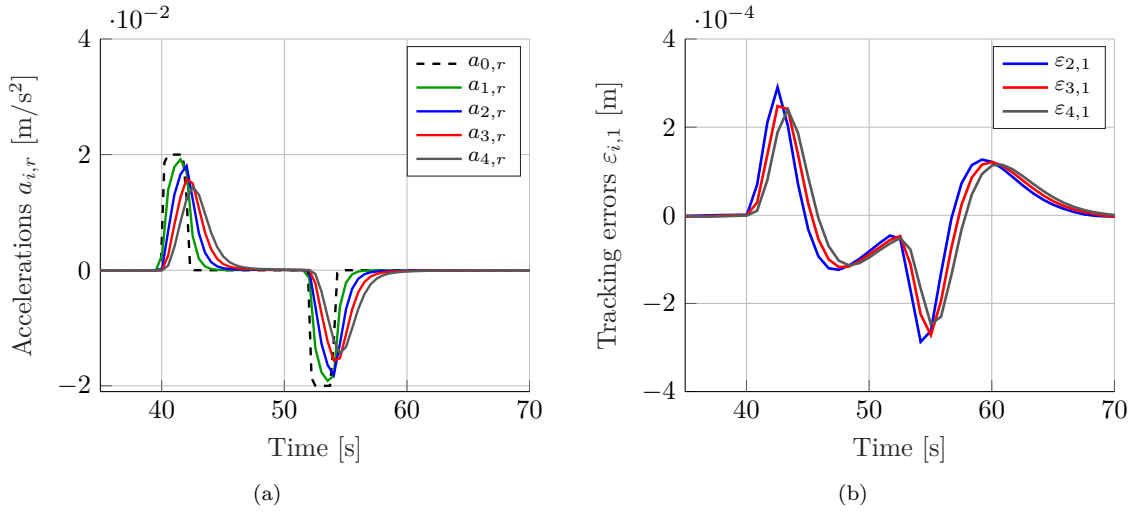


Figure 5.10: Simulation results of the alternative approach in a platoon with different vehicle dynamics: (a) accelerations $a_{i,r}$ and (b) tracking errors $\varepsilon_{i,1}$.

5.3.3 Mass estimation

This section follows Section 3.3.3 and Section 4.3.3, to validate the control structure with the assumption that the vehicle mass is unknown. The implementation on the e-puck setup, as discussed in Section 5.2, remains the same, except the longitudinal vehicle model, which is now given by

$$\begin{aligned} \dot{v}_{i,r} &= a_{i,r} \\ \dot{a}_{i,r} &= -\frac{1}{\tau} a_{i,r} + \frac{1}{\tau} u_{i,r} + \frac{1}{\tau} \frac{\tilde{m}_i}{m_i} u_{i,r}, \quad i \in S_m. \end{aligned} \quad (5.7)$$

In the vehicles for which the CACC approaches are designed, a maximum initial mass estimation error of approximately 20% is expected. Therefore, the initial mass estimates are chosen as $\hat{m}_i(0) = 0.16$ kg, for all vehicles. All other initial conditions are the same as in the previous sections. The presented simulations are used for tuning of the controller gains: the common approach is again

Table 5.5: Additional system parameters and control parameters, used in the scenario which assumes unknown vehicle masses.

Parameter	Symbol	Common	Alternative	Unit
Proportional feedback gain	k_p	1.5	1.5	-
Derivative feedback gain	k_d	5.0	5.0	-
Double derivative feedback gain	k_{dd}	0.0	0.0	-
Mass estimate gain	$\tilde{\gamma}_i$	50	500	-
Actual mass	m_i	0.20	0.20	kg

 Table 5.6: Average of the tracking error signal 2-norms $\|\varepsilon_{i,1}\|_2$ over the follower vehicles, calculated over the simulation time $t = [0 \ 70]$: a comparison between the case with and without mass estimation.

CACC approach	With mass estimate	No mass estimate
Common	0.0010	0.0011
Alternative	0.1229	0.2289

tuned such that the settling time smaller than 13 seconds for \hat{m}_i , while minimizing $\tilde{\gamma}_i$, k_p , and k_d . A settling time smaller than 13 seconds for \hat{m}_i is not achieved for the alternative approach. Therefore, these gains are tuned with the aim of minimizing the settling time, yielding a settling time of approximately 30 seconds. Table 5.5 lists the resulting values and additional parameters. The mass estimates are again fixed after these convergence periods. In line with the previous chapters, a continuous reference acceleration is specified for the first convergence period. For the remainder of the simulation $u_{0,r}$ is given by $u_{0,r} = -0.02$ for $40 < t \leq 42$, $u_{0,r} = 0.02$ for $52 < t \leq 54$, and zero for all other time periods. The corresponding accelerations are presented in Figure 5.11.

The mass estimates and tracking errors are depicted in Figure 5.12 and Figure 5.13 for the common and alternative approaches, respectively. These figures show that, for both approaches, the tracking errors are smaller than the tracking errors presented in sections 3.3.3 and 4.3.3, which is a direct consequence of the scaling of $u_{0,r}$. Moreover, Figure 5.13b shows that the alternative approach has a much larger tracking error during convergence of the mass estimates compared to the common approach. This is in line with the previous chapters and a consequence of the larger settling time and the higher sensitivity, as was explained in Chapter 4.

To compare the performance of the CACC approaches including mass estimation, the tracking errors of a second case are presented in Figure 5.14. This comparison case also assumes an unknown mass but does not use a mass estimator, i.e., $\hat{m}_i = 0.16$ kg throughout the simulation. Table 5.6 presents the average $\|\varepsilon_{i,1}\|_2$ over the follower vehicles, for the aforementioned second case and for the previously discussed case with mass estimation. This comparison case shows that utilizing the mass estimation results in a significant reduction of the tracking error in the alternative approach. Moreover, the comparison case illustrates that the mass estimation has very little influence on the tracking performance in the common approach. Hence, for both approaches, the behaviour is similar to the previous chapters, which validates the assumption that the low-level system approximates an integrator.

5.4 Experimental results

The effectiveness of the common and alternative CACC approaches was illustrated in Chapter 3 and Chapter 4, respectively, and the control structure was validated in the previous section. Now, this section presents experiment with the e-pucks to validate the simulations and provide insight into the performance of the control strategies when subject to sensor noise and delays.

First, the experiments are used to validate the theoretical results. To this end, Section 5.4.1 presents the results of the experiments in a case of regular platooning, with a focus on string

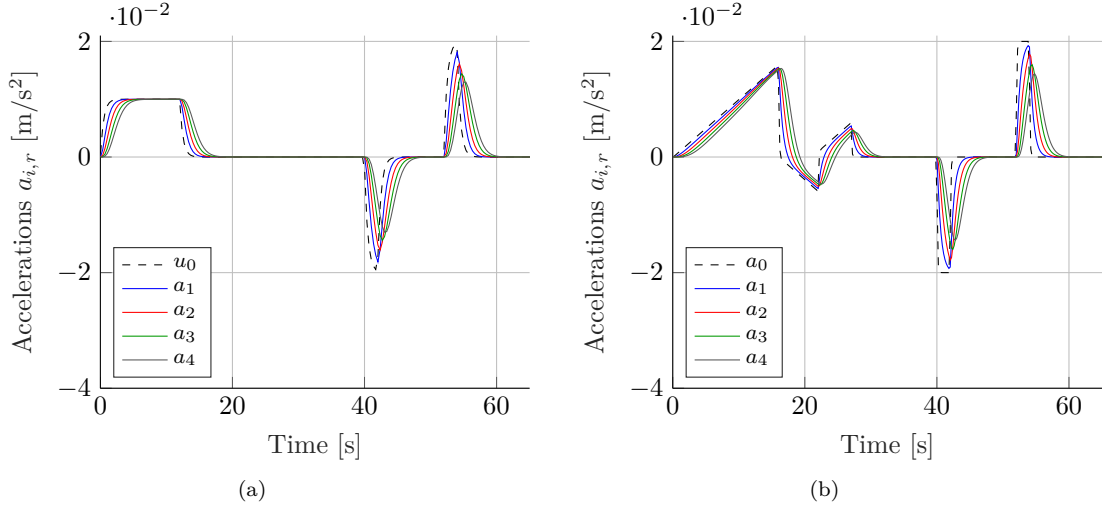
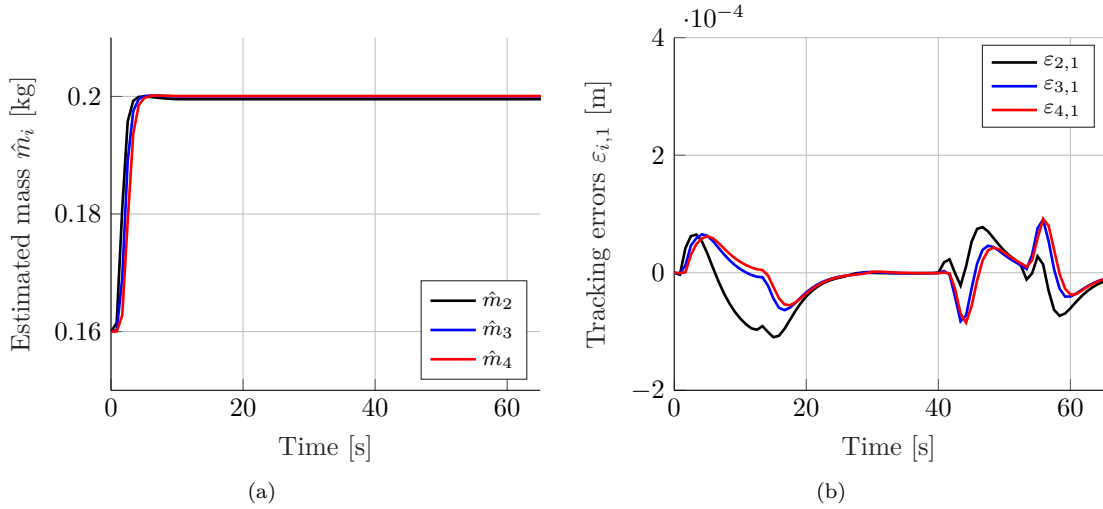


Figure 5.11: Acceleration profiles for (a) the common and (b) the alternative approach.


 Figure 5.12: Simulation results of the common approach: (a) mass estimates \hat{m}_i and (b) tracking errors $\varepsilon_{i,1}$.

stability. Next, sections 5.4.2 and 5.4.3 analyse and compare the longitudinal performance of the two approaches, focussing on the tracking errors of the follower vehicles in a heterogeneous vehicle platoon and for the case where the vehicle mass is unknown. Throughout this section the tracking errors and accelerations are used for the validation. In addition, the longitudinal positions and velocities are presented in Appendix G for completeness. All experiments in this section use (approximately) the same initial conditions, control parameters, and reference accelerations as in simulations of the previous section. Hence, the expectations of these experiments are set by the simulations presented in the previous section.

5.4.1 Regular platooning

To validate the simulations presented in Section 5.3.1 in the presence of communication delay and measurement noise, Figure 5.15a and Figure 5.16a present the accelerations $a_{i,r}$ for the common

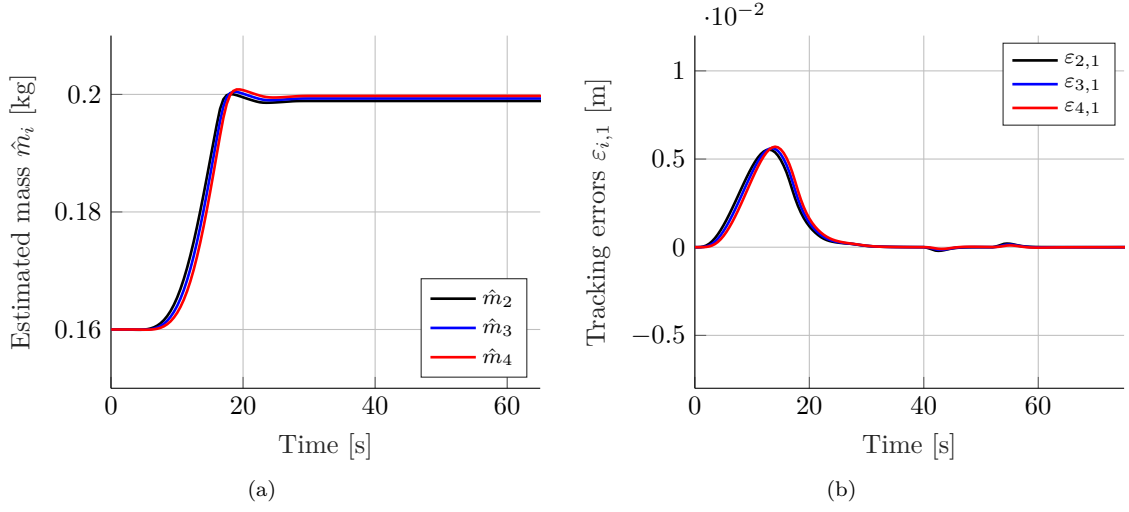


Figure 5.13: Simulation results of the alternative approach: (a) mass estimates \hat{m}_i and (b) tracking errors $\varepsilon_{i,1}$.

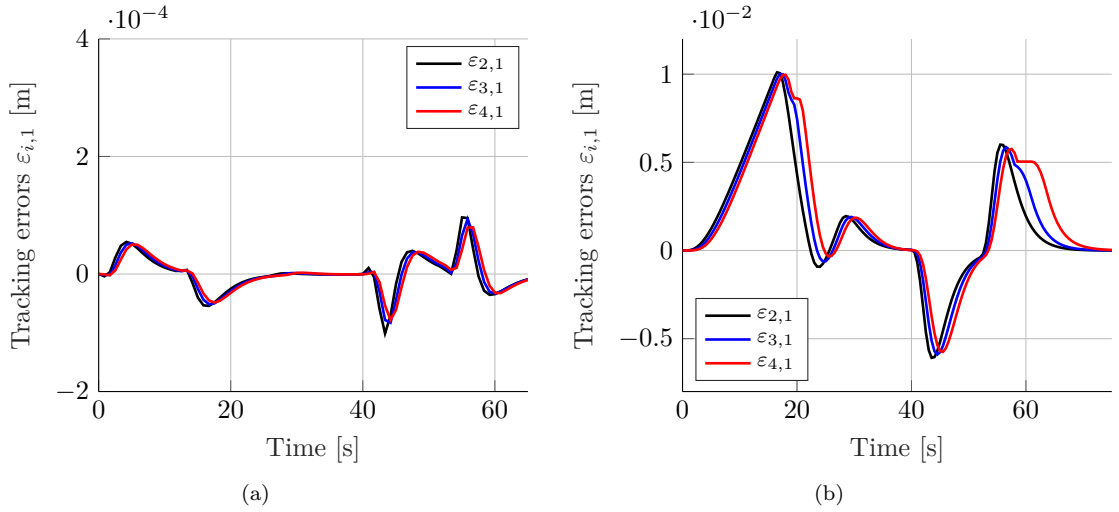


Figure 5.14: Tracking errors $\varepsilon_{i,1}$ of the case without mass estimation, for (a) the common approach and (b) the alternative approach.

and alternative approaches, respectively. Both show very strong similarities with the simulations presented in Section 5.3.1. The corresponding norms of these accelerations are given in Table 5.7 and decrease over the vehicle index, which confirms that the time gap $h = 0.5$ s yields string stability in the presence of the communication delay.

The tracking errors $\varepsilon_{i,1}$ are presented for the common and alternative approaches in Figure 5.15b and Figure 5.16b, respectively. The simulations presented in sections 3.3.1 and 4.3.1 illustrated that both approaches have a tracking error during acceleration and deceleration of the lead vehicle, which is caused by the communication delay θ . Additionally, the simulations in Section 5.3.1 illustrated that the tracking error also increases during acceleration and deceleration of the lead vehicle because the low-level system is only an approximation of a pure integrator. Hence, due to the communication delay in the experimental setup and the low-level approximation, the experimental tracking errors are larger than in the simulations. Moreover, in the experiments,

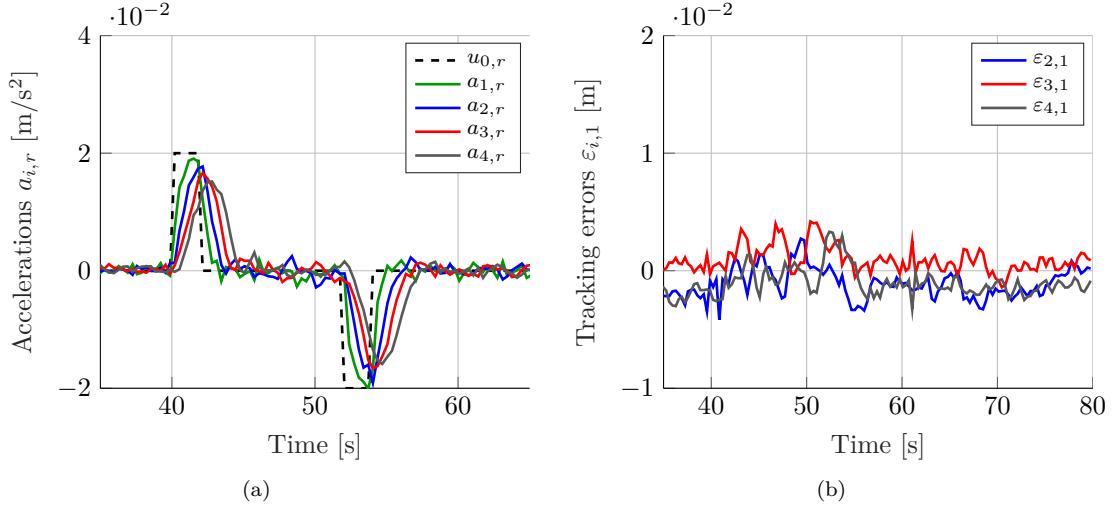


Figure 5.15: Experimental results of the common approach in a scenario of regular platooning: (a) accelerations $a_{i,r}$ and (b) tracking errors $\varepsilon_{i,1}$.

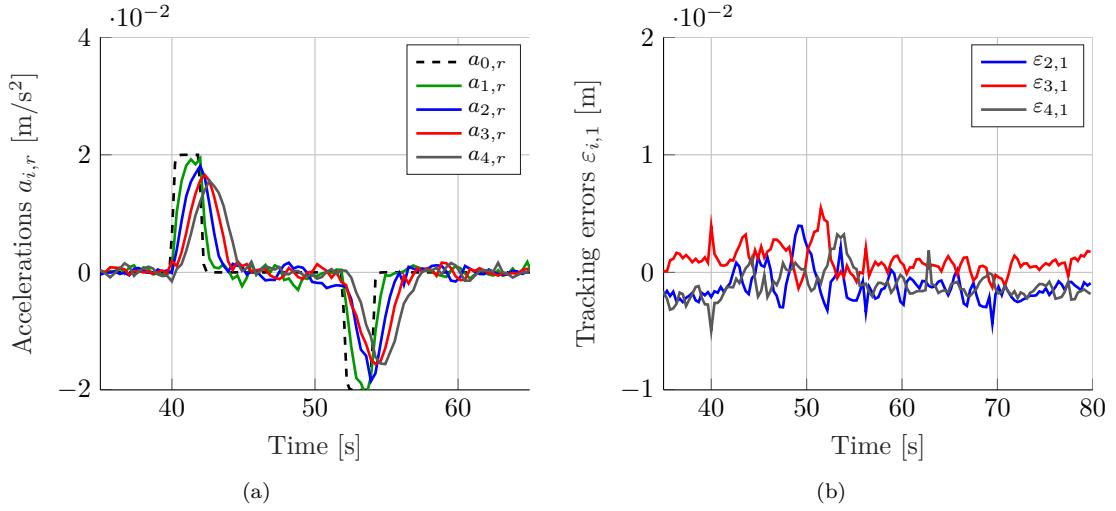


Figure 5.16: Experimental results of the alternative approach in a scenario of regular platooning: (a) accelerations $a_{i,r}$ and (b) tracking errors $\varepsilon_{i,1}$.

the tracking errors do not converge to zero because of the low sampling rate, which is limited by the frame rate of the overhead camera, and the noise which inherently exists in the experimental setup.

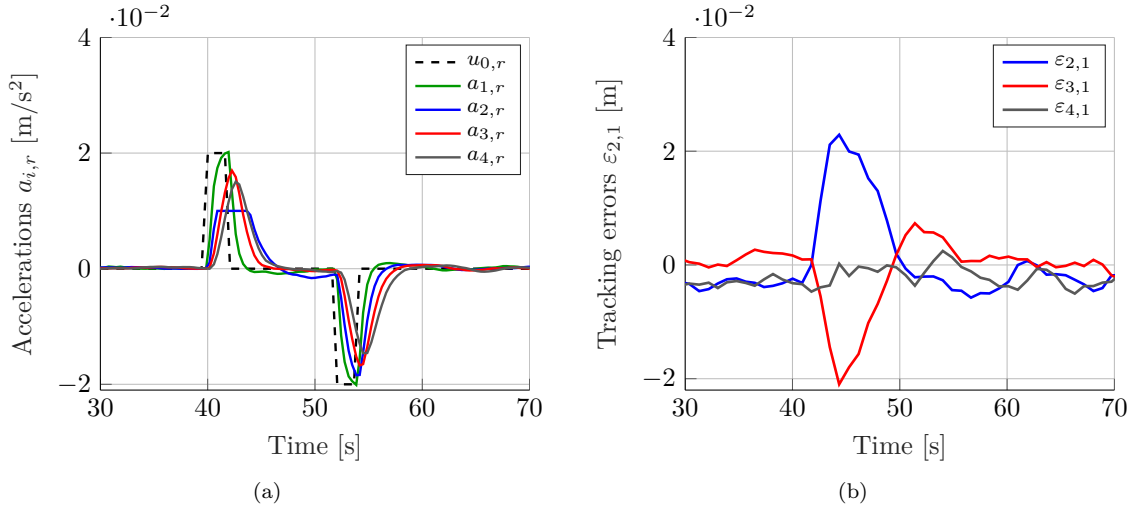
As was the case for the simulations presented in Section 5.3.1, Figure 5.15b and Figure 5.16b, illustrate that the tracking performance of the two approaches is approximately equal. This performance is achieved in a scenario of regular platooning, the following two sections analyze the tracking performance in different scenarios.

5.4.2 Heterogeneity

In this section all control parameters, system parameters and initial conditions are (approximately) equal to the simulations presented in Section 5.3.2. Hence, the expectations in this section are

Table 5.7: Acceleration norms common and alternative approach, calculated over the simulation time $t = [0 \ 80]$.

Acceleration norm	Common	Alternative
$\ a_1\ _2$	0.3400	0.3184
$\ a_2\ _2$	0.3358	0.2974
$\ a_3\ _2$	0.3162	0.2824
$\ a_4\ _2$	0.2966	0.2712


 Figure 5.17: Experimental results of the common approach in a platoon with differences in acceleration limits: (a) accelerations $a_{i,r}$ and (b) tracking errors $\varepsilon_{i,1}$.

again set by the corresponding simulations. In line with the previous chapters, two different heterogeneous vehicle platoons are considered. First, for the case where heterogeneity is caused by different acceleration limits, Figure 5.17 and Figure 5.18 present the response of the accelerations $a_{i,r}$ and tracking errors $\varepsilon_{i,1}$ of the common and alternative approaches, respectively. Second, for the case where heterogeneity is caused by different vehicle dynamics, Figure 5.19 and Figure 5.20 present the response of the accelerations $a_{i,r}$ and tracking errors $\varepsilon_{i,1}$ of the common and alternative approaches, respectively.

Based on the experimental results presented in Section 5.4.1, it was concluded that the simulation model is accurate and that the control strategies perform satisfactory in the presence of sensor noise and delays. This is again confirmed by the results presented in this section. Because of the strong similarities with the simulations presented in Subsection 5.3.2, the conclusions of that section also hold for the presented experiments. In other words, the main conclusion remains that the alternative CACC controller performs significantly better than the common CACC controller for the presented heterogeneous vehicle platoons.

5.4.3 Mass estimation

This section aims to validate the results of the simulations presented in Section 5.3.3, in the presence of delays and measurement noise. The initial conditions, system parameters, control parameters and references accelerations are (approximately) equal to those in Section 5.3.3. Figure 5.21 and Figure 5.22 present the mass estimates and tracking errors. The mass estimates of the common and alternative approach show similar differences compared to the simulation results presented in Section 5.3.3: the alternative approach has a larger settling time, resulting in larger tracking errors during convergence of the mass estimates.

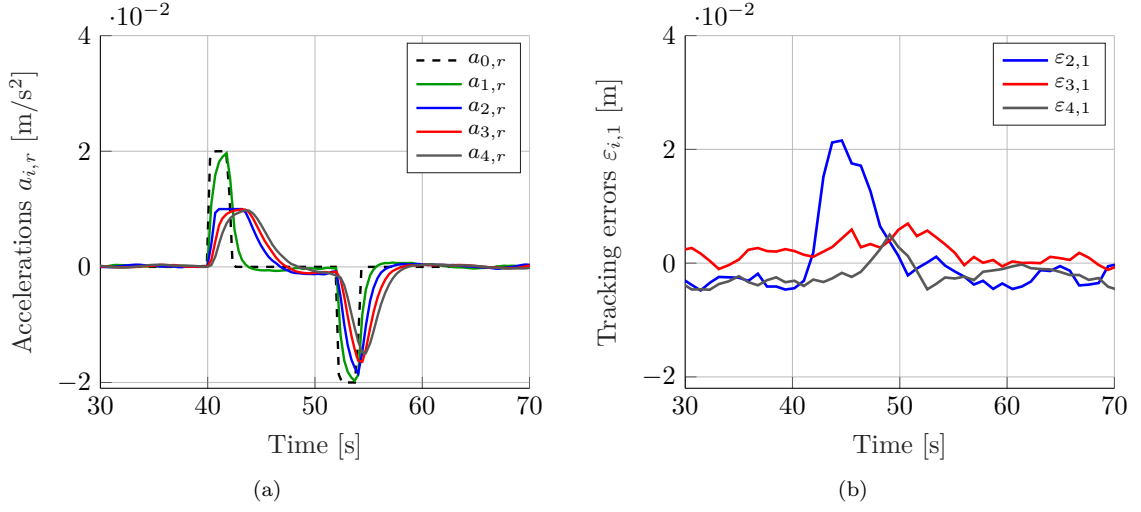


Figure 5.18: Experimental results of the alternative approach in a platoon with differences in acceleration limits: (a) accelerations $a_{i,r}$ and (b) tracking errors $\varepsilon_{i,1}$.

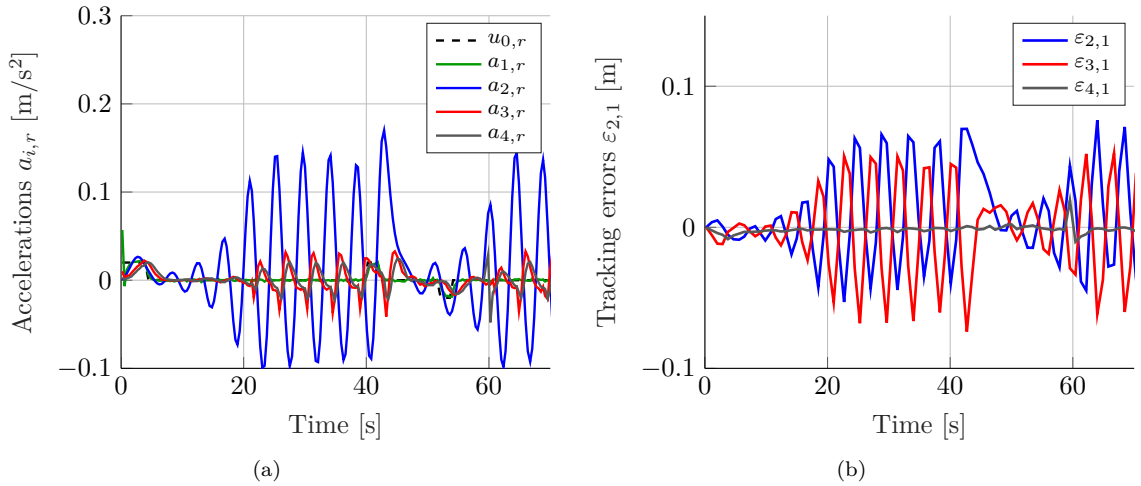


Figure 5.19: Experimental results of the common approach in a platoon with differences in vehicle dynamics: (a) accelerations $a_{i,r}$ and (b) tracking errors $\varepsilon_{i,1}$.

To validate the tracking performance, Table 5.8 and Table 5.9 present the average $\|\varepsilon_{i,1}\|_2$ of the follower vehicles, for the common and alternative approach, respectively, and show that the amplitude of the tracking errors is much larger compared to the simulations presented in Section 5.3.3. This increase can be explained by the delay, which was not considered in the simulations and is known to increase the tracking error, and by the measurements noise due to which the tracking errors do not converge to zero. Table 5.8 shows, for the common approach, that the mass estimation has little influence on the tracking error, which is conform expectation and validates simulations. However, Table 5.9 shows that, for the alternative approach, the average norm of the tracking error is larger when the mass estimation is utilized. This is not conform expectation but can be understood as follows. Figure 5.22a shows non-minimal phase behaviour which was not present in the simulations. This non-minimal phase behaviour results in a large peak in the tracking error, as illustrated in Figure 5.22b, which causes the average tracking error to be larger compared to the case without mass estimation. The expected reduction of the tracking

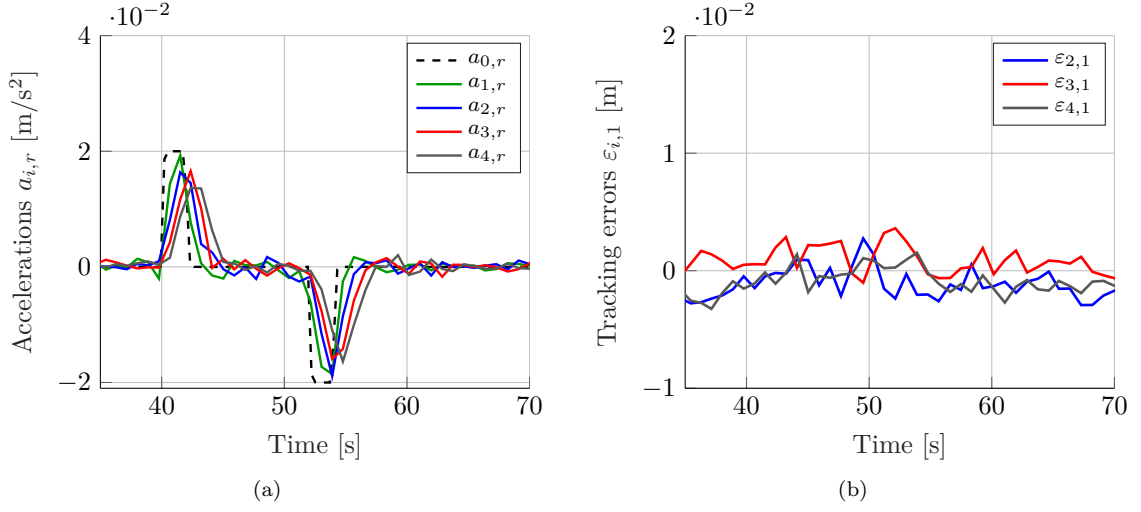


Figure 5.20: Experimental results of the alternative approach in a platoon with differences in vehicle dynamics: (a) accelerations $a_{i,r}$ and (b) tracking errors $\varepsilon_{i,1}$.

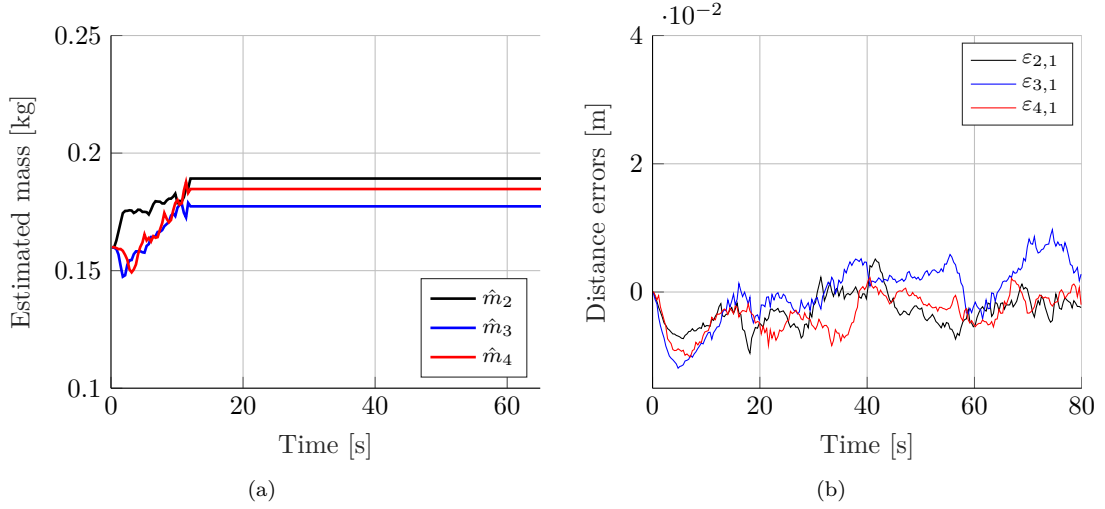


Figure 5.21: Experimental results of the common approach: (a) mass estimates \hat{m}_i and (b) tracking errors $\varepsilon_{i,1}$.

error can be seen after the mass estimates are fixed, as shown in Table 5.10 which shows the average tracking error signal 2-norms $\|\varepsilon_{i,1}\|_2$ of the follower vehicles for $t > 30$ s. Based on this, it is concluded that the mass estimation only improves the performance after the mass estimates are fixed and that the non-minimal phase behaviour poses a serious limitation on the performance of the mass estimation for the alternative approach.

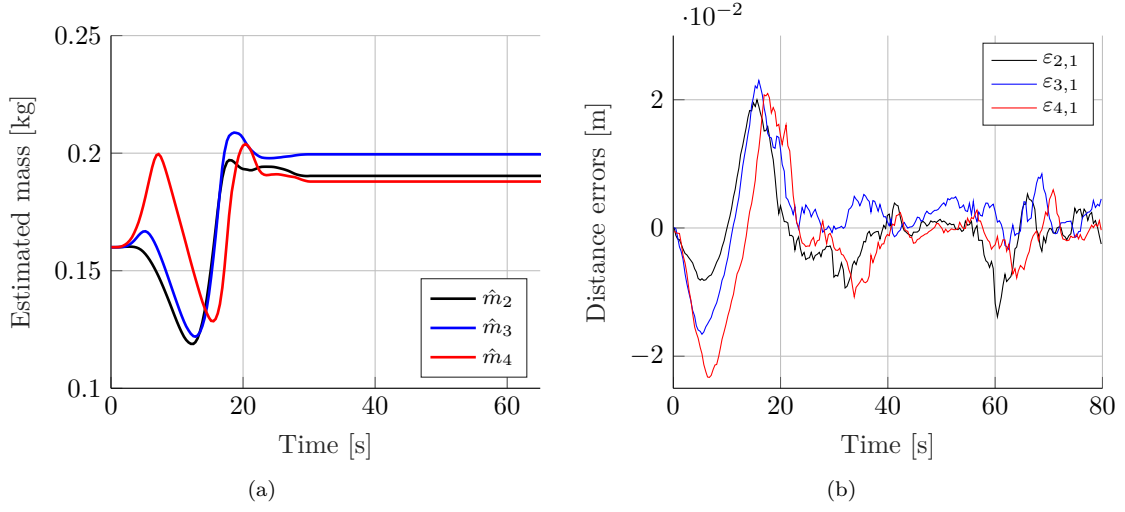


Figure 5.22: Experimental results of the alternative approach: (a) mass estimates \hat{m}_i and (b) tracking errors $\varepsilon_{i,1}$.

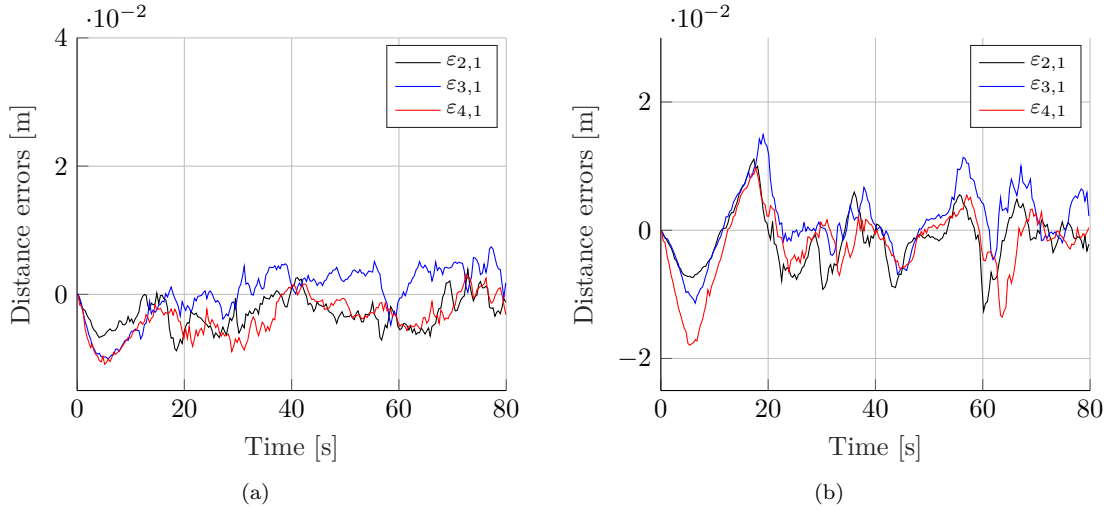


Figure 5.23: Experimental tracking errors $\varepsilon_{i,1}$ of the second case, without mass estimation, for (a) the common approach and (b) the alternative approach.

Table 5.8: Common approach average tracking error signal 2-norms $\|\varepsilon_{i,1}\|_2$ of the follower vehicles, calculated over the simulation time $t = [0 \ 80]$: comparison between the case with and without mass estimation.

Run	With mass estimate	No mass estimate
Run 1	0.2128	0.2228
Run 2	0.2126	0.2349
Run 3	0.2148	0.2057
Combined average	0.2134	0.2211

Table 5.9: Alternative approach average tracking error signal 2-norms $\|\varepsilon_{i,1}\|_2$ of the follower vehicles, calculated over the simulation time $t = [0 \ 80]$: comparison between the case with and without mass estimation.

Run	With mass estimate	No mass estimate
Run 1	0.3071	0.2525
Run 2	0.3447	0.2922
Run 3	0.3263	0.2663
Combined average	0.3260	0.2703

Table 5.10: Alternative approach average tracking error signal 2-norms $\|\varepsilon_{i,1}\|_2$ of the follower vehicles, for $t = [30 \ 70]$ s: comparison between the case with and without mass estimation.

Run	With mass estimate	No mass estimate
Run 1	0.1295	0.1560
Run 2	0.1340	0.1657
Run 3	0.1463	0.1518
Combined average	0.1366	0.1578

5.5 Summary

This chapter started in Section 5.1 with describing the experimental platform that is used for the validation of the CACC approaches presented in Chapter 3 and Chapter 4. After the introduction of the main components and characteristics of the experimental platform, the control structure used for the implementation of the CACC approaches was explained in Section 5.2. This section explained how the performance of the one-dimensional CACC approaches can be tested on the two-dimensional experimental platform, which requires a longitudinal as well as lateral controller.

Section 5.3 validated the presented control structure by comparing platoon simulations with the simulation results that were presented in the previous chapters. The three scenarios regular platooning, heterogeneity and mass estimation, which are used throughout this thesis, were followed for this validation. The first scenario illustrated that the adopted control structure introduces a tracking error because the low-level is not an exact integrator. However, this scenario also illustrated that string stability of the platoon was achieved and, therewith, illustrated the control structure can effectively be used to test the CACC approaches. Moreover, the two subsequent sections, focussing on heterogeneity and mass estimation, validated the control structure, since the simulations showed similar results compared to the previous chapters.

Finally, Section 5.4 validated the simulations presented in the previous section and provided insight into the performance of the control strategies in the presence of sensor noise and delays. The experimental results confirmed that the alternative approach is more effective in a heterogeneous vehicle platoon. Moreover, for the case with an unknown vehicle mass, the experimental results illustrated that the non-minimal phase behaviour poses a limitation on the performance of the alternative approach.

Chapter 6

Conclusions and recommendations

This chapter summarizes the main conclusions from this thesis in Section 6.1 and discusses the resulting topics for future research in Section 6.2.

6.1 Conclusions

Cooperative automated driving is a field of research, that strives to fulfil the social demand for clean, safe and efficient traffic systems, driven by technological innovation. Cooperative adaptive cruise control is a form of automated driving, which automates the longitudinal control of vehicles in a platoon. To reach its full potential in increasing traffic throughput, safety, and reducing fuel consumption, cooperative adaptive cruise controllers must achieve the control objectives of close-distance vehicle following and guaranteeing string stability of the platoon. To guarantee string stability and minimize the inter-vehicle distance between adjacent vehicles, CACC employs wireless communication.

Because of its high potential and the strong development of wireless communication technology in recent years, CACC is a well studied subject and various approaches are available in literature. A commonly adopted approach communicates the desired acceleration between platoon vehicles. As a direct consequence of communicating the desired acceleration, knowledge of the dynamic behaviour of a predecessor is required to obtain its response. This knowledge may not be available due to, for instance, reluctance of vehicle manufacturers to share this information. To overcome the absence of this information, homogeneity of the platoon dynamics is often assumed. With this assumption, the common approach can achieve both control objectives. This is partly realized by feedback linearisation of the vehicle model, which not only linearises the vehicle dynamics, but inherently also compensates for the vehicle mass, such that the resulting model is linear and independent of vehicle mass. With respect to the other model parameters, it is simply assumed that these are identical for all platoon vehicles. To enable platooning with vehicles which have an unknown and possibly varying vehicle mass, this common approach was extended with a dynamically updated mass estimation law, the result of which is used in the feedback linearisation. As a result, robustness against inhomogeneity regarding vehicle mass is obtained.

Homogeneity of the platoon is not always a realistic assumption, e.g., in case of *ad hoc* platooning, where not only the vehicle mass but also other parameters can differ between vehicles. A novel alternative CACC approach was presented, which communicates the realized acceleration instead of the desired acceleration. As a consequence, no knowledge of the dynamic behaviour of a predecessor is required to effectively achieve both control objectives in a heterogeneous vehicle platoon.

Throughout this thesis the common and alternative CACC approach were compared using three scenarios: a regular vehicle platoon with a focus on string stability, a heterogeneous vehicle platoon, and a vehicle platoon with unknown vehicle masses. Using these three scenarios the following was concluded: in the regular platooning scenario, it is possible to tune the alternative

CACC controller such that the tracking errors of both approaches show similar behaviour and such that the alternative approach allows for slightly smaller inter-vehicle distances, while guaranteeing string stability. This means that, in the regular platooning scenario, quantitative performance of the alternative approach which is at least equal to the performance of the common approach can be achieved. In a heterogeneous vehicle platoon, where the desired and realized accelerations of platoon vehicles are different or vehicles have different dynamics, the platoon can become string unstable in the common approach, which may result in unsafe behaviour. When, on the other hand, the alternative approach is adopted, the platoon remains string stable and safety is guaranteed. Finally, the control objectives were achieved in a platoon with unknown vehicle masses for both approaches, by utilizing an adaptive mass estimation law. For the alternative approach, the settling time posed a limitation. Moreover, the common approach appeared to be more robust against the remaining estimation error, resulting in a larger tracking error for the alternative approach.

6.2 Recommendations

This thesis advocates the use of the realized acceleration of preceding vehicles as feedforward input, so as to overcome issues relating heterogeneity of vehicle platoons and allow for *ad hoc* platooning without requiring knowledge of the dynamic behaviour and limitations of the preceding vehicle. The acceleration signal can be obtained in various ways, e.g., by applying a low-pass filter to the desired acceleration. However, this option would not take into account limitations of the vehicle model, such as, for instance, limitations of the driveline. It was shown in this thesis that these limitations can result in unsafe driving behaviour. Therefore, a preferred option would be to measure the acceleration signal. A consequence of using a measured input signal is that this it contains noise, the effects of this noise are not addressed in this work. Therefore, it is advised to investigate these effects before practical implementation. A feasible option to overcome the issue of noise on the realized acceleration could, for instance, be to use an estimator to obtain this signal.

Furthermore, it was discussed that the large settling time of the mass estimation poses a serious drawback to the adaptive control strategy. In particular for the alternative approach, this resulted in a decrease in performance compared to the ideal scenario where the vehicle mass is known. Additional research is recommended to improve the tuning of the alternative approach to achieve shorter settling times and, therefore, increasing the tracking performance. It is also recommended that comfortable driving behaviour, which was not explicitly considered in this work, is taken into account, since this limits the tuning possibilities. If tuning does not result in satisfactory performance, another possibility would be to consider different control methods that increase the robustness of the approach. Robust control is the most common alternative to the presented adaptive control method, when dealing with parameter uncertainty. To increase the robustness of the CACC approach, various control methods can be used. Options of control methods that are known for their robustness properties are, for instance, sliding mode control or \mathcal{H}_∞ control.

Finally, the scope of this thesis was limited to the longitudinal performance of CACC, without initial position errors. This scope is often considered as a first step towards full integration of automated driving into regular traffic. However, since it is only the first step towards full integration, future research is required on the many subsequent steps in this process. Some of these subsequent steps are, for instance, the design of a gap closing controller to take into account initial position errors, the inclusion of lateral control to allow for more advanced manoeuvres such as merging of vehicle platoons, or discussing some of the many safety related aspects, like reliability of communication or collision avoidance mechanisms.

Bibliography

- B. Aarts, S. Chalker, E. Weiner, and O. U. Press. The Oxford dictionary of English grammar, 2014. URL <https://en.oxforddictionaries.com/definition/heterogeneous>. Accessed: 2018.
- A. Al-Jhayyish and K. Schmidt. Feedforward strategies for cooperative adaptive cruise control in heterogeneous vehicle strings. *IEEE Transactions on Intelligent Transportation Systems*, 19(1): 113–122, Jan 2018.
- Allied Vision Technologies. AVT guppy technical manual, March 2008. URL https://www.stemmer-imaging.com/media/uploads/cameras/avt/50/50664-Allied_Vision_Guppy_Technical_Manual_oudZ1Ay.pdf.
- B. Arem, C. Driel van, and R. Visser. The impact of cooperative adaptive cruise control on traffic-flow characteristics. *IEEE Transactions on Intelligent Transportation Systems*, 7(4):429–436, Dec 2006.
- I. Barkana. Simple adaptive control - a stable direct model reference adaptive control methodology — brief survey. *IFAC Proceedings Volumes*, 40(13):310–327, 2007.
- M. Barth and K. Boriboonsomsin. Real-world carbon dioxide impacts of traffic congestion. *Transportation Research Record*, 2058(1):163–171, 2008.
- I. Bayezit, T. Veldhuizen, B. Fidan, J. Huissoon, and H. Lupker. Design of string stable adaptive cruise controllers for highway and urban missions. In *2012 50th Annual Allerton Conference on Communication, Control, and Computing (Allerton)*, pages 106–113, Monticello, IL, USA, Oct 2012.
- A. Bayuwindra, O. Aakre, J. Ploeg, and H. Nijmeijer. In *Combined lateral and longitudinal CACC for a unicycle-type platoon*, pages 527–532, 2016.
- T. Beumer. *Control of Platooning Mobile Robots: Experimental Validation*. Technische Universiteit Eindhoven, Department of Mechanical Engineering, 2017. Master’s thesis.
- C. Bonnet and H. Fritz. Fuel consumption reduction in a platoon: Experimental results with two electronically coupled trucks at close spacing. In *Future Transportation Technology Conference and Exposition*, Costa Mesa, CA, USA, Aug 2000. SAE International.
- F. Browand, J. McArthur, and C. Radovich. Fuel saving achieved in the field test of two tandem trucks. In *UC Berkeley: California Partners for Advanced Transportation Technology*, 2004.
- Centre for Economics and Business Research. The future economic and environmental costs of gridlock in 2030, July 2014. URL <http://www.cebr.com/reports/the-future-economic-and-environmental-costs-of-gridlock/>. Technical report, Cebr, London.
- D. Chen, S. Ahn, M. Chitturi, and D. Noyce. Truck platooning on uphill grades under cooperative adaptive cruise control (CACC). *Transportation Research Part C: Emerging Technologies*, 94: 50–66, 2018.

- C. Desjardins and B. Chaib-draa. Cooperative adaptive cruise control: A reinforcement learning approach. *IEEE Transactions on Intelligent Transportation Systems*, 12(4):1248–1260, Dec 2011.
- M. di Bernardo, A. Salvi, and S. Santini. Distributed consensus strategy for platooning of vehicles in the presence of time-varying heterogeneous communication delays. *IEEE Transactions on Intelligent Transportation Systems*, 16(1):102–112, Feb 2015.
- W. Dixon, D. Dawson, E. Zergeroglu, and F. Zhang. Robust tracking and regulation control for mobile robots. *International Journal of Robust and Nonlinear Control*, 10(4):199–216, 2000.
- J. Doyle, B. Francis, and A. Tannenbaum. *Feedback control theory*. Macmillan Publishing Co., London, United Kingdom, 1990.
- T. Gillespie. *Fundamentals of Vehicle Dynamics*. SAE Publications, 1992.
- D. Godbole and J. Lygeros. Longitudinal control of the lead car of a platoon. *IEEE Transactions on Vehicular Technology*, 43(4):1125–1135, Nov 1994.
- P. Goncalves, P. Torres, C. Alves, F. Mondada, M. Bonani, X. Raemy, J. Pugh, C. Cianci, A. Klaptocz, S. Magnenat, J. Zufferey, D. Floreano, and A. Martinoli. The e-puck, a robot designed for education in engineering. In *Proceedings of the 9th Conference on Autonomous Robot Systems and Competitions*, volume 1, Castelo Branco, Portugal, Jan 2009.
- Y. Harfouch, S. Yuan, and S. Baldi. An adaptive switched control approach to heterogeneous platooning with intervehicle communication losses. *IEEE Transactions on Control of Network Systems*, 5(3):1434–1444, Sept 2018.
- Y. Hori. Future vehicle driven by electricity and control-research on four wheel motored "UOT electric march II". *IEEE Transactions on Industrial Electronics*, 51(5):954–962, Oct 2004.
- H. Huang and C. Tsai. Adaptive trajectory tracking and stabilization for omnidirectional mobile robot with dynamic effect and uncertainties. *IFAC Proceedings Volumes*, 41(2):5383–5388, 2008. 17th IFAC World Congress, Seoul, Korea.
- International Organization for Standardization. Adaptive cruise control systems – performance requirements and test procedures, April 2010. ISO Standard 15622.
- P. Ioannou and C. Chien. Autonomous intelligent cruise control. *IEEE Transactions on Vehicular Technology*, 42(4):657–672, Nov 1993.
- Z. Jiang and H. Nijmeijer. Tracking control of mobile robots: A case study in backstepping. *Automatica*, 33(7):1393–1399, 1997.
- Y. Jong-Min and K. Jong-Hwan. Sliding mode control for trajectory tracking of nonholonomic wheeled mobile robots. *IEEE Transactions on Robotics and Automation*, 15(3):578–587, June 1999.
- A. Kalberlah. Electric hybrid drive systems for passenger cars and taxis. *SAE Transactions*, 100: 404–413, 1991.
- H. Khalil. *Nonlinear systems; 3rd edition*. Prentice Hall, Upper Saddle River, NJ, United States, 2002.
- P. Khatun, C. Bingham, N. Schofield, and P. Mellor. Application of fuzzy control algorithms for electric vehicle antilock braking/traction control systems. *IEEE Transactions on Vehicular Technology*, 52(5):1356–1364, Sept 2003.

- R. Kianfar, B. Augusto, A. Ebadighajari, U. Hakeem, J. Nilsson, A. Raza, R. Tabar, N. Irukulapati, C. Englund, P. Falcone, S. Papanastasiou, L. Svensson, and H. Wymeersch. Design and experimental validation of a cooperative driving system in the grand cooperative driving challenge. *IEEE Transactions on Intelligent Transportation Systems*, 13(3):994–1007, Sept 2012.
- D. Kostic, S. Adinandra, J. Caarls, N. van de Wouw, and H. Nijmeijer. Saturated control of time-varying formations and trajectory tracking for unicycle multi-agent systems. In *49th IEEE Conference on Decision and Control (CDC)*, pages 4054–4059, Atlanta, GA, USA, Dec 2010.
- M. Lammert, A. Duran, J. Diez, K. Burton, and A. Nicholson. Effect of platooning on fuel consumption of class 8 vehicles over a range of speeds, following distances, and mass. *SAE International Journal of Commercial Vehicles*, 7:626–639, 2014.
- R. Marino. Adaptive control of nonlinear systems: Basic results and applications. *Annual Reviews in Control*, 21:55–66, 1997.
- K. Narendra and A. Annaswamy. Persistent excitation in adaptive systems. *International Journal of Control*, 45(1):127–160, 1987.
- G. Naus, R. Vugts, J. Ploeg, M. van de Molengraft, and M. Steinbuch. String-stable CACC design and experimental validation: A frequency-domain approach. *IEEE Transactions on Vehicular Technology*, 59(9):4268–4279, Nov 2010.
- B. Netten, T. van den Broek, and G. Blom. A270 demo schokgolfdemping. In *Nationaal verkeerskundecongres*, Rotterdam, the Netherlands, Nov 2010. TNO, Integrated Safety.
- S. Öncü. *String stability of interconnected vehicles : network-aware modelling, analysis and experiments*. PhD thesis, Technische Universiteit Eindhoven, Department of Mechanical Engineering, 2014.
- J. Ploeg. *Analysis and design of controllers for cooperative and automated driving*. PhD thesis, Technische Universiteit Eindhoven, Department of Mechanical Engineering, 2014.
- J. Ploeg, D. P. Shukla, N. van de Wouw, and H. Nijmeijer. Controller synthesis for string stability of vehicle platoons. *IEEE Transactions on Intelligent Transportation Systems*, 15(2):854–865, April 2014a.
- J. Ploeg, N. van de Wouw, and H. Nijmeijer. Lp string stability of cascaded systems: Application to vehicle platooning. *IEEE Transactions on Control Systems Technology*, 22(2):786–793, March 2014b.
- J. Ploeg, E. Semsar-Kazerooni, G. Lijster, N. van de Wouw, and H. Nijmeijer. Graceful degradation of cooperative adaptive cruise control. *IEEE Transactions on Intelligent Transportation Systems*, 16(1):488–497, Feb 2015.
- F. Pourboghrat and M. P. Karlsson. Adaptive control of dynamic mobile robots with nonholonomic constraints. *Computers and Electrical Engineering*, 28(4):241–253, 2002.
- B. Powell, K. Bailey, and S. Cikanek. Dynamic modeling and control of hybrid electric vehicle powertrain systems. *IEEE Control Systems Magazine*, 18(5):17–33, Oct 1998.
- Publications Office of the European Union. Statistical office of the european communities, energy, transport and environment indicators, 2017. URL <https://ec.europa.eu/eurostat/documents/3217494/8435375/KS-DK-17-001-EN-N.pdf/18d1ecfd-acd8-4390-ade6-e1f858d746da>. Luxembourg.
- R. Ramakers, K. Henning, S. Gies, D. Abel, and H. Max. Electronically coupled truck platoons on german highways. In *2009 IEEE International Conference on Systems, Man and Cybernetics*, pages 2409–2414, Oct 2009.

- Rijksoverheid. Regeerakkoord “vertrouwen in de toekomst”, 2017. URL <https://www.rijksoverheid.nl/regering/regeerakkoord-vertrouwen-in-de-toekomst>. Website is in Dutch.
- G. Rodonyi. An adaptive spacing policy guaranteeing string stability in multi-brand ad hoc platoons. *IEEE Transactions on Intelligent Transportation Systems*, 19(6):1902–1912, June 2018.
- W. Schakel, B. van Arem, and B. Netten. Effects of cooperative adaptive cruise control on traffic flow stability. In *13th International IEEE Conference on Intelligent Transportation Systems*, pages 759–764, Funchal, Portugal, Sept 2010.
- P. Seiler, A. Pant, and J. Hedrick. Disturbance propagation in vehicle strings. *IEEE Transactions on Automatic Control*, 49(10):1835–1842, Oct 2004.
- E. Shaw and J. Hedrick. String stability analysis for heterogeneous vehicle strings. In *2007 American Control Conference (ACC)*, pages 3118–3125, San Diego, CA, USA, July 2007. New York, NY, USA.
- S. Sheikholeslam and C. Desoer. Longitudinal control of a platoon of vehicles. In *1990 American Control Conference ACC*, pages 291–296, San Diego, CA, USA, May 1990.
- S. Sheikholeslam and C. Desoer. A system level study of the longitudinal control of a platoon of vehicles. *Journal of Dynamics Systems, Measurement and Control*, 114(2):286–292, 1992.
- S. Shladover. Longitudinal control of automated guideway transit vehicles within platoons. *Journal of Dynamic Systems, Measurement, and Control*, 113(2):302–310, June 1978.
- S. Stankovic, M. Stanojevic, and D. Siljak. Decentralized overlapping control of a platoon of vehicles. *IEEE Transactions on Control Systems Technology*, 8(5):816–832, Sept 2000.
- S. Studli, M. Seron, and R. Middleton. From vehicular platoons to general networked systems: String stability and related concepts. *Annual Reviews in Control*, 44:157–172, 2017.
- D. Swaroop and J. Hedrick. String stability of interconnected systems. *IEEE Transactions on Automatic Control*, 41(3):349–357, March 1996.
- D. Swaroop, J. Hedrick, C. Chien, and P. Ioannou. A comparison of spacing and headway control laws for automatically controlled vehicles. *Vehicle System Dynamics*, 23(1):597–625, 1994.
- R. R. Teetor. Speed control device for resisting operation of the accelerator, 1948. US Patent No. US2519859A.
- S. G. Tzafestas. *Introduction to Mobile Robot Control: Adaptive and Robust Methods*. Elsevier, Oxford, United Kingdom, 2014.
- UN. United Nations Paris Agreement. <https://bigpicture.unfccc.int/content-the-paris-agreement>, 2015.
- A. Vahidi and A. Eskandarian. Research advances in intelligent collision avoidance and adaptive cruise control. *IEEE Transactions on Intelligent Transportation Systems*, 4(3):143–153, Sept 2003.
- T. van den Broek, N. van de Wouw, and H. Nijmeijer. Formation control of unicycle mobile robots: a virtual structure approach. In *Proceedings of the 48th IEEE Conference on Decision and Control (CDC) held jointly with 2009 28th Chinese Control Conference*, pages 8328–8333, Shanghai, China, Dec 2009.
- M. Vidyasagar. *Nonlinear Systems Analysis*. Society for Industrial and Applied Mathematics, second edition, 2002.

- C. Wang and H. Nijmeijer. String stable heterogeneous vehicle platoon using cooperative adaptive cruise control. In *IEEE 18th International Conference on Intelligent Transportation Systems*, pages 1977–1982, Gran Canaria, Spain, Sept 2015.
- J. Zegers, E. Semsar-Kazerooni, M. Fusco, and J. Ploeg. A multi-layer control approach to truck platooning: Platoon cohesion subject to dynamical limitations. In *2017 5th IEEE International Conference on Models and Technologies for Intelligent Transportation Systems (MT-ITS)*, pages 128–133, Napels, Italy, June 2017.
- C. Zhai, Y. Liu, and F. Luo. A switched control strategy of heterogeneous vehicle platoon for multiple objectives with state constraints. *IEEE Transactions on Intelligent Transportation Systems*, 20(5):1883–1896, May 2019.
- Y. Zhang, D. Hong, J. Chung, and S. Velinsky. Dynamic model based robust tracking control of a differentially steered wheeled mobile robot. In *Proceedings of the 1998 American Control Conference (ACC)*, volume 2, pages 850–855, Philadelphia, PA, USA, June 1998.
- K. Zheng, T. Shen, and Y. Yao. A robust nonlinear control approach for the traction problem in electrical vehicles. In *2006 IEEE Vehicle Power and Propulsion Conference*, pages 1–5, Windsor, UK, Sep. 2006.
- Y. Zheng, S. E. Li, J. Wang, D. Cao, and K. Li. Stability and scalability of homogeneous vehicular platoon: Study on the influence of information flow topologies. *IEEE Transactions on Intelligent Transportation Systems*, 17(1):14–26, Jan 2016.
- Y. Zheng, S. Li, K. Li, F. Borrelli, and J. Hedrick. Distributed model predictive control for heterogeneous vehicle platoons under unidirectional topologies. *IEEE Transactions on Control Systems Technology*, 25(3):899–910, May 2017.
- Y. Zheng, Y. Bian, S. Li, and S. E. Li. Cooperative control of heterogeneous connected vehicles with directed acyclic interactions. *IEEE Intelligent Transportation Systems Magazine*, pages 1–1, 2019.

Appendix A

Preliminaries

This appendix presents several preliminaries used throughout the thesis.

A.1 Feedback linearisation

Khalil (2002) presents the following definition regarding feedback linearisation.

Definition A.1 (Feedback linearisation) *A nonlinear system*

$$\dot{x} = f(x) + G(x)u, \quad (\text{A.1})$$

where $f : D \mapsto \mathbb{R}^n$ and $G : D \mapsto \mathbb{R}^{n \times p}$ are sufficiently smooth on a domain $D \in \mathbb{R}^n$, is said to be feedback linearisable if there exists a diffeomorphism $T : D \mapsto \mathbb{R}^n$ such that $D_z = T(D)$ contains the origin and the change of variables $z = T(x)$ transforms the system A.1 into the form

$$\dot{z} = Az + B\gamma(z)[u - \alpha(z)] \quad (\text{A.2})$$

with (A, B) controllable and $\gamma(z)$ nonsingular for all $x \in D$. Then, the state feedback control law

$$u = \alpha(z) + \beta(z)v, \quad (\text{A.3})$$

where $\beta(z) = \gamma^{-1}(z)$, can be used to transform the nonlinear system (A.1) into the linear system

$$\dot{z} = Az + Bv. \quad (\text{A.4})$$

A.2 Gronwall's lemma

Vidyasagar (2002) presents Gronwall's lemma in the following form.

Lemma A.2 (Gronwall's inequality). *Suppose a $\mathbb{R}_+ \rightarrow \mathbb{R}_+$ is a continuous function, and $b, c \geq 0$ are given constants. Under these conditions, if*

$$\dot{a}(t) \leq ca(t), \quad \forall t \geq 0, \quad (\text{A.5})$$

then

$$a(t) \leq be^{ct}, \quad \forall t \geq 0. \quad (\text{A.6})$$

A.3 Matrix submultiplicative property

Consider the following property of matrix norms:

Definition A.3 (Submultiplicative property). *The submultiplicative property of a matrix A is given by*

$$\|AB\| \leq \|A\| \cdot \|B\|, \tag{A.7}$$

where B is any other matrix of appropriate dimensions.

Appendix B

Input-to-state stability

As encore to Section 3.1.2, this appendix illustrates that input-to-state-stability of the system (3.7) can be achieved with any positive definite matrix Q of appropriate dimensions. To this end consider the Lyapunov function

$$V(x_i) = x_i^T P x_i, \quad (\text{B.1})$$

where P is a 4×4 positive definite matrix. This Lyapunov function satisfies

$$\lambda_{min}^P \|x_i\|^2 \leq x_i^T P x_i \leq \lambda_{max}^P \|x_i\|^2, \quad (\text{B.2})$$

where λ_{min}^P and λ_{max}^P are the minimum and maximum eigenvalues of the matrix P , respectively. Hence, Lyapunov function (B.1) satisfies the condition (3.10), with $\alpha_1 = \lambda_{min} \|x_i\|_2^2$ and $\alpha_2 = \lambda_{max} \|x_i\|_2^2$. Next, consider the derivative of Lyapunov function (B.1) along the trajectories of (3.7), which is given by

$$\dot{V}(x_i, u_{i-1}) = -x_i^T (PA + A^T P) x_i + 2x_i^T P B u_{i-1}. \quad (\text{B.3})$$

Suppose P is such that $PA + A^T P = Q$, where Q is any positive definite 4×4 matrix, then it follows that

$$\begin{aligned} \dot{V}(x_i, u_{i-1}) &= -x_i^T Q x_i + 2x_i^T P B u_{i-1} \\ &= -\frac{1}{2} x_i^T Q x_i - \frac{1}{2} x_i^T Q x_i + 2x_i^T P B u_{i-1}, \end{aligned} \quad (\text{B.4})$$

Then, utilizing

$$\lambda_{min}^Q \|x_i\|^2 \leq x_i^T Q x_i \leq \lambda_{max}^Q \|x_i\|^2 \quad (\text{B.5})$$

where λ_{min}^Q is the minimum and λ_{max}^Q is the maximum eigenvalue of Q , shows that

$$\begin{aligned} &-\frac{1}{2} x_i^T Q x_i + 2x_i^T P B u_{i-1} \\ &\leq -\frac{1}{2} \lambda_{min}^Q \|x_i\|^2 + 2 \|x_i\| \|PB\| \|u_{i-1}\| \\ &= -\frac{1}{2} \lambda_{min}^Q \left[\|x_i\|^2 - 2 \|x_i\| \frac{\|PB\|}{\frac{1}{2} \lambda_{min}^Q} \|u_{i-1}\| + \frac{\|PB\|^2}{\frac{1}{2} (\lambda_{min}^Q)^2} \|u_{i-1}\|^2 \right] + \frac{\|PB\|^2}{\frac{1}{2} \lambda_{min}^Q} \|u_{i-1}\|^2 \\ &= -\frac{1}{2} \lambda_{min}^Q \left(\|x_i\| - \frac{\|PB\|}{\frac{1}{2} \lambda_{min}^Q} \|u_{i-1}\| \right)^2 + \frac{\|PB\|^2}{\frac{1}{2} \lambda_{min}^Q} \|u_{i-1}\|^2 \\ &\leq \frac{2\|PB\|^2}{\lambda_{min}^Q} \|u_{i-1}\|^2. \end{aligned} \quad (\text{B.6})$$

Hence,

$$\begin{aligned}
 \dot{V}(x_i, u_{i-1}) &\leq -\frac{1}{2}x_i^T Q x_i + \frac{2\|PB\|^2}{\lambda_{min}^Q} \|u_{i-1}\|^2 \\
 &\leq -\frac{1}{4}\lambda_{min}^Q \|x_i\|^2 - \frac{1}{4}\lambda_{min}^Q \|x_i\|^2 + \frac{2\|PB\|^2}{\lambda_{min}^Q} \|u_{i-1}\|^2 \\
 &\leq -\frac{1}{4}\lambda_{min}^Q \|x_i\|^2 \qquad \qquad \qquad \forall \|x_i\| \geq \frac{4\|PB\|}{\lambda_{min}^Q} \|u_{i-1}\|.
 \end{aligned} \tag{B.7}$$

Now, input-to-state stability can be concluded in a similar manner as presented in Section 3.1.2.

Appendix C

A string stability condition

This appendix proves the claim, made in Section 3.1.3 and Section 4.1.3, that the choice $y_i(t) = a_i(t)$ guarantees existence of $\|P_1(s)\|_{\mathcal{H}_\infty}$, while this is not guaranteed if either the position or velocity is chosen as output signal.

Consider the reference input $u_r(t) = \xi_0(t)$, with output $y_1(t) = a_1(t)$, and the corresponding string stability complementary sensitivity function

$$\Gamma_i(s) = \frac{\bar{a}_i}{\bar{a}_{i-1}} = \frac{s^2 \bar{q}_i}{s^2 \bar{q}_{i-1}} = \frac{\bar{q}_i}{\bar{q}_{i-1}}, \quad (\text{C.1})$$

where the Laplace operator s is omitted for clarity. This complementary sensitivity function shows that $\bar{a}_1(s) = \Gamma_1(s)\bar{a}_0(s)$. Moreover, from the vehicle model

$$\begin{aligned} \dot{q}_i &= v_i \\ \dot{v}_i &= a_i \\ \dot{a}_i &= -\frac{1}{\tau_i}a_i + \frac{1}{\tau_i}u_i, \quad i \in S_m, \end{aligned} \quad (\text{C.2})$$

it follows that

$$\begin{aligned} \bar{a}_1(s) &= \Gamma_1(s)\bar{a}_0(s) \\ &= \Gamma_1(s)(\tau_0 s + 1)^{-1}\bar{u}_0 \\ &= \Gamma_1(s)(\tau_0 s + 1)^{-1}(h_0 s + 1)^{-1}\bar{\xi}_0. \end{aligned}$$

Hence,

$$P_1(s) = \Gamma_1(s)(\tau_0 s + 1)^{-1}(h_0 s + 1)^{-1},$$

from which it directly follows that $\|P_1(s)\|_{\mathcal{H}_\infty}$ exists if $\|\Gamma_1(s)\|_{\mathcal{H}_\infty}$ exists, due to the submultiplicative property¹ of the \mathcal{H}_∞ norm and the fact that $1/(\tau_0 s + 1)$ and $1/(h_0 s + 1)$ are stable transfer functions, provided that $\tau_0 > 0$, and $h_0 > 0$, respectively.

Next, consider the velocity v_i as output signal for vehicle i . The corresponding string stability complementary sensitivity function is again given by (C.1) and the vehicle model (C.2) shows that

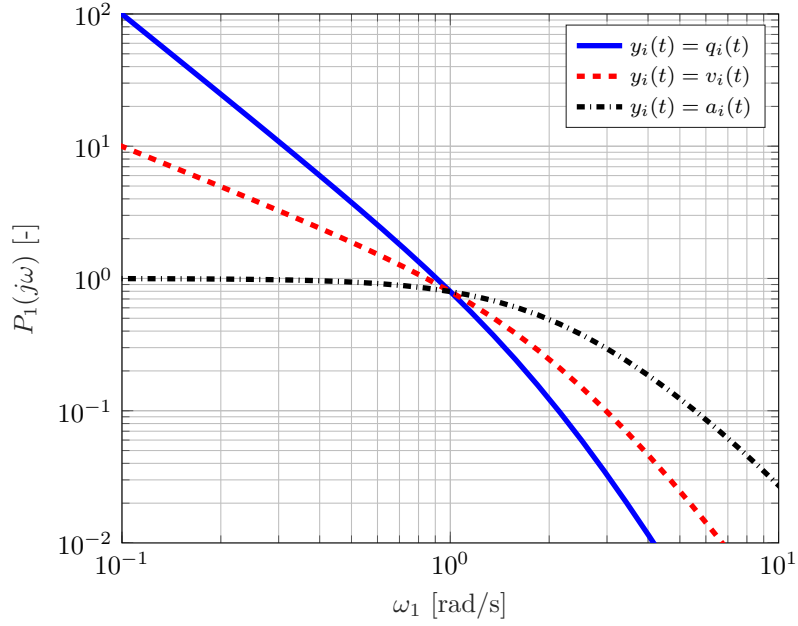
$$\begin{aligned} \bar{v}_1(s) &= \Gamma_1(s)\bar{v}_0(s) \\ &= \Gamma_1(s)\frac{1}{s}\bar{a}_0(s) \\ &= \Gamma_1(s)((\tau_0 s + 1)s)^{-1}\bar{u}_0 \\ &= \Gamma_1(s)((\tau_0 s + 1)(h_0 s + 1)s)^{-1}\bar{\xi}_0. \end{aligned}$$

Hence,

$$P_1(s) = \Gamma_1(s)((\tau_0 s + 1)(h_0 s + 1)s)^{-1}.$$

Due to the integrator, it holds that $\lim_{\omega \rightarrow 0} P_1(j\omega) = \infty$. With the same reasoning it can also be shown that $\lim_{\omega \rightarrow 0} P_1(j\omega) = \infty$ if the position is chosen as output signal, which is illustrated

¹See Appendix A for the definition of this property.


 Figure C.1: The complementary sensitivity function P_1 for different output signals.

by Figure C.1. Hence, existence of $\|P_1(s)\|_{\mathcal{H}_\infty}$ is guaranteed for $y_i(t) = a_i(t)$, but not for either $y_i(t) = v_i(t)$ or $y_i(t) = q_i(t)$. Although it may be surprising that the velocity cannot be chosen as output, this is merely a technical matter, originating in the definition of the virtual reference vehicle. Moreover, as shown by (C.1), $\Gamma_i(s)$ is independent of the output choice.

Appendix D

Negative definite quadratic form

This appendix elaborates on the negative definite quadratic form, which was used in Section 3.2.2. To this end, consider again the following Lyapunov function.

$$V(\varepsilon, u_i, \tilde{m}_i) = \varepsilon^T P \varepsilon + \frac{\alpha}{2} u_i^2 + \frac{\gamma_i}{2} \tilde{m}_i^2, \quad (\text{D.1})$$

where $\varepsilon = [\varepsilon_{i,1}, \varepsilon_{i,2}, \varepsilon_{i,3}]^T$ and $\alpha > 0$ is a constant. Differentiating this Lyapunov function with respect to time, along the solutions of (3.33), while utilizing (3.30) and (3.34) results in

$$\begin{aligned} \dot{V}(\varepsilon, u_i, \tilde{m}_i) &= -\varepsilon^T Q \varepsilon + \frac{\alpha}{h} u_i [k_p \quad k_d \quad k_{dd}] \varepsilon - \frac{\alpha}{h} u_i^2 \\ &\leq -\lambda_{min}^Q \|\varepsilon\|^2 + \frac{\alpha}{h} \|k\| |u_i| \|\varepsilon\| - \frac{\alpha}{h} |u_i|^2, \end{aligned} \quad (\text{D.2})$$

where $k = [k_p \quad k_d \quad k_{dd}]$. Next, consider the symmetric matrix

$$\begin{bmatrix} x_1 & x_2 \end{bmatrix} = \begin{bmatrix} c_1 & c_{12} \\ c_{12} & c_2 \end{bmatrix} \begin{bmatrix} x_1 \\ x_2 \end{bmatrix}, \quad (\text{D.3})$$

which is negative definite for $c_1 < 0$ and $c_1 c_2 > c_{12}^2$. Since (D.3) can be written as

$$c_1 x_1^2 + 2c_{12} x_1 x_2 + c_2 x_2^2, \quad (\text{D.4})$$

it can be easily shown that (D.2) is negative definite in $\|\varepsilon\|$ and $|u_i|$ for $0 < \alpha < \frac{4\lambda_{min}^Q h}{\|k\|^2}$. A similar analysis can be followed for the negative definite quadratic form used in Section 4.2.2.

Appendix E

Sensitivity in the presence of mass estimation errors

Section 3.3.3 and Section 4.3.3 illustrated that the alternative approach gives larger tracking errors than the common approach if a mass estimation error is present, while the tracking errors where approximately equal in a scenario of regular platooning. This appendix elaborates on the sensitivity to disturbances in the presence of mass estimation errors, for both approaches.

For the common approach, the closed-loop dynamics (3.31), with $k_{dd} = 0$, are linearised around the equilibrium point $x_{i,eq} = [0 \ 0 \ 0 \ 0 \ \bar{m}_i]$, where \bar{m}_i is 1000 kg. In other words, the initial mass estimates are not updated in this scenario. The linearised closed-loop system is given by

$$\begin{bmatrix} \dot{\varepsilon}_{i,1} \\ \dot{\varepsilon}_{i,2} \\ \dot{\varepsilon}_{i,3} \\ \dot{u}_i \\ \dot{\tilde{m}}_i \end{bmatrix} = \begin{bmatrix} 0 & 1 & 0 & 0 & 0 \\ 0 & 0 & 1 & -\frac{h}{\tau} \frac{\bar{m}_i}{m_i} & 0 \\ -\frac{k_p}{\tau} & -\frac{k_d}{\tau} & -\frac{1}{\tau} & -(1 - \frac{h}{\tau}) \frac{1}{\tau} \frac{\bar{m}_i}{m_i} & 0 \\ \frac{k_p}{h} & \frac{k_d}{h} & 0 & -\frac{1}{h} & 0 \\ 0 & 0 & 0 & 0 & 0 \end{bmatrix} \begin{bmatrix} \varepsilon_{i,1} \\ \varepsilon_{i,2} \\ \varepsilon_{i,3} \\ u_i \\ \tilde{m}_i \end{bmatrix} + \begin{bmatrix} 0 \\ 0 \\ \frac{1}{\tau} \frac{\bar{m}_{i-1}}{m_{i-1}} \\ \frac{1}{h} \\ 0 \end{bmatrix} u_{i-1}, \quad i \in S_m. \quad (\text{E.1})$$

To analyze the influence of disturbances on the tracking error, the outputs are chosen as

$$y_i(t) = C_i x_i, \quad i \in S_m, \quad (\text{E.2})$$

where $C_i = [1 \ 0 \ 0 \ 0 \ 0]$.

For the alternative approach, the closed-loop dynamics (4.16) are linearised around the equilibrium point $x_{i,eq} = [0 \ 0 \ h a_{i-1} \ \bar{m}_i]$, where \bar{m}_i is 1000 kg. In other words, the mass estimates are again not updated. The linearised closed-loop system is given by

$$\begin{bmatrix} \dot{\varepsilon}_{i,1} \\ \dot{\varepsilon}_{i,2} \\ \dot{\varepsilon}_{i,3} \\ \dot{\tilde{m}}_i \end{bmatrix} = \begin{bmatrix} 0 & 1 & 0 & 0 \\ -k_p(1 + \frac{\bar{m}_i}{m_i}) & -k_d - (k_d + \frac{1}{h} - \frac{1}{\tau}) \frac{\bar{m}_i}{m_i} & -(\frac{1}{h} - \frac{1}{\tau}) \frac{\bar{m}_i}{m_i} & 0 \\ 0 & \frac{1}{h} & -\frac{1}{h} & 0 \\ 0 & 0 & 0 & 0 \end{bmatrix} \begin{bmatrix} \varepsilon_{i,1} \\ \varepsilon_{i,2} \\ \varepsilon_{i,3} \\ \tilde{m}_i \end{bmatrix} + \begin{bmatrix} 0 \\ 1 + \frac{1}{\tau} - \frac{\bar{m}_i}{m_i} \\ 1 \\ \gamma(P_{1,2} + P_{2,2})(1 - \frac{h}{\tau}) \end{bmatrix} a_{i-1}, \quad i \in S_m. \quad (\text{E.3})$$

The outputs are again chosen as

$$y_i(t) = C_i x_i, \quad i \in S_m, \quad (\text{E.4})$$

where $C_i = [1 \ 0 \ 0 \ 0]$.

For the common approach, the system model (E.1)-(E.2) can be formulated in the Laplace domain as follows:

$$\bar{y}_i(s) = P_i(s) \bar{u}_{i-1}(s), \quad i \in S_m, \quad (\text{E.5})$$

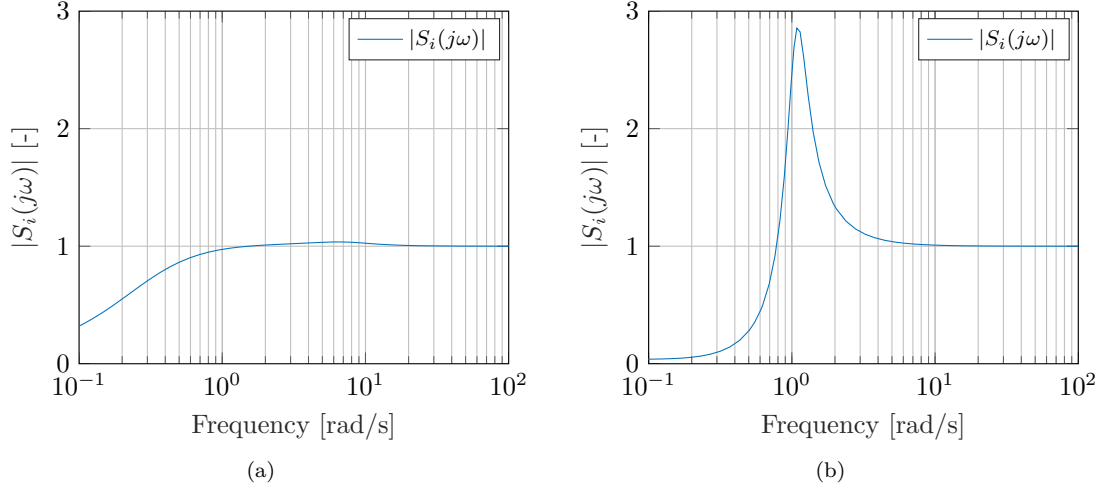


Figure E.1: Sensitivity transfer functions $S_i(j\omega)$ for (a) the common approach and (b) the alternative approach.

and, for the alternative approach, the system model (E.3)-(E.4) can be formulated in the Laplace domain as follows:

$$\bar{y}_i(s) = P_i(s)\bar{a}_{i-1}(s), \quad i \in S_m. \quad (\text{E.6})$$

For both approaches the complementary sensitivity transfer function $P_i(s)$ is given by

$$P_i(s) = C_i(sI - A_i)^{-1}B_i, \quad (\text{E.7})$$

Figure E.1a and Figure E.1b present the corresponding sensitivity transfer functions $S_i(s) = 1 - P_i(s)$, for the common and alternative approach, respectively. These sensitivity functions show a clear difference between the two approaches. For the common approach, Figure E.1a illustrates that disturbances do not have much effect: low frequency disturbances affect the tracking errors slightly, while high frequency disturbances do not have any influence. For the alternative approach on the other hand, the sensitivity plot shows a high peak. This sensitivity explains why the alternative approach has larger tracking errors if a mass estimation error is present, as was observed in Section 3.3.3 and Section 4.3.3.

Appendix F

Experimental setup limitations

This appendix illustrates the effect of communication losses during an experiment as mentioned in Section 5.1.2. The presented results are obtained during an experiment of the common CACC approach with the assumption that the vehicle mass is unknown. Therefore, the experimental settings, e.g., control parameters, system parameters and initial conditions, are conform Subsection 5.4.3.

If the communication protocol is lost during an experiment, the e-puck does not receive a control signal and comes to a full stop. Figure F.1a presents the tracking error of an experiment during which the communication is lost with the first vehicle around $t = 20$ s. It can be clearly seen that the communication loss with the first vehicle results in a positive tracking error for the first vehicle and a negative tracking error for the second vehicle. This means that the second vehicle comes too close to its predecessor, which could result in dangerous driving situations. Figure F.1b shows that due to the stop of the first vehicle, a peak also occurs in the control signal v_1 .

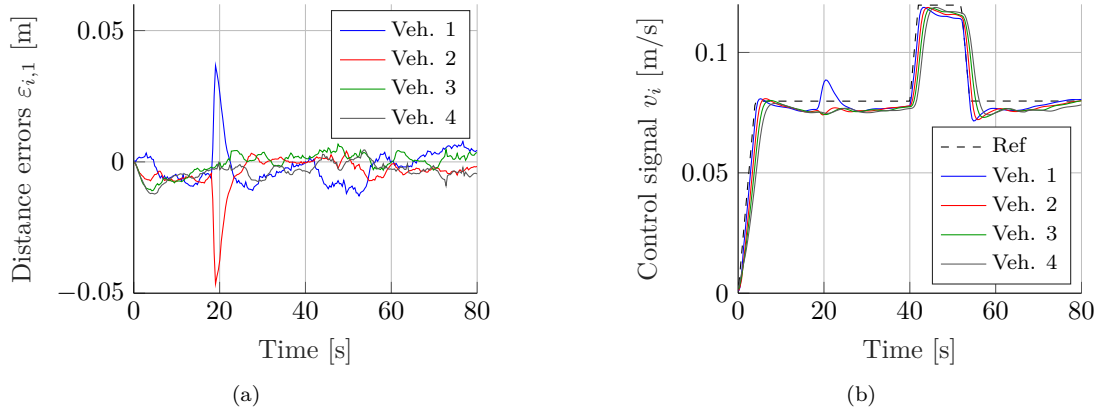


Figure F.1: Results of an experiment with communication loss: (a) realized tracking errors, and (b) control signal v_i .

After only a few seconds the communication with the first vehicle is restored and the vehicle starts to move again. Because of the short duration, the platoon is able to recover from the communication loss and goes back into the desired formation.

Appendix G

Additional experimental results

In order to present a complete picture of the experiments, this appendix presents the longitudinal positions and velocities that correspond to the experimental results presented in Section 5.4.

G.1 String stability

This section presents results obtained in a scenario of regular platooning. The presented results correspond to Section 5.4.1. Figure G.1 and Figure G.2 present the longitudinal positions $q_{i,r}$ and velocities $v_{i,r}$ for the common and alternative approaches, respectively.

G.2 Heterogeneity

This section presents results obtained in two heterogeneous scenario's. The presented results correspond to the experimental results presented in Section 5.4.2. Figure G.3 presents the longitudinal positions $q_{i,r}$ and velocities $v_{i,r}$ in a scenario where the heterogeneity is caused by different acceleration limits, for the common approach. Figure G.4 presents the longitudinal positions $q_{i,r}$ and velocities $v_{i,r}$ in a scenario where the heterogeneity is caused by different acceleration limits, for the alternative approach.

Figure G.5 presents the longitudinal positions $q_{i,r}$ and velocities $v_{i,r}$ in a scenario where the heterogeneity is caused by different τ values, for the common approach. Figure G.6 presents the longitudinal positions $q_{i,r}$ and velocities $v_{i,r}$ in a scenario where the heterogeneity is caused by different τ values, for the alternative approach.

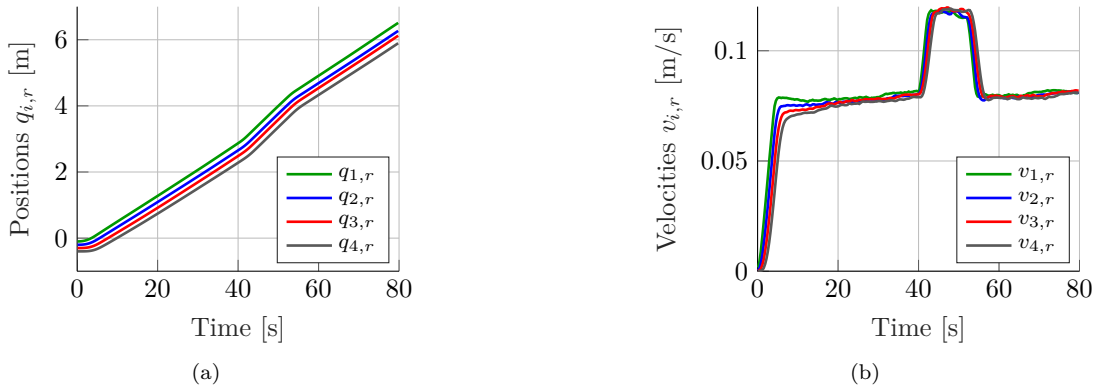


Figure G.1: Common approach in a scenario of regular platooning: (a) longitudinal positions $q_{i,r}$ and (b) velocities $v_{i,r}$.

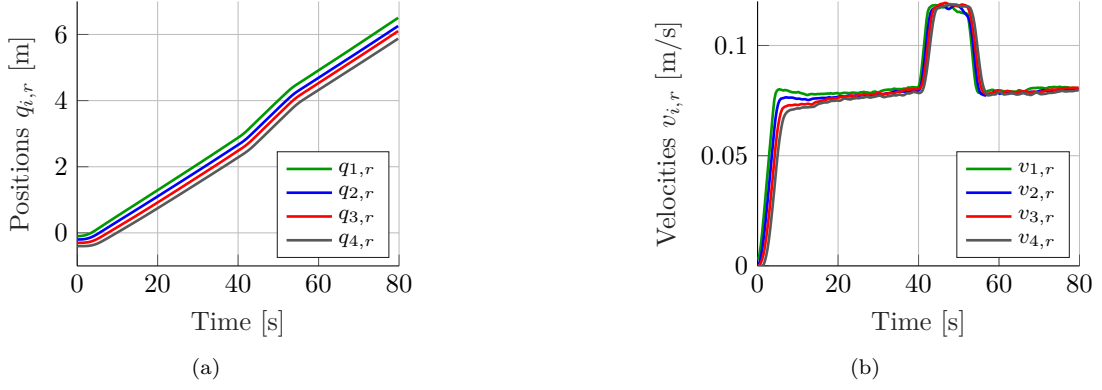


Figure G.2: Alternative approach in a scenario of regular platooning: (a) longitudinal positions $q_{i,r}$ and (b) velocities $v_{i,r}$.

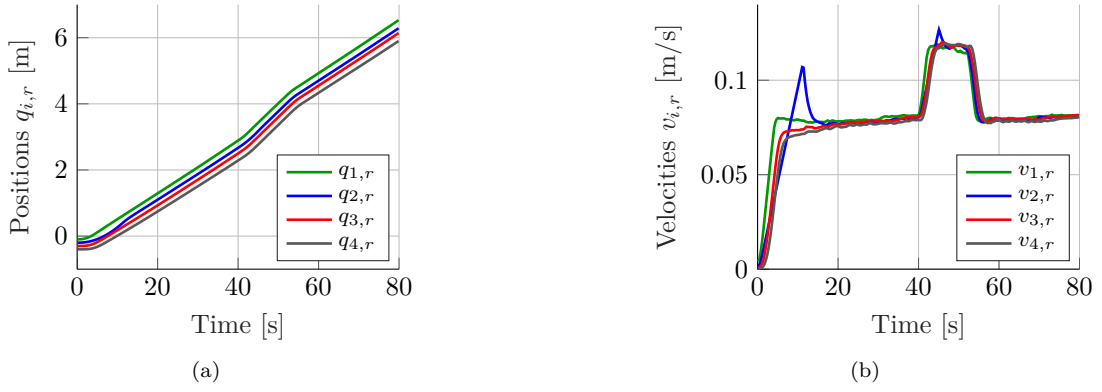


Figure G.3: Common approach in a scenario where the heterogeneity is caused by different acceleration limits: (a) longitudinal positions $q_{i,r}$ and (b) velocities $v_{i,r}$.

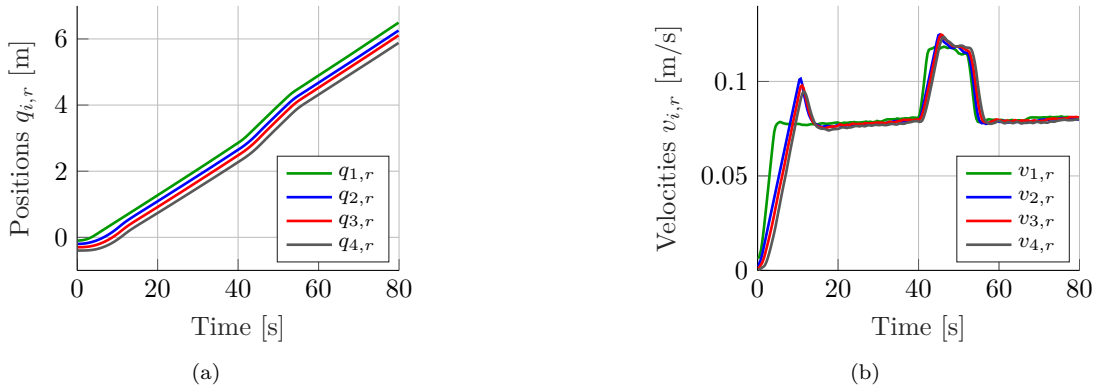


Figure G.4: Alternative approach in a scenario where the heterogeneity is caused by different acceleration limits: (a) longitudinal positions $q_{i,r}$ and (b) velocities $v_{i,r}$.

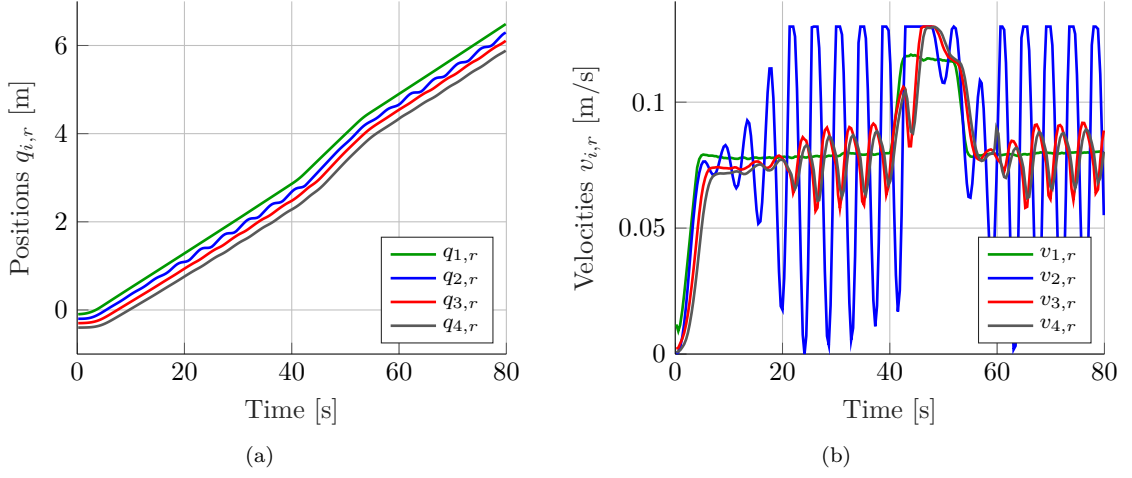


Figure G.5: Common approach in a scenario where the heterogeneity is caused by different τ : (a) longitudinal positions $q_{i,r}$ and (b) velocities $v_{i,r}$.

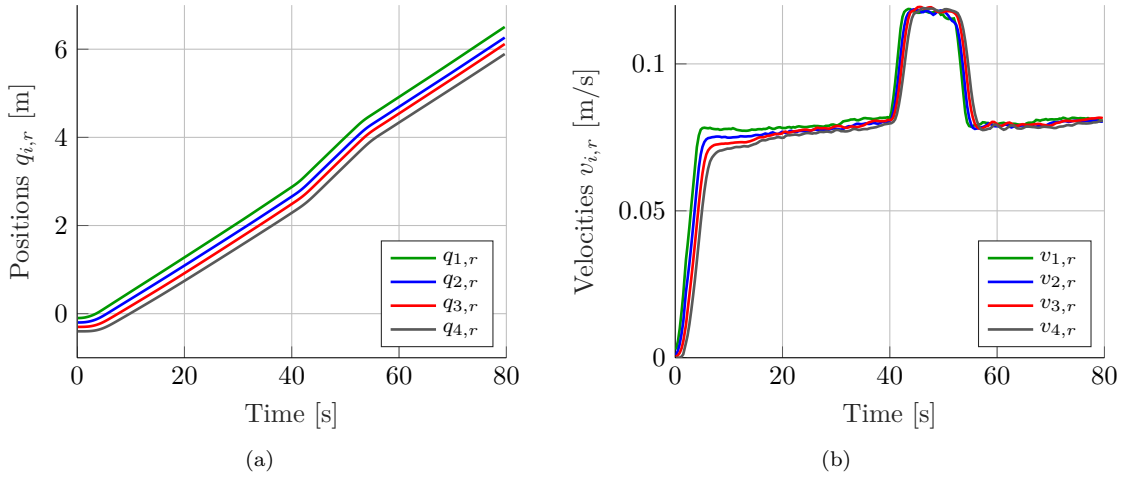


Figure G.6: Alternative approach in a scenario where the heterogeneity is caused by different τ : (a) longitudinal positions $q_{i,r}$ and (b) velocities $v_{i,r}$.

G.3 Mass estimation

This section presents results obtained in a scenario where the vehicle masses are estimated. The presented results correspond to the experimental results presented in Section 5.4.3. Figure G.7 presents the longitudinal positions $q_{i,r}$ and velocities $v_{i,r}$ for the common approach. Figure G.8 presents the longitudinal positions $q_{i,r}$ and velocities $v_{i,r}$ for the alternative approach.

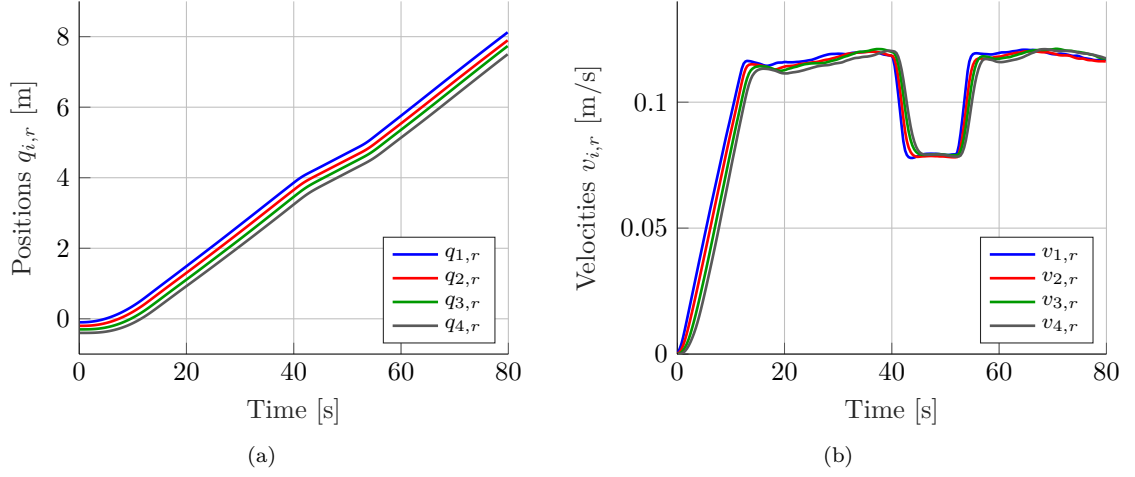


Figure G.7: Common approach in a scenario where the mass is estimated: (a) longitudinal positions $q_{i,r}$ and (b) velocities $v_{i,r}$.

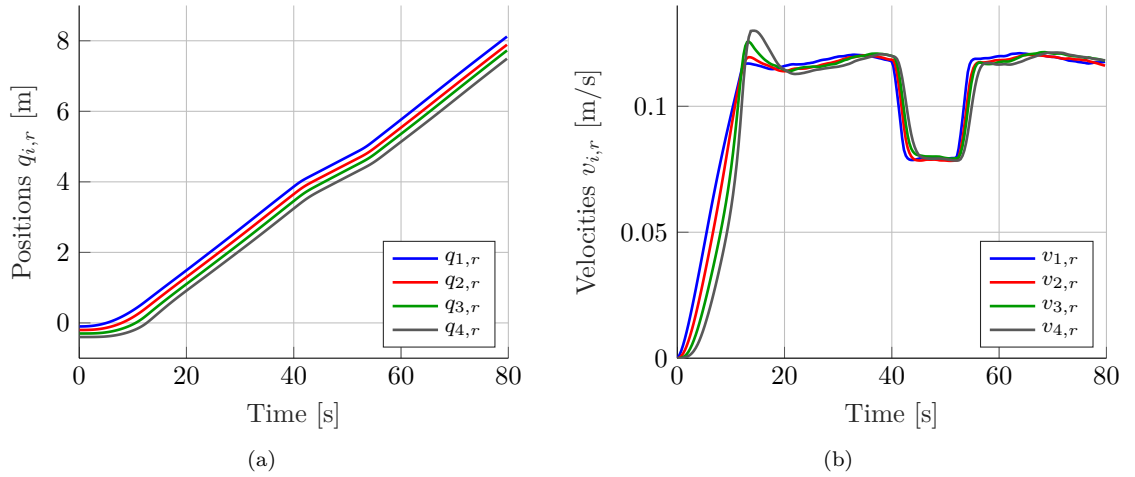


Figure G.8: Alternative approach in a scenario where the mass is estimated: (a) longitudinal positions $q_{i,r}$ and (b) velocities $v_{i,r}$.

Declaration concerning the TU/e Code of Scientific Conduct for the Master's thesis

I have read the TU/e Code of Scientific Conductⁱ.

I hereby declare that my Master's thesis has been carried out in accordance with the rules of the TU/e Code of Scientific Conduct

Date

20-08-2019

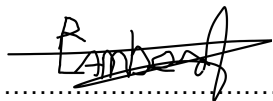
Name

Peter Lambert

ID-number

s1116821

Signature



Submit the signed declaration to the student administration of your department.

ⁱ See: <http://www.tue.nl/en/university/about-the-university/integrity/scientific-integrity/>

The Netherlands Code of Conduct for Academic Practice of the VSNU can be found here also.

More information about scientific integrity is published on the websites of TU/e and VSNU